Université Catholique de Louvain
Faculté de Médecine
Service de Cardiologie
Département de Médecine Interne

Myocardial Blood Flow and Metabolism in Left Ventricular Ischemic Dysfunction

Thesis by
Jean-Louis J. Vanoverschelde

Thèse présentée en vue de l'obtention du grade
d'Agrégé de l'Enseignement Supérieur

Co-Promoteurs:
Dr Jacques A. Melin
Dr William Wijns
1995

Author's address:

Jean-Louis Vanoverschelde, M.D.
Division of Cardiology
Cliniques Universitaires St Luc
Avenue Hippocrate 10 (2881)
B-1200 Brussels, Belgium
Tel: (32-2)-764.28.03
Fax: (32-2)-764.28.11

ACKNOWLEDGEMENTS

I would like to express my gratitude to Professor P. Macq, Rector of the University, for the medical education provided at the University of Louvain.

My deepest gratitude goes my Promoters, Professors J.A. Melin and W. Wijns, who introduced me to clinical research and always encouraged my research projects. Their continuing support and moreover their friendship is much appreciated.

I also wish to thank Professor J.-M. Detry, Chief of the Division of Cardiology, who welcomed me in the Division in 1988 and has always been supportive ever since. I am also grateful to my colleagues of the Division of Cardiology, and particularly to Professor J. Cosyns, who warmly welcomed me in the Echocardiographic Laboratory.

Most of the work summarized in this thesis was performed at the Positron Emission Tomography Laboratory in Louvain-la-Neuve and could not have been done without the invaluable help and competence of the physicists in charge of the PET scanner, namely A. Bol and C. Michel, without the expertise and skills of the cyclotron staff, particularly M. Cogneau, D. Labar and B. Georges and without the hard work of many colleagues, especially T. Baudhuin, C. Depré, B. Essamri, B. Gerber and C. Grandin. I wish also to thank A. Robert for her thoughtful statistical advises in the preparation of this thesis.

During my stay at the Cardiovascular Division of the Washington University in Saint-Louis, I was guided by Professor S.R. Bergmann. I also enjoyed the close collaboration of Drs E. Geltman, R. Gropler and O. Lowry. I wish to thank them for introducing me to basic cardiac metabolism and biochemistry.

I would like to acknowledge the members of my thesis committee, who critically reviewed this manuscript and helped me to improve its content and presentation: Professor L. Opie from the University of Cape Town; Professor D. Buxton from the University of California, Los Angeles; Professor M. Borgers, from the University of Maastricht and the Janssen Research Foundation; Professors H. Pouleur, A. Charlier, J.-M. Gillis, L. Hue, C. Michel and J.-M. Detry.

Finally, I wish to express my deepest thanks to my wife Martine Cransquin for her patience and her continuing support during the preparation of this thesis. Together, we share the joys, disillusions and hopes of an ever more demanding scientific and clinical career.

Table of Content

Page No

Chapter 1 Background and definitions

Modern therapy of coronary artery disease increasingly involves interventional strategies aimed at directly restoring blood flow to the ischemic myocardium. Over the recent years, the emergence of coronary artery bypass surgery, percutaneous transluminal coronary angioplasty and thrombolytic therapy has helped to change the natural course of ischemic heart diseases and contributed to the significant reduction in the mortality from both acute myocardial infarction [82] and chronic coronary artery disease.[1,61,151] This new sophistication in revascularization therapy has also heightened our awareness of the diverse effects of perfusion on cardiac function. Since the pioneering works of Tennant and Wiggers, it is known that total ischemia leads to a prompt cessation of contraction198 and eventually results in the appearance of cell damage and irreversible myocardial necrosis.[106] Accordingly, in the mind of many cardiologists, the discovery of an abnormal regional contraction in a patient with coronary artery disease has long been equated with the presence of irreversible myocardial necrosis. With the advent of reperfusion therapy, however, evidence progressively accumulated that prolonged regional "ischemic" dysfunction did not always arise from irreversible tissue damage and, to some extent, could be reversed by restoration of blood flow.[160] From laboratory and clinical investigations of reperfusion of ischemic myocardium, several associated phenomena were described, which have come to be known as myocardial "stunning" [20,21,25,113,128] and myocardial "hibernation."[26,113,128,161] Stunning is a reversible form of contractile dysfunction that can occur after restoration of coronary blood flow following a relatively brief period of coronary occlusion.[95] Myocardial hibernation is a postulated condition of chronic sustained abnormal contraction due to chronic underperfusion in patients with coronary artery disease in whom revascularization or an improved oxygen supply-demand balance causes recovery of regional function.[160,161]

Despite the rich and still evolving variety of eponyms that are used to describe these new myocardial states, uncertainties remain about their pathophysiology.128 From a conceptual standpoint, it seems that a first logical approach to the elucidation of potential pathophysiological factors could be to describe these new states in terms of perfusion-contraction matching.[169] Studies on regional flow-function relations during acute ischemia have indeed indicated that there is a close coupling between the supply of myocardial substrates, including O_2, of which the measurement of regional perfusion provides a rough estimate, and myocardial energy demand, as reflected by the steady state level of regional contraction.[68-70] Thus, whether or not flow and function are appropriately matched in stunning and hibernation can provide us with important clues as to their origin. Unfortunately, while it is quite easy to obtain accurate measurements of regional perfusion and contraction in experimental animals, it is far more difficult to obtain these same measurements in man. In this regard, recent refinements in myocardial function and perfusion imaging have greatly enhanced our ability to measure flow and function directly in patients. In the present thesis, I wish to review my contribution to the elucidation of the pathophysiologic factors associated with left ventricular ischemic dysfunction in humans. Before going into the details of the different studies performed, I would like to set the stage and define more comprehensively some of the pathological conditions we will be dealing with throughout this thesis.

Acute perfusion-contraction matching or acute myocardial ischemia. Acute ischemia is a condition of low coronary blood flow associated with a proportional reduction of contraction and

a steady-state matching of energy supply and demand.[69,169] Reperfusion after very short periods of ischemia (less than 10 minutes) usually results in rapid and complete restoration of cardiac performance. There is no necrosis, and myocardial ultrastructure is normal.[106,213] More prolonged periods of ischemia, up to 15-20 minutes, do not usually cause tissue necrosis, but, with reperfusion, are associated with a prolonged, albeit reversible, dysfunction which has been termed stunning (see below).[95] Further increases in the duration of ischemia result in the appearance of irreversible cell damage, the ultrastructural characteristics of which include cellular swelling, membrane rupture, and cell contracture.[86,104-106,215-216] In vivo, irreversible damage occurs first in the subendocardial myocardium. With longer periods of ischemia, a wavefront of cell death moves from the subendocardial zone across the wall to involve progressively more of the transmural thickness of the ischemic zone (wavefront phenomenon).[106] As a consequence, the amount of necrosis in the ischemic zone increases over time, and until completion of the process (3 to 6 hours in dogs, probably more in humans), both reversibly and irreversibly injured cell populations may coexist within the same area. Reperfusion of severely ischemic myocardium usually results in a marked gain in cellular calcium, worsening of contracture,[87,88,213] exaggerated enzyme release[86] and failure to replenish high energy phosphate. There is usually no recovery of contractile function. The healing process involves the formation of a fibrotic scar, typical of chronic myocardial infarction.

Acute perfusion-contraction mismatch or myocardial stunning. Stunning is a reversible form of contractile dysfunction that can occur after restoration of coronary blood flow following a relatively brief period of coronary occlusion, as originally described by Heyndrickx et al.[95] Stunning is also postulated to occur in humans and to account in part for the prolonged contractile dysfunction seen after thrombolytic therapy or following attacks of unstable angina.[21,145,165,229] Myocardial stunning is considered to be a form of reperfusion injury,[213] whereby reintroduction of oxygen after a period of deprivation provokes a transient overload of calcium in cardiac myocytes and damages the contractile machinery.[57,122,123,128] The ensuing contractile dysfunction typically lasts for hours or days, despite adequate restoration of myocardial blood flow and the absence of tissue necrosis. Nonetheless, in the absence of subsequent ischemic episodes, function always returns spontaneously and completely back to normal.

As mentioned above, several lines of evidence support the hypothesis that transient calcium overload during early reperfusion is critical in the pathogenesis of myocardial stunning.[57,122,123,128] Kusuoka et al. showed that when isolated ferret hearts are exposed to elevated extracellular calcium during reperfusion, stunning inevitably ensues, whereas reperfusion with low calcium in the perfusion medium improves postischemic recovery.[122] The same group also showed that a transient increase in cellular calcium in the absence of ischemia mimics stunning physiologically, metabolically and histologically.[117] Additional evidence for the role of calcium overload in the genesis of myocardial stunning is provided by the results of experiments in which the transport of calcium across the plasma membrane [57] or its release from the sarcoplasmic reticulum were specifically manipulated at the time of reperfusion. Release of oxygen-centered free radicals at the time of reperfusion has been proposed as the triggering event for altering calcium homeostasis.[20,147] The role of oxygen-centered free radicals in the pathogenesis of myocardial stunning is supported by the results of several studies in which free-radicals-scavenging agents attenuated the severity of stunning.[147] Their involvement is also supported by the results of studies in isolated hearts, in which exogenous administration of a free radicals mixture caused calcium overload and subsequently contractile failure.[46] It is noteworthy that oxygen centered free-radicals are capable of inhibiting glycolysis,[46] whose integrity is critical for calcium homeostasis during reperfusion.[107] It is therefore tempting to hypothesize that myocardial stunning might

result from damage to the glycolytic pathway, perhaps mediated by free radicals, leading secondarily to impaired calcium homeostasis, calcium overload and contractile failure. The molecular mechanisms by which reperfusion-mediated calcium overload provokes reversible contractile dysfunction is currently under intense investigation. The most recent explanation relates stunning to a decreased sensitivity of the myofibrils to calcium.[72,123] The observation that calcium transients are increased in stunned myocardium, while function is severely depressed, supports this hypothesis.[123] It has been postulated that, during the initial period of overload, calcium could trigger a series of deleterious biochemical events, such as activation of calcium-dependent proteases or protein kinases, and thereby modify the properties of the contractile proteins,8 including their sensitivity to calcium. The reduction in the maximal calcium activated force observed in stunned hearts,[122] as well as the time course of recovery of stunned myocardium, which corresponds to the natural turnover rate of the contractile proteins in vivo, supports this hypothesis.

Sustained perfusion-contraction matching or short-term hibernation. Short-term hibernation is a condition of low coronary blood flow that lasts from 1 to several hours (up to 5 hours) and is associated with a sustained proportional reduction of contraction.[27,62,134] No myocardial necrosis ensues provided that there is sufficient residual coronary blood flow. Despite continuing low-flow and dysfunction, some of the metabolic markers of ischemia spontaneously resolve over time and phosphocreatine regenerates back to nearly normal levels.[3,150] Short-term hibernation is a remarkably unstable condition, as super-imposition of a chronotropic or inotropic stress invariably results in increased lactate production, decreased phosphocreatine and eventually myocardial necrosis.[182] Short-term hibernation is also postulated to occur in humans and to account for the prolonged contractile dysfunction seen during prolonged attacks of unstable angina.[169]

Chronic perfusion-contraction matching or chronic hibernation. Myocardial hibernation is a term first used by Rahimtoola for a postulated condition of chronic sustained abnormal contraction due to chronic underperfusion in patients with coronary artery disease in whom revascularization or an improved oxygen supply-demand balance causes recovery of regional function.[160,161] In his original description of the condition, Rahimtoola postulated that myocardial hibernation resulted from a "relatively uncommon response to reduced myocardial blood flow at rest whereby the heart downgrades its myocardial function to the extent that blood flow and function are once again in equilibrium, and as a result, neither myocardial necrosis or ischemic symptoms are present."[161] Although suggestive evidence supports the existence of hibernation in humans, there is no experimental demonstration that such a perfusion-contraction matching can persist for weeks or months in chronic animal preparations, let alone in the intact individual.

Ischemic preconditioning is yet another concept whereby the myocardium downgrades its energy requirements and becomes more tolerant to ischemia (i.e. develops less ischemic injury) because it has been primed or preconditioned by a preceding transient episode of ischemia followed by reperfusion.[105] Whether or not ischemic preconditioning bears any relationship with either myocardial stunning or hibernation remains largely unknown.

As briefly outlined in the preceding paragraphs, the mechanisms responsible for regional left ventricular dysfunction in patients with chronic coronary artery disease are obviously multiple and complex. Their precise delineation thus necessitates the simultaneous assessment of myocardial function, perfusion and metabolism, which, until recently, has remained elusive, owing mainly to the difficulty of obtaining quantitative measurements of myocardial blood flow and metabolism noninvasively in humans. The recent advent of powerful imaging modalities, such as positron emission tomography (PET), has greatly facilitated such investigations. In the present thesis, I will focus

on the insights gained into the pathophysiology of left ventricular ischemic dysfunction in humans by the use of PET. In Chapter 2, I will briefly review some of the concepts underlying the use of this modality for the quantification of myocardial perfusion and metabolism. In Chapter 3, I will concentrate on the study of the flow and metabolic correlates of myocardial infarction, myocardial stunning and myocardial hibernation in humans as well as on the structural changes shown to occur in the hibernating myocardium. Finally, in Chapter 4, I will illustrate how the concepts derived from these studies can be applied to the clinical identification of which patient is most likely to benefit from coronary revascularization.

Chapter 2 Assessment of Myocardial Blood Flow and Metabolism with Positron Emission Tomography

2.1 Principles of Positron Emission Tomography

Interest in positron emission tomography (PET) imaging arises from its capacity to measure regional physiologic function by tracing the biological fate of compounds that have been tagged with positron-emitting radioisotopes. Making accurate measurements with PET requires great care. Attenuation, scatter, accidental coincidences, and finite resolution effects, among many factors, may distort images and affect the reliability of the physiologic information derived from PET. In addition, physiologic parameters are often obtained by use of mathematical models that describe how biochemical concentrations vary with time. Depending on how these models are applied, factors affecting the reliability of the data can be minimized, while others become more important. Therefore, to acquire and analyze PET data accurately, one must be aware of the origin and nature of the distorting factors. This chapter briefly reviews some of the principles pertinent to the interpretation of cardiac PET studies.

2.1.1 The Basics of Positron Decay

Radioactive β–decay results from the emission of an electron or a positron from an unstable atom. Except for their opposite charges, positrons are identical to electrons: they have the same mass and behave similarly. Positrons are the "antimatter" of electrons. When a positron and an electron are in close proximity for more than the briefest interval, both disappear, a phenomenon termed annihilation, and their mass is converted into energy in the form of 2 gamma rays traveling in almost opposite directions (Figure 2-1). Thus, when the nucleus of a positron-emitter located in the myocardium decays, it emits a high-energy (from 3 MeV to 640 GeV) fast-moving positron. Initially, the positron is moving so fast that it does not spend enough time near any electron to annihilate. However, after traveling a few millimeters in tissue, the positron loses energy, slows down and eventually arrives in the close vicinity of an electron with which it annihilates, liberating 2 gamma rays of 511 keV of energy each (the energy equivalent to the mass of each particle).

2.1.2 Tomographic Detection of Positron Emission

PET scanners are built to detect pairs of gamma rays resulting from the annihilation of a positron with an electron. The detection is made by use of a ring containing hundreds or thousands of detectors that encircle the field-of-view. The mechanical assembly holding all these detectors is called the "gantry." All the detectors are connected together by electronic circuits and grouped by pairs. When a positron annihilates within the field of view, the 2 resulting gamma rays may strike and be detected by the 2 members of an opposing pair of detectors in the

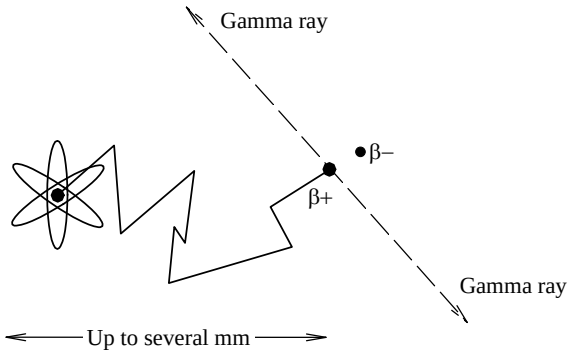

Figure 2-1. Positron decay of a nucleus. After the positron is emitted, it travels through tissue, bouncing off nearby atoms, and losing energy until it finally comes nearly to rest and annihilate with an electron. The electron and the positron annihilate, giving off 2 photons of 511 keV each traveling in almost opposite directions.

ring. When this happens, each of the detectors produces an electronic pulse at almost exactly the same time. The 2 detectors record what is called a *"coincident event."* Detection of such coincident events in pairs of detectors constitutes the basics of PET. It implies that an annihilation event has occurred somewhere along the line between the 2 detectors and assumes that the radioactive atom that decayed is located along the same line. By determining the lines along which gamma rays were generated in the field-of-view, PET scanners produce an image showing where the decaying atoms were located.

As mentioned above, although the 2 gamma rays causing a coincident event are assumed to strike their respective detectors simultaneously, this is seldom the case. As photons travel at the speed of light, it takes them about 1.33 nanoseconds to travel the 40 cm or so from the center of the ring to one of the detectors. If the annihilation has taken place somewhere other than at the center, 1 of the 2 gamma rays will reach its detector a few tenths of a nanosecond earlier than the other. Unfortunately, most current detector/photomultiplier combinations are not able to produce electronic pulses timed more accurately than within a few nanoseconds. Therefore, simultaneous detection refers to detection within a so-called *"resolving time,"* which is set electronically in the PET scanner, and is typically of 10 to 20 nsec. Any photons that are detected within this resolving time are considered to have occurred in coincidence. Accordingly, it is quite possible for 2 photons that did not come from the same annihilation event to be erroneously identified, quite by accident, as having occurred simultaneously, i.e. within the resolving time of the scanner. Such false coincidences are called *"accidental,"* or "random" coincidences. They account for background activity in the reconstructed image. They are dependent on the amount and location of activity detected by the scanner and on the resolving time of the tomograph. Consideration of the rate of singles detection on each detector allows to correct for accidental coincidences with a fairly small error. One can also measure the coincidence rate in the so-called "delayed coincidence time-window," subtract it from that measured in the "prompt coincidence time-window" and estimate thereby the true coincidence rate.

2.1.3 Attenuation and Scattering

When annihilation photons pass through tissue, they frequently interact with electrons in the tissue. Of those that interact, some do so by a process called *photoelectric effect*, whereby all the energy of the photon is absorbed by an electron, while others interact with neighboring electrons by a process called *Compton scattering*, whereby the photon is deflected and loses some of its energy. The higher the angle of deflection, the higher the energy loss. In biological tissues, most of the interaction results from Compton scattering. As a consequence, some fraction of the emitted photons is diverted from its original course and never reaches the detectors in the ring. The resulting loss of detected events is termed *"attenuation."* The number of photons that make it through unscathed decreases exponentially with the thickness of the interposed tissue as:

$$No = e^{-\mu(d1+d2)},$$

where μ is the attenuation coefficient (0.096 cm^{-1} in soft tissues), and d1 and d2 the distances traveled by photons before reaching their detectors. Typically, for a 70 kg subject, attenuation by factors of 10 to 20 is common. Although attenuation is a serious problem with PET because both photons in a pair must survive intact, accurate attenuation correction is possible. In contrast, with methods such as single-photon emission computed tomography (SPECT) in which only one photon is involved, such correction is quite difficult because the attenuation factor, $e^{-\mu d1}$, depends on measurement of the depth at which the isotope is located in the tissue. This measurement can hardly be made before imaging. The value necessary for attenuation correction of PET images, however, is (d1+d2). This quantity is independent of how deep the isotope is located and depends only upon the attenuation through the total body thickness, which can be measured

accurately.

The most common method for making these corrections is to calculate an attenuation correction factor for each pixel of the field-of-view. This is done by performing a "blank" and an "attenuation" scan (often called transmission scan). Before the patient to be imaged is placed in the ring, a small positron-emitting source is placed at one side and a scan, called the blank, is made. The position of the source is maintained and the patient is positioned in the ring. A second scan, the attenuation scan, is then performed. The difference in counts detected in the blank and the attenuation scans result from attenuation by the patient. The ratio of the blank scan counts to the transmission scan counts gives the factor $e^{-\mu * D}$ which is the factor needed to correct for attenuation for this pair of detectors. Making similar measurements for all the detector pairs permit complete attenuation correction on a pixel per pixel basis. It is important to note that precise attenuation correction requires either long acquisitions or spatial/angular smoothing. For practical reasons, however, acquisition times seldom exceed 15 to 20 minutes.

Scattering may cause other problems. Although the great majority of scattered photons never reach the detectors, a small number of them may still hit a detector and register a coincident event. When this occurs, the scanner erroneously computes the position of a radioactive atom. This may cause false counts to appear in cold areas of an image when a hot spot is nearby. Most scanners are designed, however, to reduce scatter detection by quantifying photon energy and rejecting those photons with energy below a certain threshold.

2.1.4 Finite Resolution Effects

The *spatial resolution* of a PET scanner is a measure of how well the scanner can distinguish between 2 small objects placed closely together. The resolution of a PET scanner is mainly dependent on 3 factors: 1- the design of the machine (including crystal size and spacing, ring diameter, etc. ...); 2- the positron range(which relates to how far positrons travel into the tissue before being annihilated) and deviation of annihilation photons from exact colinearity; 3- image reconstruction and post-processing (including filtering and smoothing) of reconstructed images.

Besides its influence on the ability to discriminate between 2 objects, the spatial resolution of a scanner also influences the accuracy of count measurements. To understand better what are the effects of the finite resolution of a tomograph on its measuring accuracy, let's assume that a perfect tomograph exists, and is used to image a 2 cm diameter cylinder of radioactivity. Assume further that after imaging for 100 seconds, 100.000 coincident events have been recorded (1000 events per second) in a transaxial slice of the cylinder. The perfect scanner will produce a perfect image, in which all the pixels have the same value, while all pixels outside the object would have the value zero. Placing a 2 cm diameter region of interest around the image of the object would yield the total number of coincidences per second coming from the object and all the coincidences detected would be measured within the region of interest.

If the same 2 cm diameter cylinder was imaged with an imperfect scanner (one with a 7 mm resolution for instance), the same 100.000 coincidences would be detected, but some of the coincidences would be blurred or spread out. Some counts from pixels near the edge would be smeared into the region outside the object. The pixels from the center of the object would not be affected as much as the pixels at the periphery because as many counts would be blurred out as blurred into them from their neighboring pixels. The net result is that part of the total radioactivity present in the object is now measured outside the object. Consequently, the same 2 cm diameter region of interest would now produce a value of 785 events per second, the other 215 events per second being detected outside the region of interest. The percentage of the counts retained in the region of interest is termed *"recovery coefficient,"* 78.5% in this case, while the percentage of counts spreading outside the region of interest is termed *"spillover*

fraction," in this case 21.5%. The term "*partial volume effect*" describes the resolution effect by which counts obtained from a region of interest applied to an image with finite resolution are fewer than those in the same region of interest applied to an image from an "ideal" PET scanner. The poorer the resolution, the more blurred the data will be and the fraction of counts "recovered" within a given region of interest will be lower.

It is clear from the above example, that if one wants to measure the total number of events in the object, simply increasing the size of the region of interest will be sufficient to recover a greater number of counts. In practice, however, PET data are seldom used to assess the total number of events within a given organ, but rather to measure regional activity concentrations, in counts per pixel per second. In this case, drawing too large a region of interest in an effort to recover all the counts will just have the opposite effect, as it will reduce the measured counts per pixel per second by increasing the total number of pixels. If the region of interest were decreased in size, however, it would no longer include pixels near the edge and the activity concentration would more closely approximate the correct value. Unfortunately, as the region of interest gets smaller, so does the total number of events contained in it, causing statistical fluctuations to increase. Also, if the size of the imaged object is less than twice the actual resolution of the tomograph, the activity concentration will be underestimated, even in the pixels near the center of the imaged object.[98]

It is theoretically possible to correct for the partial volume and spillover effects.10,98 If the true anatomic dimensions of the imaged object and the resolution of the tomograph producing the image are known, it is possible to calculate the recovery coefficients and spillover fractions and use them to correct the data.76 These corrections are an absolute prerequisite to the measurements of myocardial blood flow and metabolism in absolute terms, in ml.(min.g)$^{-1}$ or in µmol.(min.g)$^{-1}$, with PET.

From a theoretical standpoint, the true tracer concentrations in blood (C_b, left ventricular [LV] cavity) and myocardium (C_m) can be computed from their imaged concentrations (C_{ib} and C_{im}) by use of the following equations:

$$C_m = k \cdot (F_{bb} \cdot C_{im} - F_{bm} \cdot C_{ib})$$
$$C_b = k \cdot (F_{mm} \cdot C_{ib} - F_{mb} \cdot C_{im})$$

Where

$$k = 1/(F_{bb} \cdot F_{mm} - F_{mb} \cdot Fbm)$$

and F_{bb} and F_{mm} are the recovery coefficients for blood pool and myocardium, respectively, and Fbm and Fmb are the spillover fractions from blood pool to myocardium and from myocardium to blood pool, respectively.

The magnitude of the 4 correction factors (F_{bb}, F_{mm}, F_{bm} and F_{mb}) is mainly dependent on the geometric dimensions of the objects, on their relative distance and on the resolution function of the tomograph. To determine these factors, we have developed a Monte Carlo simulation that assumes a bigaussian spatial resolution in the tomographic plane and tested its accuracy in both phantom and in vivo dynamic studies.[17,210] The different steps of the method are briefly outlined below.

Step 1

The shapes and sizes of the LV cavity and myocardium are first determined by isocontours on a selected image of the dynamic study where all the activity is concentrated in the myocardium. The geometric dimensions determined by use of such isocontours compare favorably with the known sizes of various heart phantoms (within 3%). Also, the mean radii of the contours measured on images obtained 70 minutes after FDG injection are in good agreement with those measured on the corresponding anatomical slices ($y = 0.062 + 0.921\,x$, $r = 0.98$). It should be pointed out, however, that this approach necessitates images with high count statistics and is likely not valid in very small objects, typically less than 6 mm. For these small objects, the geometric

dimensions should be measured by use of imaging modalities with a better spatial resolution, such as magnetic resonance imaging or echocardiography.

Step 2

From the cavity and myocardial contours, 4 images are randomly generated: the "true" uniform activity distributions in both cavity and myocardium and the corresponding "imaged" distributions, distorted by the resolution effect. The measured in-plane spatial resolution of our tomograph (ECAT III, model 911/01, CTI Inc., Knoxville, TN) follows a gaussian distribution with a full-width-at-half-maximum (FWHM) of 8 mm when reconstructed with a Hann filter at a cutoff frequency of 0.5.[99] When this resolution function is implemented in the Monte Carlo simulation, the recovery coefficients computed as a function of object size are in excellent agreement with those measured with a hot spot phantom. The degree of agreement is less, however, when the same resolution function is applied to in vivo dynamic FDG studies. Because of heart motion, the geometric dimensions determined from dynamic imaging are averaged over the cardiac cycle, introducing errors in the computation of the correction factors. To compensate for these errors, a simplified model of wall motion derived from gated studies was added to the Monte Carlo simulation. In this model, the outer contours of the myocardium are kept constant, while the cavity radius is allowed to vary between 2 extreme values determined from contours drawn at end-diastole and end-systole. Simulation studies were performed to evaluate specifically the effects of spatial averaging. The results of these studies clearly indicated that neglecting the effects of wall motion led to overestimation of recovery coefficients and underestimation of spillover factors. Thus, ideally, gated studies should be performed in every patient to correct for the effects of heart motion. Gated dynamic studies are tedious to perform, however. Therefore, despite the above limitations, we finally decided to use the averaged dimensions from nongated studies and to compensate for the discrepancies in the correction factors by increasing the FWHM of the resolution function from 8 to 10 mm, in accordance to previous in vitro measurements.

Step 3

The regions of interest defined on the dynamic PET study are projected on the Monte Carlo images. Their integral ratios with and without the resolution effect allow computation of the recovery coefficients for each region of interest and the spillover factors between the different regions.

Comparison with in vitro measurements

To evaluate the accuracy of the correction factors provided by the Monte Carlo simulation, dynamic PET imaging was obtained in 8 dogs after intravenous administration of 5 mCi of FDG. In the 8 dogs studied, the blood pool curves derived from corrected PET data compared favorably with those obtained by rapid arterial sampling and well-counting. The mean of all angular coefficients obtained by linear regression of the tomographic data on the in vitro arterial counts improved from 0.82 to 0.95 when corrections for finite resolution were applied. In 4 studies, the dogs were sacrificed at the end of the PET acquisition, and tissue samples from the imaged slice were counted in a

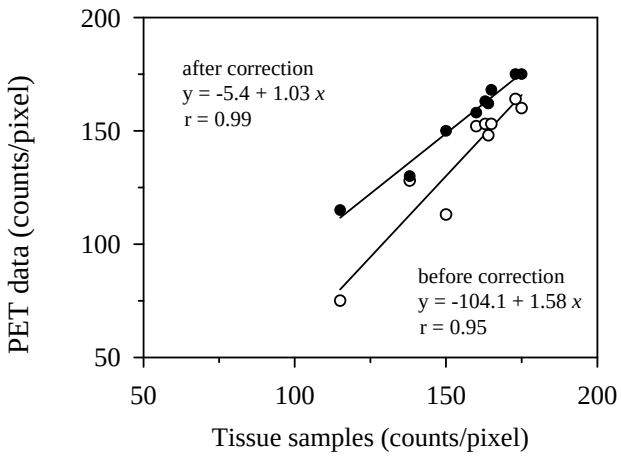

Figure 2-2. Scatterplots of correlation between in vitro and in vivo tissue concentrations before (○) and after (●) correction of PET data for finite resolution effects. Adapted from Ref. 210.

cross-calibrated well counter. As shown in a representative example (Figure 2-2) PET data corrected for the finite resolution effects correlated well with in vitro measurements.

2.1.5 Radiopharmaceuticals for Cardiac PET

In contrast to most single-photon emitters, many positron-emitting radionuclides are unique because their naturally occurring counterparts (hydrogen, carbon, nitrogen and oxygen) are predominant constituents of biological compounds. Positron-emitting isotopes of fluorine, carbon, nitrogen, and oxygen may replace their stable counterparts in the synthesis of metabolic substrates, receptors ligands, drugs, and other biologically active compounds without disrupting biochemical properties or activity. Also, as the labeled compounds are administered in only tracer amounts, they do not usually interfere with the physiological or metabolic processes under study.

Positron-emitting radionuclides can be produced in 2 ways: with a cyclotron or with a generator. Use of an on-site cyclotron can support production of oxygen-15 (^{15}O, half-life of 2.0 minutes), nitrogen-13 (^{13}N, half-life of 9.9 minutes), carbon-11 (^{11}C, half-life of 20.4 minutes), and fluorine-18 (^{18}F, half-life of 110 minutes). Many different radiopharmaceuticals incorporating these labels have been developed for studies of myocardial perfusion and metabolism with PET. However, because of their short half-life, incorporation of these positron-emitters into the tracer of interest often requires the use of novel, rapid, synthetic schemes. These in turn necessitate the expertise of highly-specialized radiochemists or radiopharmacists, and strict quality controls pertinent to the delivery and administration of radiopharma-ceuticals to human subjects.

Production of positron-emitting radio-nuclides with generators, whereby a short-lived daughter radionuclide is rapidly separated from a longer-lived parent, offers the advantage that the parent radionuclide can be produced at a remote site and less expensively than cyclotron-produced radiopharmaceuticals. To date, however, generator-produced radiopharmaceuticals suitable for cardiac studies are limited to agents used to image the blood pool or to estimate perfusion (^{68}Ga, ^{82}Rb).

2.2 Quantification of Myocardial Perfusion with Positron Emission Tomography

2.2.1 General Considerations

Quantification of myocardial perfusion in absolute terms, i.e. in ml.(min.g)$^{-1}$, is crucial for determination of the physiologic significance of coronary artery disease and for evaluation of the efficacy of pharmacological, mechanical, or surgical interventions designed to augment nutritive perfusion. Quantitative estimates of myocardial perfusion are also mandatory for the evaluation of patients in whom the uptake and clearance of flow tracers are homogenous, such as those with chest pain and angiographically normal coronary arteries, cardiac allografts or cardiomyopathies, or when regional disparities are not obvious because of balanced or multivessel coronary artery disease.

The severity of stenosis, as determined visually from coronary angiograms, does not accurately predict maximal flow in response to a physiologic or pharmacological stimulus.129 Even though quantitative arteriography has improved the accuracy of assessment of epicardial vessels,[75,204] such measurements do not define nutritive perfusion per se. Intracoronary flow velocity measurements by use of miniaturized Doppler flow probes have been recently proposed to achieve this goal.[129] Yet, these measurements reflect only bulk conductance flow in limited vascular territories, and unless they are coupled with the measurement of vessel dimensions, they do not allow flow to be measured. In addition, nutritive perfusion may not parallel macrovascular flow, as collateral flow is not taken into account.

Nuclear medicine techniques such as planar or single-photon emission computed tomography (SPECT) with perfusion agents such as ^{201}Thallium or ^{99m}Tc isonitriles are increasingly

used to assess myocardial perfusion and perfusion reserve. Despite their convenience, these methods are of limited accuracy because of inadequate correction for tracer extraction, photon attenuation and finite resolution effects. Accordingly, they cannot be used to assess myocardial perfusion in absolute terms.

Because of its quantitative capabilities, PET has emerged as a promising method for quantification of nutritive myocardial perfusion. When mathematically and physiologically appropriate models are used to describe the biological behavior of the administered radiotracers in blood and myocardium, it becomes possible to obtain quantitative estimates of regional myocardial perfusion.[15,19,93] Among the different positron-emitting radiopharmaceuticals available for perfusion studies, ^{13}N-ammonia, ^{15}O-water and ^{82}Rubidium are the most commonly used.

2.2.2 Quantification of Myocardial Perfusion with ^{13}N-ammonia.

A number of experimental and clinical studies have shown the feasibility of qualitative and quantitative estimates of myocardial blood flow with ^{13}N-ammonia and PET. Although ammonia is a gas, it falls into the category of cation-type tracers, since at physiological pH, its major form is NH_4^+. Although the mechanisms of transport across the sarcolemmal membrane have not been delineated conclusively, carrier-mediated transport appears to be involved. ^{13}N-ammonia exhibits high, single pass extraction (greater than 80% at physiological flow rates).[176,186] Once extracted by the heart, its biological half-life is 80 to 400 minutes. Clearance from the blood is usually rapid. Accordingly, ^{13}N-ammonia provides good to excellent images of the myocardium.[175]

^{13}N-ammonia extraction by the myocardium is inversely and non linearly related to flow.[176,186] Net uptake plateaus at flows greater than 2 to 2.5 ml.(min.g)$^{-1}$. Thus, net ^{13}N-ammonia uptake is not very sensitive to changes in the hyperemic flow range. The extraction and retention of ^{13}N-ammonia by the heart are also related to myocardial oxygenation and metabolism.[14,118,164] Because the trapping of ^{13}N-ammonia is dependent on the conversion of ammonia to glutamine by the glutamine synthase pathway, factors that influence flux through this pathway can theoretically affect tracer kinetics independent of flow. In practice, however, these effects are negligible. Estimation of regional perfusion with ^{13}N-ammonia is usually achieved by use of a 2- or a 3-compartment model, which accounts for the forward and the backward transfer rates of ^{13}N-ammonia into the myocardium and for the metabolic trapping of ^{13}N-ammonia in the form of ^{13}N-glutamine.[19,74,100,120,138] Use of such models requires dynamic imaging to record time-activity curves in arterial blood (for input function) and myocardium. Several studies have shown that PET derived input functions were in good agreement with their invasive counterparts,[19,224] provided that blood pool and tissue time-activity curves are corrected for partial volume and spillover effects.

Additional corrections for contamination of the arterial input function by ^{13}N-labeled metabolites may be required to obtain reliable flow data.[168] In dogs, the proportion of administered ^{13}N-ammonia that is degraded to metabolic intermediates (predominantly urea and glutamine) is 91 ± 9% and 57 ± 19% at 1 and 2 minutes respectively after intravenous administration, and increases with adenosine. In humans, however, accumulation of 13N-labeled metabolites is slower, the proportion of the total radioactivity in blood retained in form 13N-ammonia at 1 and 2 minutes after injection being 99 ± 1% and 90 ± 4% respectively.[19]

The accuracy of quantitative estimates of myocardial blood flow with PET and ^{13}N-ammonia has been evaluated by several investigators in both open-chest and conscious animals over a wide range of flow conditions induced by coronary stenosis and pharmacological vasodilation.[19,74,138] In general, the best results are obtained when data are corrected for both finite resolution effects and for the presence of labeled metabolites (Figure 2-3). Without these corrections, the correlation with microspheres deteriorates with systematic underestimation of flow and larger random variability. The correlation with microspheres is poorer in the septum than in any other regions, presumably because of spillover from the right ventricle. In myocardium made necrotic by permanent coronary occlusion, good agreement between PET and microspheres flow estimates has also been reported (Figure 2-4). Thus, the dependence of ^{13}N-ammonia extraction on cell integrity suggested by Rauch et al.[164] does not seem to affect significantly myocardial blood flow estimates with ^{13}N-ammonia. Accordingly, ^{13}N-ammonia is used extensively in humans for both qualitative and quantitative imaging of myocardial perfusion. As mentioned earlier, it usually provides images of good quality (except in patients with lung diseases), allowing for the assessment of myocardial blood flow in both relative and absolute terms.

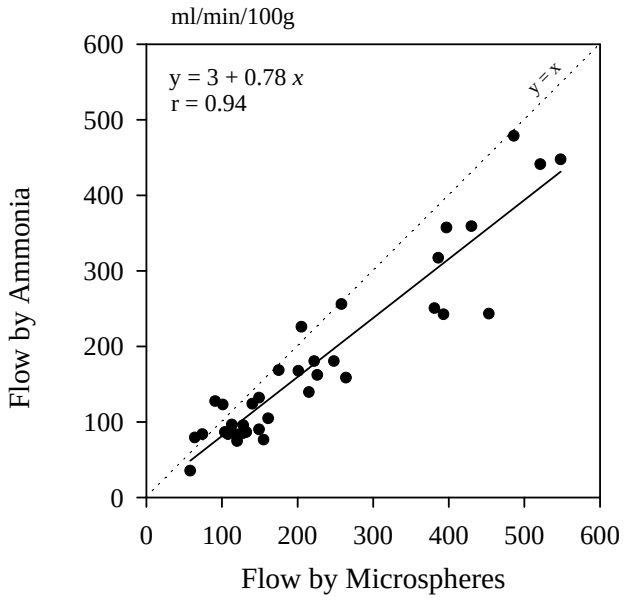

Figure 2-3. Scatterplot showing the correlation between myocardial blood flow estimated by ^{13}N-ammonia and PET and that obtained with microspheres over a wide range of flow conditions in dogs. PET data were corrected for finite resolution effects and for the accumulation of ^{13}N-labeled metabolites in the arterial blood. Adapted from Ref. 19.

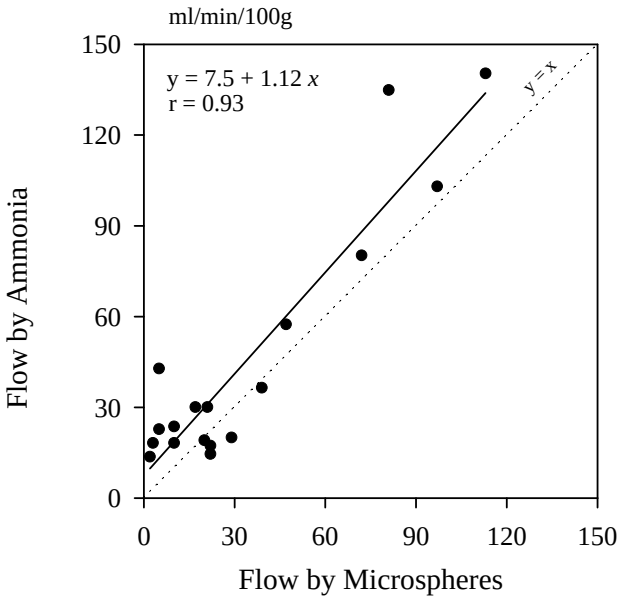

Figure 2-4. Scatterplot showing the correlation between myocardial blood flow estimated by ^{13}N-ammonia and PET and that obtained with microspheres in 22 infarcted regions in dogs. Adapted from Ref. 1

In normal subjects, the uptake of ^{13}N-ammonia is usually homogenous throughout the left ventricle, although slightly lower levels of tracer uptake may be noted in the lateral free wall. Absolute levels of myocardial blood flow estimated with the 3-compartment model average 88 ± 22 ml.(min.100g)$^{-1}$ at rest and increase linearly with increases in cardiac work. With adenosine or dipyridamole, flow rates usually increase markedly, up to 3 to 4-fold.[47,100]

2.2.3 Quantification of Myocardial Perfusion with ^{15}O-water.

In contrast to ^{13}N-ammonia, ^{15}O-water is relatively freely diffusible across capillary and

cellular membranes. Its first pass extraction fraction is close to unity and thus insensitive to flow changes. In theory, the advantage of using freely diffusible tracers is that their kinetics of accumulation and clearance from myocardium is far less complex than those of partially extractable tracers. Bergmann et al. demonstrated that the limitations to free diffusibility of water were modest, constant, and not altered by flow.[15] Thus, ^{15}O-water can be considered as freely diffusible in the heart. Regional uptake of ^{15}O-water was found to correlate closely with regional uptake of microspheres.[15] In most centers, 15O-water is directly cyclotron-produced and administered as an intravenous bolus.[15,16,19] Alternatively, it can be produced from the inhalation of ^{15}O-carbon dioxide (which is converted to ^{15}O-water by lung and blood carbonic anhydrase), which requires more prolonged infusion protocols.[4,101] The fact that ^{15}O resides in blood as well as in myocardium necessitates the use of a separate scan (like ^{15}O-carbon monoxide) to label the blood pool to visualize the myocardium.

Assessment of myocardial perfusion in absolute terms is performed with a modification of equations derived by Kety to encompass correction for finite resolution effects.[15,19,92,110] As with ^{13}N-ammonia, dynamic imaging is required to measure the time-activity curves in arterial blood and in myocardium. Several assumptions underlie the use of the single-compartment Kety model for quantification of myocardial perfusion with ^{15}O-water including [109-111] : 1- that the uptake of tracer is flow dependent and not diffusion limited, 2- that no arteriovenous shunts or bypasses are present, 3- that the solubility of the tracer is constant, and 4- that the flow is constant and more importantly homogenous throughout the region interrogated during the imaging interval. As mentioned above, limitations to free diffusibility are modest, constant and not affected by flow. Significant shunts or bypasses are probably not present in the heart. However, the assumption that flow is uniform is probably not valid in patients with coronary artery disease and a previous myocardial infarction.

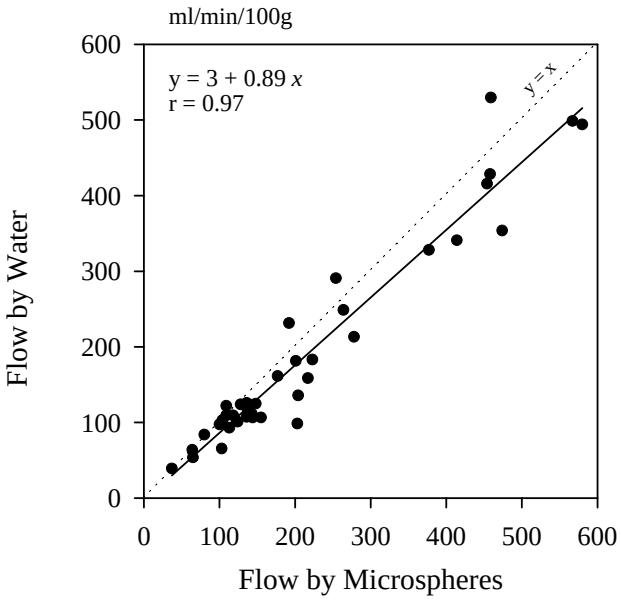

Figure 2-5. Scatterplot showing the correlation between myocardial blood flow estimated by ^{15}O-water and PET and that obtained with microspheres over a wide range of flow conditions in dogs. PET data were corrected for finite resolution effects before the fitting procedure. Adapted from Ref. 19.

The accuracy of quantitative estimates of myocardial blood flow with PET and ^{15}O-water has also been evaluated by several investigators in both open-chest and conscious animals over a wide range of flow conditions induced by coronary stenosis and pharmacological vasodilation.[15,19,138] Tripp et al.[202] demonstrated a close correlation between measurements of myocardial blood flow obtained with tritiated water and microspheres. In several studies, good correlations were also observed between estimates of myocardial blood flow derived from ^{15}O-water (injected as a bolus) and PET and those measured with microspheres (Figure 2-5). Similar correlations were also reported with the inhalation approach, although the accuracy at hyperemic flows was less than with bolus injections.

In myocardium made necrotic by permanent coronary occlusion, the degree of agreement between PET and microspheres flow estimates is reportedly poor (Figure 2-6). Although it was originally proposed that overestimation of flow by ^{15}O-water and PET in infarcted tissue was

due to partial resolution effects and poor count statistics,[15] this explanation is unlikely as these factors should equally affect flow estimates with other tracers, such as ^{13}N-ammonia.[19] Therefore, these inaccuracies must either reflect intrinsic kinetic characteristics of ^{15}O-water or be related to problems in model parameters estimation. Based on results obtained in patients with a previous myocardial infarction, Iida et al. have recently proposed that the ^{15}O-water method estimates flow per unit of mass of perfusable tissue excluding scar tissue, as opposed to the conventional microspheres technique which would also include the nonperfusable space.[52,102,231] Although attractive, this explanation implies that, somehow, the diffusibility of water into scar tissue is restricted, a possibility that has been recently ruled out by Herrero et al. who performed direct measurements of ^{15}O-water content in chronically infarcted canine myocardium.94 These authors proposed that overestimation of infarcted blood flow by 15O-water resulted from errors in parameters estimation in the presence of heterogeneous blood flow.[94]

In normal subjects, the myocardial uptake and clearance of ^{15}O-water are homogenous throughout the left ventricle. Estimated levels of absolute myocardial blood flow are usually slightly higher than those measured with ^{13}N-ammonia and average 95 ± 17 ml.(min.100g)$^{-1}$. Lower values are measured in the septum, probably because of spillover from the right ventricle. As with ^{13}N-ammonia, estimated flow rates increase in proportion to cardiac work. Due to its short half-life, ^{15}O-water is well suited for the assessment of myocardial perfusion reserve. With adenosine or dipyridamole, flow rates usually increase 3-5 fold.[204]

2.3 Quantification of Regional Myocardial Oxidative Metabolism with Positron Emission Tomography

2.3.1 General Considerations

Myocardial oxygen consumption (MVO_2) is often used to measure cardiac energy utilization because as much as 90 to 95% of adenosine

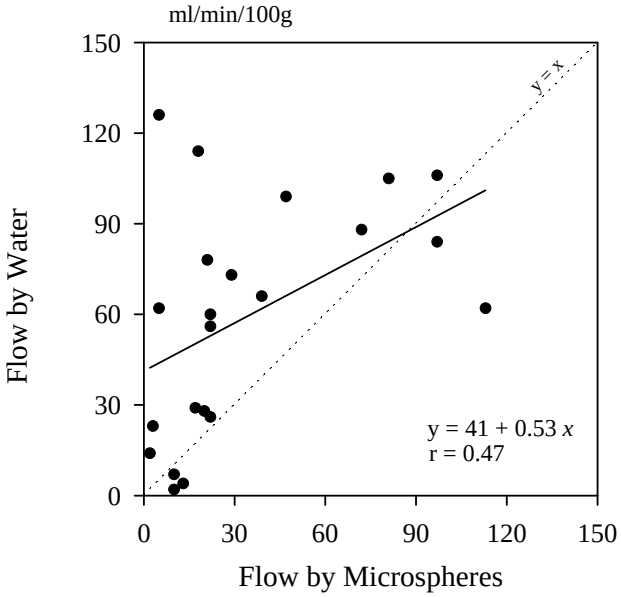

Figure 2-6. Scatterplot showing the correlation between myocardial blood flow estimated by ^{15}O-water and PET and that obtained with microspheres in 22 infarcted regions. Adapted from Ref. 19.

triphosphate in the heart is produced by aerobic metabolism, via oxidative phosphorylation in the mitochondria.[135] Measurement of regional MVO2 is needed for investigations designed to define the relative efficacy of therapeutic interventions implemented to reduce myocardial oxygen requirements, increase supply, or both. It is also needed to identify pathophysiologic factors in conditions such as cardiomyopathies or chronic ischemic heart disease. Cardiac derangements of clinical significance are indeed often attributable to impaired oxidative metabolism leading ultimately to contractile dysfunction and pump failure. Their detection has been greatly facilitated by advances in cardiac PET. Although cardiac PET can interrogate specific metabolic pathways, quantification of overall oxidative metabolism has been elusive because of varying contributions of the various substrates to overall energy utilization under physiologic conditions.[39,141,162,194] This dilemma reflects the capacity of the heart to utilize a wide variety of substrates for energy production, including fatty acids, glucose, lactate, pyruvate, ketone bodies and amino acids. The particular pattern of

substrate utilization depends on the concentrations of substrates in arterial blood, myocardial perfusion and oxidative capacity, and the neurohumoral milieu.39 Under aerobic conditions, fatty acids are usually the preferred metabolic substrate for oxidative energy production. With ischemia, fatty acid oxidation decreases, and glucose utilization predominates.[127,139] With reperfusion, oxidative fatty acids utilization is again predominant.[166] Therefore, estimation of overall oxidative rates based only on the utilization pattern of individual substrates is nearly impossible.

2.3.2 Assessment of Myocardial Oxidative Metabolism with ^{11}C-palmitate

Because fatty acids are the preferred substrate for oxidation under aerobic conditions, PET and ^{11}C-palmitate have been proposed for quantification of myocardial oxidative metabolism.[177,178,180,181] Generally speaking, before a tracer like ^{11}C-palmitate can be used for the measurement of oxidative metabolism, 2 basic assumptions must be fulfilled: 1- the utilization pattern of the tracer must accurately reflect the turnover rates of the tricarboxylic acid (TCA) cycle, 2- the externally detectable kinetics of the radiotracer must faithfully reflect its metabolism. Unfortunately, in the case of ^{11}C-palmitate, neither of these assumptions appears to be valid.

Although it is generally accepted that fatty acids are the preferred metabolic fuel for the heart, it is also known that the heart can oxidize a wide variety of other fuels, including glucose, lactate, pyruvate and ketone bodies [39,141,162,194,230] and adjust their relative contributions to oxidative metabolism according to their plasma concentrations. Therefore, estimation of overall oxidative rates based only on the utilization pattern of palmitate is elusive. In addition, the myocardial ^{11}C clearance curves, which are used to assess palmitate oxidation, do not only reflect the oxidation of the labeled compound but also the complexity of the metabolic pathways involved in long-chain fatty acid metabolism, from initial uptake and activation to acetyl-CoA to incorporation as triglycerides into the endogenous lipid pool, or to mitochondrial transport via the carnitine shuttle and shunting into ß-oxidation and TCA cycle.

After intravenous or intracoronary administration of ^{11}C-palmitate, the tracer initially accumulates in the myocardium in proportion to blood flow.[180] Thereafter, it clears biexponentially from normal myocardium. The late slow clearance phase is thought to reflect incorporation and release of the tracer from the intracellular lipid pool, while the early rapid phase has been associated with its oxidation.[177,180] Unfortunately, factors other than cellular uptake and metabolism also influence the myocardial kinetics of the tracer. In addition to delivery by myocardial perfusion, backdiffusion of labeled molecules,[58,67,209,227] washout of both non-metabolized tracer and labeled metabolites, and multiple fates of isotope contribute to the complex kinetics of this tracer.

2.3.3 Assessment of Myocardial Oxidative Metabolism with ^{11}C-acetate

There has been growing interest in acetate as a tracer of myocardial oxidative metabolism because of the relative simplicity of its oxidation pathway. Indeed, after initial uptake, acetate is rapidly activated into acetyl-CoA by means of the acetyl-CoA synthase. In myocardial cells, this activation primarily takes place in the mitochondrial matrix, where acetyl-CoA becomes immediately available for shunting into the TCA cycle. Even though acetate is readily oxidized by myocardium, the concentration of acetate in plasma is so low under physiologic conditions (30 to 400 µM) that its oxidation contributes negligibly to overall production of ATP in the heart. In the rat heart, under steady-state conditions, myocardial oxygen consumption of acetate is less than 90 nmol.(min.g)$^{-1}$. Several experimental studies have demonstrated that the TCA cycle could be traced accurately with either ^{14}C- or ^{11}C-acetate and that the flux through the cycle correlated closely with MVO_2.[28,33] Although variations in the pattern of substrate utilization can alter the

ratio of TCA cycle flux to oxygen consumption, the magnitude of these changes is usually small. For example, if the heart used exclusively glucose, lactate or palmitate as sole substrate for oxidative metabolism, it would consume 3.0, 3.0, and 2.9 moles of oxygen per mole of acetyl CoA consumed, respectively. Thus, if oxidative metabolism shifted from exclusive oxidation of palmitate to exclusive oxidation of glucose, the maximal error in the estimate of MVO_2 based on the assessment of TCA cycle flux would be 4%.

Theoretically, the rate of oxidation of radiolabeled acetate should not be affected by a change in the particular substrate that serves as a precursor to acetyl CoA as long as the size of the precursor pool is small compared with that of glutamate, the main form in which the label is trapped, and as long as the pool size of glutamate remains constant. As judged from results of numerous studies, these assumptions appear valid. Acetyl-CoA can also be incorporated into fatty acid by de novo synthesis or chain elongation. However, in normoxic hearts, the rate of such incorporation is less than 1% of the TCA cycle flux.[162] Even though this rate can increase up to 12-fold with hypoxia [85] and ischemia, the fraction of acetyl-CoA incorporated into lipids remains small compared with the total intracellular pool of acetyl-CoA. Acetate can also be incorporated into amino acids and ketone bodies.[28] However, the magnitude of acetate flux through these synthetic pathways is so modest under diverse conditions, including ischemia, that the use of radiolabeled acetate for estimation of MVO_2 is unlikely to be compromised.

In the isolated rabbit heart, the steady-state extraction fraction of acetate averages 62%. Oxidation of radiolabeled acetate, assessed from the rate of efflux of radiolabeled CO_2 in venous effluents, was found to correlate closely with MVO_2 under conditions of normoxia, ischemia, hypoxia and reperfusion.28,33 Under conditions of ischemia, more than 80% of the efflux of label is attributable to labeled CO_2 despite a slight increase in the production of non-CO_2 labeled metabolites.[28] Also, with ischemia, modest backdiffusion of labeled acetate occurs.[28]

In dogs, the steady-state extraction of unlabeled acetate averages 33%. The unidirectional extraction fraction of labeled acetate is even greater (47 - 70%).[6] Experiments using simultaneous intracoronary injection of 14C- and ^{11}C-acetate have demonstrated that clearance of radioactivity from the myocardium after injection of labeled acetate occurs almost exclusively in form of labeled CO_2 and that external measurements of ^{11}C myocardial clearance kinetics closely parallel the removal of ^{14}CO2 from the coronary sinus effluent.[29,34] Studies with PET have revealed that ^{11}C radioactivity is cleared in a biexponential fashion from the myocardium and that the rate constants k_1 and k_{mono} of the early rapid clearance closely correlate with MVO_2 over a wide range of physiologic conditions. The clearance kinetics was shown to be largely insensitive to changes in myocardial substrate availability[30] and to be independent of myocardial blood flow.[6] Finally, the relationship between k_1, k_{mono}, and MVO_2 was found to be unaffected by ischemia, reperfusion or both.[6]

After intravenous administration of ^{11}C-acetate in humans, extraction of the tracer by the myocardium is usually avid and clearance from the blood is rapid. Accordingly, images of the myocardium are of high quality. In most subjects, clearance from the myocardium is mono-exponential at rest [5,90,212] (at least with short imaging protocols)[5] but becomes biexponential at higher myocardial workloads (Figure 2-7).[90,212] In normal subjects, the clearance of radioactivity is homogenous throughout the left ventricular myocardium and averages 0.054 ± 0.008 min^{-1}, corresponding to a biological half-life of approximately 13 minutes.[212] Use of the relationship between kmono and MVO_2 established in canine hearts enables to calculate an MVO_2 of 189 ± 33 µmol.(min.100g)$^{-1}$, a value close to that previously obtained directly with invasive procedures.

Several investigators have reported that the myocardial clearance kinetics of ^{11}C-acetate correlated closely with the rate-pressure product,[90,121,212] a rough estimate of the global cardiac energy demand, and with PET estimates of MVO_2, obtained by use of ^{15}O-labeled molecular oxygen, over a wide range of levels of work and oxygen consumption.[18] The correlation with rate-pressure product is even better when time-activity curves are fitted to a 2-compartment model to account for possible recirculation of labeled acetate during the scanning period.[32] These characteristics lend considerable support to the use of ^{11}C-acetate and PET for the accurate noninvasive assessment of myocardial oxidative metabolism in vivo.

2.4 Quantification of Regional Myocardial Glucose Uptake with Positron Emission Tomography

Assessment of exogenous myocardial glucose utilization in vivo with PET can be achieved by use of the glucose analog 2-deoxy-2-18F-D-glucose (FDG). FDG competes with glucose for facilitated transport sites and also for phosphorylation by hexokinase to yield FDG-6-phosphate. However, FDG-6-*P* is not a significant substrate for either glycogen synthase, phosphoglucose isomerase, glucose-6-phosphate dehydrogenase or phosphoglucomutase. In addition, dephosphorylation back to free FDG occurs slowly in heart and the phosphorylated compound has a low membrane permeability. Therefore, the FDG-6-*P* is effectively trapped in the tissue as the end product of the phosphorylation reaction. These properties permit imaging of myocardium in vivo using PET and the application of a tracer kinetic model to calculate the rate of exogenous glucose uptake.

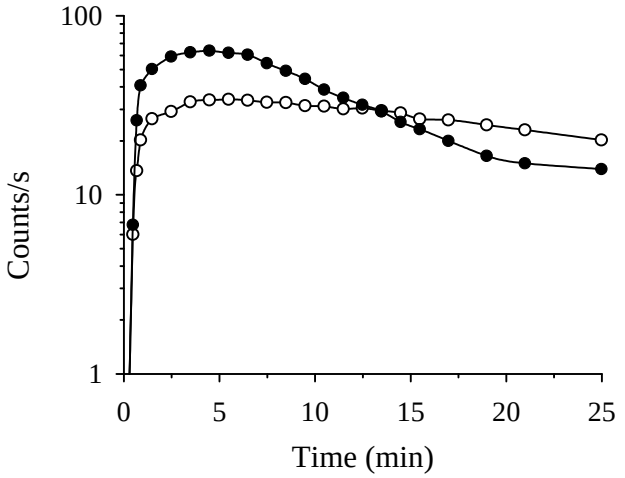

Figure 2-7. Plot of myocardial time-activity curves obtained at rest (open circles) and during infusion of dobutamine (closed circles). Myocardial activity was determined from a large volume of interest encompassing septal, anterior and lateral left ventricular myocardium. Note that myocardial ^{11}C clearance is monoexponential at rest and becomes biexponential during infusion of dobutamine. Adapted from Ref. 212.

The mathematical tracer kinetic model that is used was first developed by Sokoloff et al.[191] for autoradiographic studies of brain using the glucose analog 2-^{14}C-deoxyglucose. This model was further extended by Phelps et al.[154] to include possible hydrolysis of FDG-6-*P* to FDG. It consists of the 3 compartments shown in Figure 2-8: a vascular compartment for both FDG and glucose denoted by P; an extravascular or tissue compartment for FDG and glucose, which includes the interstitial and cellular spaces, denoted by E; and a compartment within the cell for the FDG-6-*P* and glucose-6-*P* denoted by M. The forward and reverse transport rate constants between compartments P and E, which include transport from the vascular space to the interstitial space as well as transport across the plasma membrane of the myocytes, are k_1 and k_2 for glucose. The rate constants between compartments E and M, denoting the phosphorylation and dephosphorylation reactions, are k_3 and k_4. The respective *k's* for FDG and FDG-6-*P* are denoted with an asterisk. The application of this model permits the estimation of the rate constants for FDG forward and reverse transport between plasma and tissue, phosphorylation of FDG and dephosphorylation of FDG-6-*P*. The myocardial metabolic rate of exogenous glucose utilization can be calculated using these derived rate constants and a lumped

constant. The lumped constant is a term based on the principles of competitive substrate kinetics that corrects for the differences in transport and phosphorylation between FDG and glucose. This lumped constant is used to transform measured values of FDG metabolism to corresponding metabolic rates of exogenous glucose utilization. It is made up the following six constants: the maximum velocities (V_{max} and V_{max}*) and Michaelis-Menten constants (K_m and K_m*) for the hexokinase reaction for glucose and FDG, respectively; λ, which is the ratio of distribution volumes (i.e., tissue to plasma concentrations ratios) of FDG and glucose; and ϕ, which is the fraction of phosphorylated glucose that is metabolized. The FDG model has been validated in the isolated, arterially perfused rabbit septum and in isolated working rat hearts, with the estimated utilization rates for exogenous glucose correlating well with those derived by the Fick method or from detritiation of tritiated glucose, over a wide range of perfusion, workload and metabolic conditions.[119]

Application of this model to FDG PET data is complicated by the slow convergence in fitting for the different rate constants of the FDG model, due to noise levels typically encountered in dynamic in vivo studies. A simplified method, using the Patlak graphic analysis, has therefore been proposed to avoid these problems.71 This technique, usable for general models in which the tracer is irreversibly trapped in a system, was first proposed and described by Patlak et al.[152] and can be applied to dynamic FDG studies if one assumes the dephosphorylation constant *k4** to be equal to 0. The following equation constitutes the basics of the Patlak analysis:

$$\text{Am(t)/Cp(t)} = [(K_1 \times k_3)/(k_2 + k_3)] / \int_0^t Cp(t)Cp(s)ds + W,$$

where Am(t) is the myocardial tissue 18F activity at time t, Cp(t) is the plasma activity at time t and W is a function of the steady state volume of the reversible compartments and the effective plasma volume. The plot of

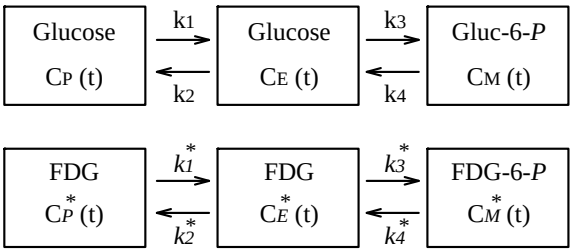

Figure 2-8. Compartment model used to describe the kinetics of glucose and FDG in myocardium. The left compartments represent the vascular space for glucose and FDG; the middle compartments represent tissue or extravascular (interstitial and intracellular) space for glucose and FDG; the right compartments represent the cellular space for glucose-6-P and for FDG-6-P. Glucose and glucose-6-P concentrations in the 3 compartments is denoted as C_P, C_E and C_M, respectively. The corresponding FDG and FDG-6-P concentrations are denoted with an asterisk.

Am(t)/Cp(t) versus $\int_0^t Cp(s)ds/Cp(t)$ has been shown to be linear at late times with a slope equal to $K = (K_1 \times k_3)/(k_2 + k_3)$ and a Y intercept equal to W, that is $K_1k_2/(k_2+k_3)$. The Y intercept represents a kinetic volume and has no particular physical meaning. The graphic approach allows for an estimation of glucose uptake by simply giving an estimate of K from the slope of the linear regression of the plot. Regional myocardial glucose uptake is then calculated as rMGU = (Cp/LC) x K, where Cp is the plasma concentration of glucose, K is the slope of the graphic analysis and LC is the lumped constant that accounts for differences in the transport and phosphorylation of FDG and glucose. In humans, the lumped constant is generally assumed to be 0.665. From these data and from the measured levels of absolute myocardial blood flow (which can be obtained with 13N-ammonia and PET for instance), one can calculate backward the extraction of glucose from the arterial blood as the ratio of regional myocardial glucose uptake to regional myocardial blood flow.[193] Normalized glucose extraction can also be calculated as the ratio of absolute glucose extraction in the risk region to that in the remote region (Table 2-1).

There are potential limitations to the use of FDG and PET for assessment of exogenous glucose uptake, particularly in the setting of ischemic heart disease. The basic assumption underlying the use of FDG and PET for assessing myocardial glucose uptake is that the lumped constant, which relates the steady-state uptake and phosphorylation rates of FDG to those of glucose, is insensitive to changes in dietary state and hormonal conditions, and is not affected by ischemia, reperfusion or both. As glucose analogs are favored over glucose in most membrane transport systems, while at the same time, glucose is favored over its analogs by most plant and mammalian hexokinases, the value of the lumped constant is unlikely to remain constant under all conditions. Switch from one type of glucose transporter to another, such as occurs with insulin stimulation or ischemia, is thus likely to affect the lumped constant and consequently the reliability of the metabolic information derived from FDG studies. In fact, significant changes in the value of the lumped constant with insulin [142,170] and ischemia [119] have been reported in isolated heart preparations.

In humans, estimation of regional myocardial glucose utilization can be obtained under various physiologic, metabolic and pathophysiologic conditions. Under fasting conditions, myocardial glucose utilization is usually low, as it is inhibited by the high circulating free fatty acid levels.[97,163] Fasting also results in significant regional heterogeneity in FDG retention, the uptake of the tracer in the septum and anterior wall being only 80% of that in the lateral and posterior walls.[78,97] In patients, most FDG studies are performed under glucose loading, either oral or intravenous, or during hyperinsulinemic euglycemic clamp.[49,114] This is mainly aimed at standardizing the dietary state and at maximizing glucose uptake by normal myocardium (usually 2 to 3 times) while minimizing regional heterogeneity in FDG uptake.

We have recently studied 6 normal male volunteers aged 21 to 28 years during a hyperinsulinemic euglycemic glucose clamp.

TABLE 2-1. Definitions relevant to PET FDG metabolism

Metabolic concept	Proposed definition
FDG uptake	Apparent overall 18F activity in a given segment of the myocardium; always expressed in % of maximal activity at the same imaging level.
Mismatch pattern	Discordant reduction of overall levels of ^{18}F and ^{13}N in a given myocardial segment
Match pattern	Concordant reduction of overall levels of ^{18}F and ^{13}N in a given myocardial segment
Glucose uptake148	Absolute quantity of glucose taken up by the myocardium per unit of time; requires dynamic FDG imaging; expressed as $\mu mol.(min.100g)^{-1}$.
Normalized glucose uptake	Ratio of the absolute glucose uptake in the risk region to that in a remote normal region; expressed as % of remote.
Glucose extraction148,193	Arterio-venous difference of glucose across the myocardium. Calculated backward from uptake data and flow; expressed as $\mu mol.ml^{-1}$.
Normalized glucose extraction	Ratio of the absolute glucose extraction in the risk region to that in a remote normal region; expressed as % of remote.

During the clamp, blood insulin levels increased significantly (from 12 ± 4 µU/ml at baseline to 85 ± 14 µU/ml the end of the procedure, $p<0.001$), plasma glucose levels remained unchanged (from 92 ± 5 mg/dl to 87 ± 10 mg/dl, p=ns) and the arterial concentration of fatty acid decreased (from 532 ± 205 µM to 132 ± 91 µM, $p<0.001$). At the same time, regional myocardial glucose uptake increased from 24 ± 9 (ranging from 15 to 33) to 53 ± 11 (ranging from 40 to 76) $\mu mol.(min.100g)^{-1}$, and was similar among the different myocardial regions. Myocardial blood flow and oxidative metabolism were unaffected. Similar results can be obtained by use of drugs that acutely reduce circulating free fatty acid levels, such as acipimox or nicotinic acid.[115] Nonetheless, of all these methods, the hyperinsulinemic euglycemic clamp technique

gives the best results and is the only one applicable to patients with insulin-dependent diabetes mellitus.[220] It is noteworthy that, with hyperinsulinemic euglycemic clamp, changing free fatty acid levels does not alter regional FDG uptake. This suggests that the effects of insulin on myocardial glucose uptake are largely independent of its effects on circulating free fatty acids. The lack of apparent changes in glucose utilization by the heart implies that a change in the metabolic fate of exogenous glucose occurs, likely in the form of rerouting towards glycogen synthesis such as shown in the isolated heart.[216]

2.5 Summary

PET is a sophisticated technique that permits assessment and quantification of regional metabolic and physiologic processes directly in vivo by means of the availability of biologically active positron-emitting radiopharmaceuticals. When mathematically and physiologically appropriate models are used to describe the biological behavior of the administered radiotracers in blood and myocardium, it becomes possible to obtain quantitative measures of the processes in which these tracers are involved. In contrast to most single-photon emitters, many positron-emitting radionuclides are unique because their naturally occurring counterparts (hydrogen, carbon, nitrogen and oxygen) are predominant constituents of biological compounds. Positron-emitting isotopes of fluorine, carbon, nitrogen, and oxygen may replace their stable counterparts in the synthesis of metabolic substrates, receptors ligands, drugs, and other biologically active compounds without disrupting biochemical properties or activity.

Thanks to these unique features, it is now not only possible but also practical to interrogate with PET a specific region of the heart muscle, with a specific positron-emitting radioisotope, and to obtain noninvasively quantitative information regarding absolute levels of tissue perfusion, oxygen consumption or exogenous glucose uptake and phosphorylation. This information is crucial not only to elucidate the pathophysiologic factors underlying reversible left ventricular ischemic dysfunction in humans, but also to design better and perhaps more appropriate diagnostic and therapeutic strategies.

Chapter 3 Myocardial Blood Flow and Metabolism in Patients with Left Ventricular Ischemic Dysfunction

3.1 Introduction

With the advent of recanalization therapy to salvage ischemically jeopardized myocardium in humans, delineation of dysfunctional but potentially reversible (so-called "viable") from irreversibly damaged and thus "nonviable" myocardium has gained increasing importance in the management and risk stratification of patients with ischemic heart disease. Although assessment of tissue viability after an acute ischemic episode has long relied on the simple examination of regional wall motion, evidence has accumulated that regional wall motion can remain impaired for a prolonged period of time after an ischemic insult, even in reversibly injured tissue.[25,26] Two associated phenomena have been described, which have come to be known as myocardial stunning [20,21,25,113,128] and myocardial hibernation.[26,113,128,161] As discussed in chapter 1, stunning is a reversible form of contractile dysfunction that occurs after restoration of flow following a relatively brief period of coronary occlusion, while hibernation is a postulated condition of chronic sustained abnormal contraction due to chronic underperfusion in patients, whereby the heart spontaneously downgrades its myocardial function and, as a result, no myocardial necrosis ensues.

While the existence of these altered myocardial states was receiving increasing recognition among basic and clinical cardiologists, ways to identify them in the clinical setting became one of the most active areas of research in the field of ischemic heart diseases. Because regional contractile ischemic dysfunction reflects underlying alterations of myocardial perfusion and metabolism, flow and metabolic imaging with PET has focused much attention. Results of studies in patients with left ventricular dysfunction due to chronic coronary artery disease have indicated that PET with ^{18}F-deoxyglucose could accurately identify viable myocardium, by showing an increased FDG uptake relative to blood flow (so-called flow-metabolism mismatch), while a concordant depression of flow and FDG uptake (flow-metabolism match) was usually found in necrotic segments.[196,200] Theoretically, an appealing alternate way to identify reversible injury would be to assess residual myocardial oxidative metabolism, as the energy required for contraction can only be provided by aerobic metabolism. Studies in both experimental animals [225] and in humans [79-81] have recently shown that maintenance of oxidative metabolism in dysfunctional myocardium portended its functional recovery after revascularization. The noninvasive determination of myocardial oxygen consumption might thus prove useful to assess the potential for recovery of the postischemic dysfunction.

There are situations, however, where flow and metabolic imaging with PET lacks accuracy. In patients with myocardial infarction, estimates of glucose uptake by PET was shown to overestimate the capacity for recovery of function after revascularization.156,183 Similarly, assessment of oxidative metabolism with ^{11}C-acetate has been of limited value shortly after infarction because of the time-dependence of the return of mitochondrial function after ischemia,[91,195] and because of the non-transmural character of injury. Obviously, an improved understanding of the flow, metabolic, and structural correlates of the conditions of myocardial infarction, stunning and hibernation is needed to elucidate underlying pathophysiologic factors and to design better and perhaps more specific diagnostic strategies. This chapter will review some of the insights into the mechanisms of left ventricular ischemic dysfunction gained from the study of myocardial blood flow and

metabolism with PET in carefully selected patients with chronic coronary artery disease. In this chapter, I will focus successively on the flow, metabolic and structural correlates of:

1- reperfused Q-wave myocardial infarction,[210]
2- isolated myocardial stunning[229] and
3- chronic myocardial hibernation.[211]

The clinical implications of the findings of these studies for the delineation of myocardial viability will be the focus of the next chapter.

The PET methodology is common to all studies. All acquisitions were performed with the ECAT III tomograph and the patients were studied after overnight fasting. However, to standardize the dietary state and to maximize the exogenous glucose uptake by normal myocardium, all patients received a continuous intravenous infusion of a 10% dextrose in water solution, at a rate of 15 μmol.(kg.min)$^{-1}$. The stability of the plasma glucose levels during the 4 hours PET study and glucose infusion was checked in 10 patients, none of whom showed more than 15% variation of their plasma glucose levels during the infusion. Myocardial perfusion was assessed with ^{13}N-ammonia, myocardial oxidative metabolism with ^{11}C-acetate and exogenous glucose uptake with ^{18}F-deoxyglucose. All tracers were injected intravenously, by means of a calibrated infusion pump. After collection of the attenuation data, 15 mCi of ^{13}N-ammonia was injected over 20 seconds. Beginning with tracer injection, 28 serial cross-sectional images were acquired in a decay compensated mode for 10 minutes. After a 50 minute interval for decay of ^{13}N radioactivity to baseline levels, 15 mCi of ^{11}C-acetate was injected over 20 seconds, and, beginning with tracer injection, 25 serial cross-sectional images were acquired for 25 minutes. After an additional interval of 60 minutes for decay of ^{11}C radioactivity to baseline, 15 mCi of FDG was infused over 60 seconds, followed by the acquisition of 34 serial cross-sectional images for 45 minutes.

One midventricular transaxial tomographic slice was analyzed for dynamic studies per patient. Ten regions of interest (9 in myocardium and 1 in blood pool) were drawn on each PET image. ^{13}N-ammonia and ^{18}F-FDG cross-sectional images were analyzed with an operator-interactive computer program using circumferential profiles. The program normalizes ^{18}F and ^{13}N counts within a given myocardial cross-section to maximal activity in the same ventricular slice. Each cross section of the left ventricle is then divided into serial 30° segments. The activity within each segment was expressed in relative terms (reported as relative ^{18}F and ^{13}N uptake) as percent of maximal activity normalized to peak ^{13}N-ammonia segmental activity at the same level. A pattern of flow-metabolism "mismatch" was considered to be present when the segmental FDG/ammonia activity ratio exceeded 1.2, according to data obtained in normal volunteers (with a FDG/ammonia ranging from 1.02 to 1.12).[210] Regions of interest in tomograms obtained after administration of ^{13}N-ammonia were subdivided to encompass regions of interest in remote and risk tissue. In patients with left anterior descending coronary artery disease, remote (normal) regions were identified as the 4 segments from the lateral free wall and the basal septum. Risk regions were identified as the 3 segments from the anterior wall. In patients with previous anterior infarction, regions of interest in tomograms were also subdivided to encompass remote, adjacent and infarcted tissue. Remote (normal) regions were identified as those with normal perfusion (>80% of maximal activity in the same slice). Infarct-related regions were identified as anterior or septal regions with <80% of maximal ^{13}N-ammonia activity in the same slice. The regions of interest located in the center of the zone of hypoperfusion were defined as central infarct. Adjacent regions were delineated as those located at the borders of the infarct zone (on both sides).

The quantitation of tomographic data was performed as described in Chapter 2. Regional myocardial perfusion was quantified by use of the ^{13}N-ammonia 3-compartment model. No correction for circulating metabolites was applied. The kinetics of ^{11}C-acetate were used to evaluate TCA cycle turnover. ^{11}C-acetate

clearance from the myocardium under resting conditions was always monoexponential. Finally, the Patlak graphic analysis was used to estimate absolute regional myocardial glucose uptake. Glucose extraction was calculated as the ratio of regional myocardial glucose uptake to regional myocardial blood flow. Normalized glucose extraction was calculated as the ratio of absolute glucose extraction in the risk region to that in the remote region.

3.2 Myocardial Blood Flow and Metabolism in Patients After Recovery from Reperfused Anterior Myocardial Infarction

Absolute levels of myocardial perfusion and metabolism were first investigated in patients with Q-wave anterior myocardial infarction and a patent infarct-related coronary artery to define the flow and metabolic patterns associated with irreversible injury. The patients were studied at an average of 42 days after myocardial infarction, at a time when residual dysfunction was unlikely to be related to residual myocardial stunning.

Methods

We studied 15 patients (13 men, mean age 56 ± 10 years, range 38 - 67 years) admitted to the coronary care unit for treatment of a first acute anterior myocardial infarction (MI). Upon admission, 13 patients received intravenous thrombolytic therapy and 2 were treated with intravenous heparin. Nine patients received streptokinase (500.000 IU) and 4 received recombinant human tissue-type plasminogen activator (100 mg). The interval from onset of chest pain to beginning of thrombolytic therapy was 207 ± 183 minutes. Peak serum creatine kinase activity averaged 2393 ± 1249 U/l (normal values 40 to 160 U/l). All patients subsequently developed anterior Q-waves on 12-leads surface EKGs. PET acquisitions were performed at an average of 42 days (range 13 - 90 days) after the acute event.

Coronary arteriography and contrast left ventriculography in the 30° right anterior oblique projection were performed in every patient at an average of 20 days after the acute event, and visually interpreted by two observers. In each patient, the infarct-related coronary artery, i.e. the left anterior descending coronary artery, was found to be patent, with a residual luminal diameter stenosis of 80 ± 11% (range 50 to 95%). Eight patients had single-vessel and 7 multivessel disease, including 6 with 2-vessel and 1 with 3-vessel coronary disease. None of the patients underwent angioplasty or bypass surgery before the PET study. The regional ventricular wall motion was reviewed by 2 experienced observers and defined in each of 5 segments (anterobasal, anterolateral, apical, inferior and posterobasal) as normal -0-, hypokinetic -1-, akinetic -2- or dyskinetic -3-. A dysfunctional wall motion score was calculated by summing the scores of the 3 anterior segments. Severe anterior dysfunction was observed in 14 patients: 7 patients had akinesis and 7 had dyskinesis. The remaining patient showed mild hypokinesis of the anterior wall. Mean global left ventricular ejection fraction was 52 ± 11% (range 29 to 70%) and mean wall motion score was 5.0 ± 1.3.

Results

Relative regional myocardial blood flow and glucose metabolism. PET revealed diminished perfusion in 71 anterior and/or septal segments, corresponding to the tomographic area of infarction in all 15 patients. Relative ^{13}N-ammonia uptake in these segments averaged 61 ± 13% of maximal activity. Segments with decreased blood flow showed 3 different patterns of FDG uptake: a parallel decrease of ^{13}N-ammonia and FDG uptake (flow-metabolism match), increased uptake of FDG relative to flow throughout the infarcted zone (central flow-metabolism mismatch) and a combination of concordant decrease of flow and FDG uptake in the center of the infarcted zone with increased FDG uptake relative to flow at the periphery of the infarcted zone (peripheral flow-metabolism mismatch). As indicated in Table 3-1, 8 patients showed concordant decrease of flow and metabolism in the infarcted area (FDG/flow ratio: 0.9 - 1.06), 2 patients had

TABLE 3-1. Individual Values of FDG-to-Ammonia Ratios in Hypoperfused Segments and Corresponding Ratios of Hypoperfused-to-Remote Absolute Flow and Glucose Utilization

Patients with flow-metabolism match	FDG-to-ammonia ratio in hypoperfused regions	No. of hypoperfused regions (*n*=38)	Hypoperfused-to-remote ratio of MBF	Hypoperfused-to-remote ratio of rMGU
P542	1.06	5	0.50	0.51
P568	1.01	4	0.75	0.82
P582	0.99	5	0.62	0.69
P601	0.95	4	*	0.84
P658	0.99	6	0.66	0.55
P668	0.90	5	0.51	0.25
P683	0.91	6	0.58	0.47
P699	0.99	5	0.56	0.62
Mean±SD	0.97 ± 0.05	4.8 ± 0.7	0.60 ± 0.09	0.59 ± 0.19
Patients with flow-metabolism mismatch	**FDG-to-ammonia ratio in mismatch regions**	**No. of mismatch regions (*n*=24)**	**Hypoperfused-to-remote ratio of MBF**	**Hypoperfused-to-remote ratio of rMGU**
P537	1.35	1	0.73	0.95
P602	1.25	3	0.80	1.06
P611	1.21	2	*	0.79
P622	1.79	3	0.52	1.22
P652	1.99	5	0.68	1.76
P669	1.64	5	0.63	1.13
P701	1.76	5	0.66	1.68
Mean±SD	1.57 ± 0.30	4.4 ± 1.6	0.67 ± 0.09	1.23 ± 0.36

FDG, ^{18}F-fluorodeoxyglucose; MBF, myocardial blood flow; rMGU, regional myocardial glucose uptake; *, not available.

peripheral flow-metabolism mismatch (FDG/flow ratio: 1.25 and 1.35) and 5 patients had central flow-metabolism mismatch (FDG/flow ratio: 1.21 - 1.99). The average values of the FDG/flow ratios were 1.57 ± 0.3 in patients with a mismatch pattern, and 0.97 ± 0.05 in patients with a match pattern. Relative ^{13}N-ammonia uptake averaged 60 ± 10% in infarcted segments with flow-metabolism mismatch and 61 ± 14% in infarcted segments without flow-metabolism mismatch (p=ns). In the same segments, relative FDG uptake was 108 ± 26% and 60 ± 15%, respectively. No difference in regional wall motion score was observed between patients with and without increased FDG uptake (5.1 ± 1.5 versus 4.9 ± 1.4, p=ns). Similarly, ejection fraction was not different in the 8 patients with concordant decrease of flow and metabolism versus the 7 patients with flow-metabolism mismatch (53 ± 10 versus 51 ± 13%, p=ns).

Acetate kinetics in reperfused anterior infarcted segments. Plate 3-1 illustrates the myocardial uptake and clearance of ^{11}C-acetate in a patient with anterior myocardial infarction and central flow-metabolism mismatch. The clearance of ^{11}C-acetate was reduced in the center of the infarcted region, compared to remote segments (0.027 ± 0.012 versus 0.055 ± 0.013 min^{-1}, p<0.001). Adjacent segments also showed reduced uptake and clearance of the tracer, albeit to a lesser extent than in the center of the infarcted area (0.041 ± 0.012 min^{-1}, p<0.001 versus central, p<0.001 versus remote). Comparing segments with and without flow-metabolism mismatch but with identical levels

TABLE 3-2. Relative Perfusion, Glucose Uptake, and Acetate Clearance in Normally Perfused and Hypoperfused Segments with and Without "Flow-Metabolism" Mismatch

Flow-metabolism pattern	*n*	Flow (%)	FDG (%)	k (min^{-1})
Normal flow/FDG	47	89 ± 6	89 ± 8	0.057 ± 0.015
↓ Flow ↑ FDG	24	66 ± 13 *	111 ± 26 *	0.041 ± 0.015 *
↓ Flow ↓ FDG	38	68 ± 7 *	68 ± 7 *	0.037 ± 0.014 *
↓↓ Flow ↓↓ FDG	9	39 ± 7 *†	38 ± 8 *†	0.017 ± 0.006 *†

FDG, ^{18}F-fluorodeoxyglucose; k, acetate clearance slope; %, percent of maximal activity within the same slice, normalized to peak ^{13}N-ammonia segmental activity at the same level.

*p<0.01 vs. normal flow/FDG.

†p <0.01 vs. ↓ flow ↑ FDG and vs. ↓ flow ↓ FDG.

of hypoperfusion (Table 3-2), no differences in ^{11}C-acetate clearance were found (0.041 ± 0.015 min^{-1} in mismatch segments versus 0.037 ± 0.014 min^{-1} in match segments). In segments with hypoperfusion (<80% of maximal activity) ranked according to different values of ^{11}C-acetate clearance (Table 3-3), the corresponding myocardial blood flow values were significantly different while absolute glucose uptake and relative FDG/ammonia ratios were not different.

Absolute myocardial blood flow and glucose metabolism. Estimation of regional myocardial blood flow was not possible in 2/15 patients because of inadequate left ventricular input function. In the remaining 13 patients, absolute transmural myocardial blood flow averaged 80 ± 16 ml.(min.100g)$^{-1}$ in remote segments, 67 ± 15 ml.(min.100g)$^{-1}$ in adjacent segments and 49 ± 11 ml.(min.100g)$^{-1}$ in segments located in the center of the infarcted area. Compared with segments without flow-metabolism mismatch, those segments exhibiting increased glucose uptake relative to flow had significantly higher residual myocardial blood flow: 54 ± 13 versus 45 ± 8 ml.(min.100g)$^{-1}$ (p<0.01). Similarly, residual oxidative metabolism was better preserved in segments with flow-metabolism mismatch (0.035 ± 0.014 min^{-1}) than in segments with concordant decrease of flow and metabolism (0.023 ± 0.009 min^{-1}, p<0.01). Individual metabolic rates for glucose utilization in remote, adjacent and central infarct regions are shown in Table 3-4. Both flow-metabolism patterns were associated with a wide range of absolute regional myocardial glucose uptake. Rates of utilization in remote myocardium were lower in patients with mismatch (25 ± 15 μmol.(min.100g)$^{-1}$) than in patients without mismatch (55 ± 20 μmol.(min.100g)$^{-1}$). Patients with mismatch had also higher plasma fatty acid levels. This could suggest that the presence of a match/mismatch pattern is partially dependent on the level substrate utilization in remote myocardium and thus on overall metabolic conditions, including fatty acid levels. As indicated in Table 3-1, the

TABLE 3-3. Myocardial Blood Flow, Glucose Utilization, and FDG-to-Ammonia Ratios in Hypoperfused Segments With Different Acetate Clearance Values

k categories	k (min^{-1})	MBF [ml.(min.100g)$^{-1}$]	rMGU [μmol.(min.100g)$^{-1}$]	FDG-to-ammonia ratio
< 0.020	0.015 ± 0.003	40 ± 6	19 ± 11	1.16 ± 0.48
0.020-0.030	0.026 ± 0.003	49 ± 7	29 ± 17	1.14 ± 0.34
0.030-0.040	0.034 ± 0.003	56 ± 11	30 ± 22	1.26 ± 0.50
0.040-0.050	0.047 ± 0.001	70 ± 8	32 ± 15	1.32 ± 0.51
> 0.050	0.069 ± 0.006	75 ± 7	41 ± 19	1.41 ± 0.41
p	<0.001	<0.001	NS	NS

p values are from one-way analysis of variance

FDG, ^{18}F-fluorodeoxyglucose; k, acetate clearance slope; MBF, myocardial blood flow; rMGU, regional myocardial glucose uptake.

TABLE 3-4. Individual Regional Myocardial Blood Flow, Glucose Utilization, and Acetate Clearance Among Remote (Normal Relative Perfusion), Adjacent, and Infarcted Segments (<80% of Relative Perfusion) in Patients With and Without Flow-Metabolism Mismatch.

	Remote regions			Adjacent regions			Central infarct					
	MBF	rMGU	k (min^{-1})	MBF	rMGU	k (min^{-1})	MBF	rMGU	k (min^{-1})	RPP	Glucose	FA
Flow-metabolism match												
P542	80±14	72±10	0.057±0.015	65±14	66±23	0.049±0.015	40±5	36±13	0.021±0.005	7,920	115	339
P568	72±6	74±6	0.044±0.006	67±2	63±5	0.040±0.004	54±2	62	0.030±0.004	6,930	114	390
P582	80±12	39±3	0.064±0.008	68±6	30±4	0.047	50±10	27±8	0.040±0.011	6,750	140	235
P601	*	31±3	0.053±0.007	*	26±2	0.042	*	30±2	0.041±0.002	5,520	94	234
P658	73±9	55±4	0.047±0.010	60±2	38±8	0.033±0.008	48±6	30±4	0.022±0.008	8,960	109	290
P668	87±10	60±10	0.064±0.008	82	44±3	0.045±0.002	44±10	15±5	0.020±0.008	10,250	81	530
P683	77±10	30±5	0.050±0.007	68±7	37±5	0.046	45±4	14±5	0.023±0.003	7,020	127	151
P699	95±14	81±4	0.061±0.005	86±16	50±16	0.051±0.016	53±3	64±20	0.028±0.002	7,580	164	382
Mean (SD)	80 (14)	55 (20)	0.055 (0.011)	71 (11)	44 (21)	0.043 (0.009)	47 (8)	34 (9)	0.027 (0.009)	7,635 (1,157)	118 (26)	319 (118)
Peripheral flow-metabolism mismatch												
P537	86±4	42±3	0.056±0.015	63±17	27±20	0.032±0.018	41±4	10±5	0.012±0.003	7,680	106	850
P602	56±6	17±6	0.038±0.002	45±4	14±2	0.032±0.002	43±12	16±1	0.024±0.002	6,100	88	539
Mean (SD)	69 (18)	28 (13)	0.045 (0.013)	54 (14)	21 (17)	0.032 (0.010)	42 (7)	14 (5)	0.017 (0.007)	6,890	97	695
Central flow-metabolism mismatch												
P611	*	48±6	0.077±0.011	*	38±3	0.060±0.002	*	35±3	0.055±0.004	8,640	103	756
P622	78±4	9	0.063±0.008	61	9±1	0.049±0.004	35±17	11±2	0.023±0.007	7,920	78	2,312
P652	81±7	13±2	0.051±0.007	41±4	22±14	0.043±0.014	55±8	23±2	0.037±0.007	8,100	83	560
P669	75±11	23±4	0.053±0.004	45±7	29±6	0.040±0.009	47±6	26±2	0.026±0.007	7,440	101	390
P701	111±16	22±5	0.082±0.004	90±14	31±6	0.061±0.010	73±9	37±5	0.056±0.009	9,800	150	302
Mean (SD)	87 (18)	25 (14)	0.069 (0.015)	74 (13)	26 (12)	0.052 (0.013)	53 (13)	24 (11)	0.036 (0.016)	8,340 (902)	103 (28)	864 (828)

FA (mM), fatty acids; k, acetate clearance slope; MBF [$ml.(min.100g)^{-1}$], myocardial blood flow; rMGU [$\mu mol.(min.100g)^{-1}$], regional myocardial glucose uptake, RPP(mm Hg per beat per minute), rate-pressure product; * not available.

ratios of glucose utilization in infarcted over remote myocardium were >1 in all but 1 patient with mismatch (1.23 ± 0.36). Conversely, these ratios were <1 in all patients with a match pattern (0.59 ± 0.19). There was no relationship between absolute glucose utilization in infarcted myocardium and fatty acid levels either in mismatch or in match regions. Also, there was no relationship between glucose utilization measurements and plasma insulin levels. As shown in Figure 3-1, a positive correlation ($r=0.89$, $p<0.001$) was found between absolute transmural myocardial blood flow and acetate clearance slope, irrespective of the flow-metabolism pattern. No relationship was found in the hypoperfused regions with a match pattern between regional glucose uptake and myocardial blood flow or acetate clearance slope. However, in the 24 regions with flow-metabolism mismatch, there was a relationship between regional myocardial glucose uptake and myocardial blood flow ($r=0.66$, $p<0.001$) and acetate clearance slope ($r=0.74$, $p<0.001$).

Plasma substrate concentrations. Venous plasma glucose, fatty acid, lactate and insulin

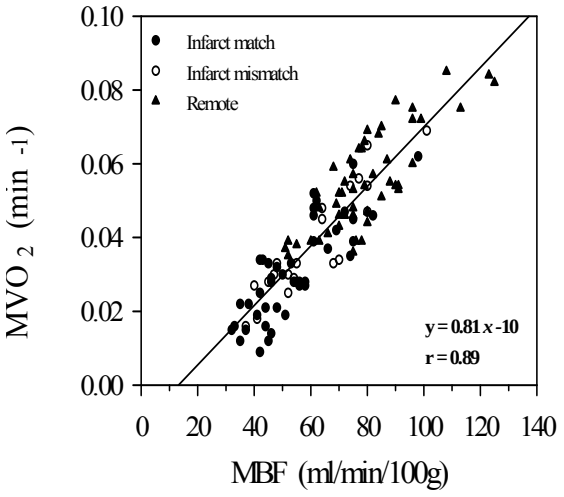

Figure 3-1*. Scatterplots of correlation between MVO2 and myocardial blood flow, in absolute terms in all regions;*
○, *Hypoperfused myocardium with a match pattern;*
●, *Hypoperfused myocardium with a mismatch pattern;*
▲, *Normally perfused myocardium.*

Adapted from Ref. 210.

concentrations obtained at the end of the FDG study are listed in Table 3-5. A significant difference ($p<0.05$) in fatty acid plasma levels was observed among patients with and without flow-metabolism mismatch.

Discussion

The results of this study indicate that, 40 days after an acute myocardial infarction, regional myocardial blood flow and oxidative metabolism are reduced by an average of 51% in the area of infarction, compared to remote normal myocardium. Adjacent but infarcted segments also manifest reduced flow and oxidative capacity, albeit to a lesser extent than central infarct segments. Our findings thus confirm and extend previously reported data showing that early after myocardial infarction, oxygen consumption is reduced in both infarcted and peri-infarction segments.[108,222]

The present data also demonstrate that regional oxidative metabolism in reperfused segments remains tightly coupled to regional myocardial blood flow, irrespective of the presence of a flow-metabolism mismatch. A similar degree of covariance between myocardial blood flow and oxygen consumption has been documented previously in normal myocardium, over a wide range of flow and metabolic conditions.[116] In reperfused myocardium, however, reports on the relation between myocardial blood flow and oxygen consumption have produced conflicting results. Studies in open-chest dogs have shown that the extraction of oxygen by regionally stunned myocardium was quite variable,[125,192] depending on the severity of regional dysfunction. In patients with reperfused infarction, Henes et al.[91] showed that myocardial perfusion, assessed by ^{15}O-water and PET, returned rapidly (18 ± 6 hours) to normal following reperfusion, while oxidative metabolism recovered more progressively and remained "in fine" (9 ± 7 days) significantly depressed ($68 \pm 17\%$ of normal). More recently, Czernin et al.[48] observed a close, albeit nonlinear, relation between flow and oxygen consumption in patients studied within the first week of a reperfused infarction. There are several potential explanations to the apparent discrepancies between these studies. First, they could be related to intrinsic differences in the severity and duration of ischemia, in the completeness and duration of reperfusion, and perhaps also in the methods used to measure myocardial blood flow. For instance, while most animal studies were looking at stunned myocardium, all human studies, including ours, focused on infarcted myocardium, which is composed of a mixture of necrotic, reversibly injured, and perhaps normal cell populations, all coexisting within the same risk area.[184] Thus,

TABLE 3-5. Plasma Substrates Levels

	Glucose (mg/100 ml)	Insulin (μU/ml)	Fatty acids (μM)	Lactate (mM)
All	110 ± 25	19 ± 9	555 ± 548	1.02 ± 0.28
Flow-metabolism match	118 ± 26	16 ± 7	347 ± 103	0.91 ± 0.21
Flow-metabolism mismatch	102 ± 24	22 ± 11	778 ± 724 *	1.16 ± 0.31

* $p<0.05$

tissue heterogeneity may have contributed to the differences in oxidative metabolism seen in stunned and infarcted myocardium. Other factors may have contributed as well, including the persistence of a significant residual stenosis on the infarct-related artery in patients with infarction or the presence of reperfusion-induced microvascular failure (the so-called "no-reflow" phenomenon),[112] as both of these conditions may limit oxygen supply to post-ischemic myocardium, possibly blunting any uncoupling between flow and oxidative metabolism.

The finding of a similarly depressed level of oxidative metabolism in similarly hypoperfused segments despite opposite patterns of exogenous glucose extraction is also of interest. Increased glucose uptake relative to flow has been considered as a useful marker of the presence of viable myocardium in mechanically dysfunctional areas. This approach was shown to allow accurate distinction between irreversibly injured and potentially viable myocardium.[196,200,221] On the other hand, maintenance of a normal oxidative metabolism has also been shown to portend the return of contractile function following reperfusion.[79-81] Combining both approaches in patients with reperfused infarction, we were unable to find any difference in oxidative metabolism between similarly hypoperfused myocardial segments with and without flow-metabolism mismatch. Although we cannot dismiss the possibility that this was related to the persistence of a significant residual epicardial coronary artery stenosis, possibly limiting blood and oxygen supply to the infarcted segments, our observation nevertheless suggests that the combined assessment of myocardial oxidative and glucose metabolisms can sometimes produce conflicting results in terms of myocardial viability. It should be stressed, however, that only the serial measurement of mechanical function following reperfusion allows determination of the reversibility or irreversibility of injury. Further studies are thus warranted to address the relative impact of assessing glucose and oxidative metabolisms upon the prediction of functional recovery in patients with reperfused infarction.

In summary, the results of our study indicate that, at an average of 40 days after an acute myocardial infarction, oxidative metabolism is significantly reduced in the area of infarction, irrespective of glucose metabolism and that regional oxidative metabolism remains intimately coupled to myocardial blood flow.

3.3 Myocardial Blood Flow and Metabolism in Patients with Unstable Angina and Persistent Postischemic Dysfunction despite Coronary Recanalization

Having characterized the flow and metabolic correlates of healed myocardial infarction, we investigated the same parameters in patients with unstable anginal symptoms and persistent anterior wall dysfunction despite successful angioplasty of the culprit lesion. As all patients eventually resumed normal regional function and showed no evidence of infarction at the time of the initial event, we considered that they fulfilled the criteria for acute myocardial stunning.

Methods

We studied 10 patients (5 men, mean age 63 ± 14 years, range 42 - 79 years) with unstable angina and well defined coronary anatomy. By reviewing all diagnostic coronary angiograms performed at 2 clinical sites, we selected prospectively patients with unstable angina, persistent anterior wall dysfunction, precordial T-wave inversion on 12-leads surface EKG, and significant left anterior descending coronary artery stenosis. All had a single vessel coronary artery disease and underwent successful angioplasty of the culprit lesion, despite which anterior wall dysfunction persisted at least to the time of the PET study, i.e. 48 hours after the angioplasty. Importantly, *no patient developed acute myocardial infarction* by clinical, enzymatic and standard 12 lead EKG criteria.

Resting 2D-echocardiograms were obtained and digitized in a cineloop, quad-screen format before and after revascularization in all patients.

Regional wall motion was assessed in 16 segments (basal, midventricular and apical levels of the septum, lateral, anterior and inferior walls; and basal and midventricular levels of the anteroseptal and posterior walls) and defined as normal (1), hypokinetic (2), or akinetic (3).[2] Normal wall motion was defined as 5 mm of endocardial excursion and obvious systolic wall thickening. Hypokinesis was defined as <5 mm of endocardial excursion and reduced wall thickening. Akinesis was defined as near absence of endocardial excursion or thickening. A "dysfunctional" wall motion score was calculated by summing up the scores of all dysfunctional LAD-dependent segments, normalized for the number of abnormal segments. Left ventricular volumes were calculated from the apical 4- and 2-chamber views by use of the Simpson's method. Repeated 2D-echocardiograms were obtained 48 hrs and again 4-8 weeks after PTCA. As judged from the changes in segmental wall motion (in 6 ± 2 abnormal segments out of 16) from the time of PET to the follow-up echocardiographic study, regional dysfunction was entirely reversible in 9/10 patients.

Results

Effects of coronary revascularization on global and regional left ventricular function. At the time of follow-up echocardiography, all patients were asymptomatic and showed normalized resting 12-lead surface EKG. In the 9 patients with improved wall motion after revascularization, global segmental wall motion score improved from 2.4 ± 0.3 to 1.2 ± 0.1 at late follow-up, left ventricular ejection fraction increased from 54 ± 8 to $61 \pm 7\%$ ($p < 0.01$) and end-systolic volume decreased from 38 ± 15 to 27 ± 14 ml/m² ($p < 0.05$). There were no changes in left ventricular end-diastolic volume (from 77 ± 18 to 72 ± 25 ml/m², p=ns).

Regional myocardial blood flow in stunned myocardium. PET revealed homogenous ^{13}N-ammonia uptake in 8/10 patients, while it showed moderately depressed anterior wall perfusion in 2 patients, one of whom had persistent left ventricular dysfunction at follow-up. Baseline absolute myocardial blood flow was measured in the 9 patients with improved wall motion at follow-up in both remote and stunned myocardial regions. Absolute levels of myocardial perfusion were within the normal range in 8/9 patients (95 ± 21 ml.(min.100g)$^{-1}$, range 60 - 124 ml.(min.100g)$^{-1}$), while it was decreased (33 ml.(min.100g)$^{-1}$) in the remaining patient. On average, absolute myocardial blood flow was similar among stunned and remote normally contracting myocardial segments (88 ± 28 versus 85 ± 25 ml.(min.100g)$^{-1}$, p=ns).

Regional oxidative metabolism in stunned myocardium. The monoexponential slope of ^{11}C-acetate clearance, kmono, was measured in 4 patients. ^{11}C-acetate clearance was slightly, albeit non significantly, faster in remote compared with reperfused stunned segments (0.065 ± 0.036 versus 0.057 ± 0.030 min^{-1}, p=ns).

Discussion

This study was designed to evaluate the flow and metabolic correlates of acute myocardial stunning in humans. For this purpose, we carefully selected a human model of prolonged postischemic dysfunction which fulfilled the experimental criteria for myocardial stunning. All the patients included in this study presented with unstable anginal symptoms, T-wave inversion on precordial EKG, anterior wall dysfunction and significant left anterior descending coronary artery disease.[165] They all underwent flow and metabolic imaging by PET within 48 hours of a successful angioplasty of the culprit lesion, despite which anterior wall dysfunction persisted on 2D-echocardiograms. The results indicate that, in these patients, persistently dysfunctional but reperfused myocardium exhibits absolute levels of myocardial perfusion and oxidative metabolism similar to those measured in remote, normally contracting, segments. To the best of our knowledge, this is the first unequivocal demonstration that, following attacks of unstable angina, myocardial stunning occurs in humans.

Since its first description in 1975 by Heyndrickx

et al.,[95] it is now well established that brief periods of myocardial ischemia produced by temporary coronary artery occlusion in the dog can be followed by prolonged depression of regional contractile performance, which may extend for hours or days despite adequate restoration of blood flow and the absence of tissue necrosis. This condition has been termed "stunned myocardium."[25] Although the concept of myocardial stunning is well established in experimental animals, definite demonstration of its existence in humans has been elusive, owing mainly to the difficulty of measuring myocardial blood flow in absolute terms.[21] In addition, the diagnosis of stunning can only be made in retrospect, as it requires 1- documentation of *complete recovery* of contractile function after *full restoration of nutritive perfusion*, and 2- proof of *absence of myocardial necrosis*. In the present study, both criteria were used to identify the presence of stunned myocardium in patients; the recovery of regional function was followed up for 2 months after coronary recanalization and plasma creatine kinase activity was regularly monitored at the time of the acute event to rule out significant myocardial necrosis. Of the 10 patients initially considered for inclusion into the study, one did not show any improvement of regional function at follow-up. Despite the absence of significant enzyme release at the time of the acute event, this patient was nonetheless considered to have a small non Q-wave myocardial infarction and was therefore excluded from further analysis. In 8/9 of the remaining patients, quantitative assessment of myocardial perfusion by PET revealed completely normal perfusion in the area of dysfunction.

The finding of similar levels of overall oxidative metabolism among stunned and remote normal myocardial segments is also of interest. Previous studies on the measurement of regional oxygen consumption in stunned myocardium have produced conflicting results.[35,125,192] Studies using ^{11}C-acetate and PET to assess regional oxidative metabolism in canine models of myocardial stunning have shown that reduced contractile function in reperfused stunned myocardium was associated with reduced oxygen consumption, despite normalization of blood flow.[35,96,228] Similar observations were also made by Schaper et al.[174] who used regional venous blood sampling, a more direct measurement of oxygen consumption. Yet, other investigators have found opposite results, i.e. that myocardial oxygen consumption was normal or even increased in stunned myocardium.

These apparently discordant results likely reflect differences in the severity of regional dysfunction observed in these various studies. Indeed, in the studies of Stahl et al.[192] and Laxson et al.,[125] as in the present study, measurements of oxygen consumption were made at a time when postischemic segments were still akinetic or even dyskinetic, at least during the first third of systole. As early as 1932, Feng reported that stretching of isolated muscle strands caused a proportional increase in heat production and oxygen consumption.[63] It is therefore conceivable that oxygen consumption of stunned myocardium is proportional to the severity and duration of systolic bulging.[73] In support of this view, we offer from our laboratory the observation that moderately stunned myocardial segments made to bulge by rapid asynchronous right ventricular pacing exhibits a disproportional increase in oxygen consumption.[206]

In summary, the results of this study indicate that myocardial stunning does occur in human subjects following attacks of unstable angina and is associated with normal levels of myocardial perfusion and oxygen consumption, as initially observed in dogs following transient ischemia.

3.4 Myocardial Blood Flow and Metabolism in Patients with Noninfarcted Collateral Dependent Myocardium: a Human Model of Chronic Hibernation

So far, we have investigated the flow and metabolic correlates of chronic infarction and acute stunning. As expected from experimental data, healed infarction was associated with

reduced flow and oxygen consumption, while stunning was characterized by a significant degree of perfusion-contraction mismatch. To investigate the flow and metabolic correlates of chronic hibernation, we carefully selected patients whose clinical and angiographic characteristics were quite similar to those initially reported by Rahimtoola.[161] All had symptomatic coronary artery disease, no previous myocardial infarction and complete chronic occlusion of a major coronary artery. In these patients, the myocardium that was normally supplied by the occluded vessel had thus become totally dependent on collateral flow. Some of these patients presented with a completely normal left ventricular function, while others displayed severe regional dysfunction despite no previous infarction. This latter group of patients thus fulfilled the criteria for chronic hibernation, as defined by Rahimtoola, and gave us the opportunity to study the pathophysiologic factors associated with this peculiar condition.

TABLE 3-6. Clinical and Angiographic Data

	Group 1	Group 2
Wall motion in collateral dependent segments	Normal	Abnormal
No. of patients	9	17
Age (years)	60 ± 7	61 ± 9
Sex	8M, 1F	11M, 6F
Anginal class		
CHA I + II	8/9	10/17
CHA III + IV	1/9	7/17
Diseased vessels		
LAD	8/9	13/17
LAD + Cx	-	-
LAD + RCA	1/9	2/17
LAD + RCA + Cx	-	1/17
Cx + RCA	-	1/17
Collateral Score	2.3 ± 0.5	2.2 ± 0.6
Rate-Pressure Product (mm Hg x bpm)	8,871 ± 2,637	9,368 ± 1,035
LV end-diastolic index (ml/m^2)	92 ± 22	112 ± 17
LV end-systolic index (ml/m^2)	27 ± 10	47 ± 13
LV ejection fraction (%)	68 ± 9	52 ± 13
Regional wall motion score	0.4 ± 0.7	4.5 ± 1.2

CHA, Canadian Heart Association; Cx, circumflex artery; LAD, left anterior descending artery; LV, left ventricle; RCA, right coronary artery; bpm, beats per minute.
No statistical analysis was applied to the differences in left ventricular function, which are build in by study design.

Methods

We studied 26 patients (19 men, mean age 60 ± 9 years, range 46 - 75 years) with angina pectoris and well defined coronary anatomy. By reviewing all diagnostic coronary angiograms performed at 2 clinical sites, we selected prospectively patients having a *complete* occlusion of a proximal coronary artery, retrogradely filled by collateral vessels. Twenty-five patients showed occlusion of the left anterior descending coronary artery, among whom 2 had a totally occluded right and 1 an occluded left circumflex coronary artery. The remaining patient had a proximal circumflex and right coronary artery occlusion with a normal left anterior descending. None of the patients had left main stenosis. Importantly, *no patient had suffered from a previous myocardial infarction* by clinical or enzymatic criteria and standard 12 lead EKG's showed no abnormal Q-waves.

Coronary arteriography and contrast left ventriculography was performed in every patient an average of 14 days (range 1 - 48 days) before the PET study. Significant disease was defined as a >70% luminal diameter stenosis in any major coronary branch. The collateral circulation was graded as follows: 0 = no visible collaterals, 1 = poor (thread like, poorly opacified distal arterial segment), 2 = fair (good distal arterial segment lightly and slowly opacified), 3 = adequate (good distal arterial segment, normally and quickly opacified).[54] Left ventricular volumes and ejection fraction, as well as regional wall motion score were calculated as described above. In the patients undergoing revascularization, either by bypass surgery (n=11) or by angioplasty (n=12), a functional follow-up was requested. Coronary angiography and contrast left ventriculography were obtained in 12 patients with chronic

dysfunction between 5 and 8 months after revascularization. The same analysis of global and regional ventricular function was performed. In 7 patients with left anterior descending coronary artery occlusion undergoing bypass surgery, a transmural needle biopsy specimen was obtained from the anterior myocardium and analyzed for morphological changes. This study protocol was approved by the Ethical Committee of our institutions and no complications resulted from any part of the study.

PET was performed as described earlier. Myocardial perfusion was assessed with ^{13}N-ammonia, myocardial oxidative metabolism with ^{11}C-acetate and exogenous glucose uptake with ^{18}F-deoxyglucose (FDG). Fifteen patients had flow and metabolic imaging at rest, using the 3 tracers. In the remaining 11 patients, myocardial blood flow was studied at baseline and following intravenous administration of dipyridamole (0.56 mg/kg over 4 min, followed by 0.28 mg/kg over 6 min) to assess myocardial flow reserve in remote and collateralized segments.

Morphological tissue analysis. Two transmural biopsies (20 mm 14-gauge needle) were obtained from the anterolateral wall, between the first and second diagonal branches, before induction of extracorporeal circulation.[64-66] Biopsies were taken at a site showing dysfunction at cineventriculography and where metabolic data were available with PET. All samples were transmural, but were immediately divided into a subendocardial and a subepicardial portion of equivalent sizes. The specimens were fixed in 3% glutaraldehyde fixative buffered at pH 7.4 with 1M natrium dihydrogenophosphate, postfixed in osmium tetroxide and routinely embedded in Epon. Light microscopy was used to quantify cellular alterations and the amount of fibrosis and to select regions of interest to be subsequently assessed with electron microscopy. Semi-thick sections stained with toluidine-blue and Periodic-Acid Schiff (PAS) reaction were obtained from each biopsy specimen. Each section was examined using a special grid dividing the field in 121 identical squares to measure the percentage of the biopsy surface covered by fibrosis or by cardiomyocytes. This procedure was repeated several times on different zones of the biopsy. Subsequently, 100 - 200 cardiomyocytes sectioned through their nucleus were examined and their morphological characteristics were studied. Ultrathin sections were stained with uranyl acetate and lead citrate and examined with a Philips EM300 electron microscope to further qualify the structural alterations in the cardiomyocytes.

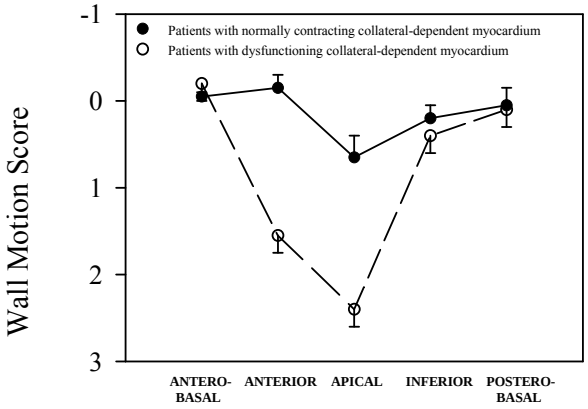

Figure 3-2. *The mean wall motion score along the ventricular silhouette is shown in patients from group 1 (closed circles) and group 2 (open circles). There is no significant difference in the regional wall motion score in group 1. No statistical analysis was applied to the differences between groups, which is build in by study design. Adapted from Ref. 211.*

Results

Clinical and angiographic patient characteristics. According to resting regional wall motion in collateral dependent segments (Table 3-6), the patients were divided in 2 groups:

- Group 1: 9 patients (8 men, mean age 60 ± 7 years, range 49 - 73) with normal or minimal regional wall motion abnormalities (mean regional wall motion score: 0.4 ± 0.7; range 0 - 2).

- Group 2: 17 patients (11 men, mean age 61 ± 9 years, range 46 -75) with severe regional dysfunction (mean regional wall motion score: 4.5 ± 1.2; range >2 - 7).

Figure 3-2 shows the wall motion score along the ventricular silhouette in the patients from both groups. Angiographic collateral grade was similar among the 2 groups. There was a non significant ($p = 0.12$) trend towards more severe anginal symptoms (Canadian Heart Association class III or IV) in patients with dysfunctional collateral dependent myocardium.

Baseline regional myocardial blood flow and metabolism. The baseline absolute myocardial blood flow was measured in all 26 patients and is shown in Figure 3-3 both in remote and collateral dependent myocardial regions. No regional differences were found in patients with normal resting regional wall motion. In patients with abnormal resting wall motion, myocardial blood flow was higher in remote compared to collateral dependent segments (95 ± 27 vs. 77 ± 25 ml.(min.100g)$^{-1}$, $p < 0.001$). Yet, no difference was found among collateral

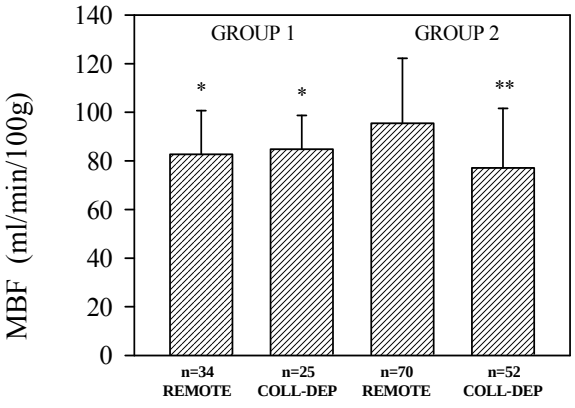

Figure 3-3. *The baseline myocardial blood flow (MBF) measured with ^{13}N-ammonia in all remote and collateral dependent regions is shown for both patient groups. A significant difference was found in patients with left ventricular dysfunction between remote and collateral dependent regions. MBF in the remote regions was significantly lower in group 1 than in group 2. * $p < 0.05$, ** $p < 0.01$. Adapted from Ref. 211*

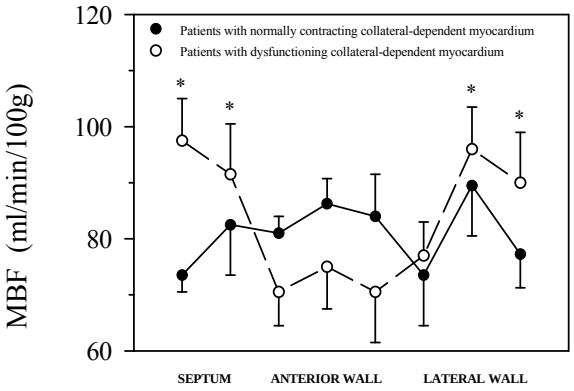

Figure 3-4. *The absolute transmural myocardial flow profile (MBF) is shown in the patients with left anterior descending coronary artery occlusion from both groups. There is a significant difference between the increased flow in the septal and lateral walls compared with that in the anterior wall in the patients with dysfunctional collateral dependent myocardium. * $p < 0.05$. Adapted from Ref. 211.*

dependent segments from patients with and without abnormal wall motion (77 ± 25 versus 85 ± 14 ml.(min.100g)$^{-1}$, p=ns). Figure 3-4 shows the same data, but compares the flow profile along the tomographic image in the patients with left anterior descending coronary occlusion. The only significant ($p < 0.01$) difference relates to the increased flow in the septal and lateral walls relative to the anterior wall in the patients with dysfunctional collateral dependent myocardium.

Table 3-7 compares myocardial blood flow, absolute glucose uptake, relative ^{18}F-FDG to ^{13}N-ammonia circumferential profiles, oxygen consumption and mean estimated wall thickness (by use of the Monte Carlo simulation) in the subgroup of 15 patients in whom these data were available. Absolute myocardial flow values in this subgroup of patients were similar to those measured in the total population. The metabolic rates for exogenous glucose utilization in remote and collateral dependent myocardium were highest in dysfunctional patients, respectively 42 ± 20 and 38 ± 16 μmol.(min.100g)$^{-1}$. Identical values were found between remote and collateralized regions in group 2 patients

TABLE 3-7. Myocardial Blood Flow, Exogenous Glucose Uptake, Oxidative Metabolism, and Mean Wall Thickness in Remote and Collateral-Dependent Myocardium

	MBF	rMGU	FDG/NH_3	k	Wall thickness (mm)
Group 1 (*n*=6 patients)					
Remote segments (*n*=25)	78 ± 8 *	33 ± 12 *	1.1 ± 0.1	0.058 ± 0.008 *	13.3 ± 0.8
Collateralized segments (*n*=18)	75 ± 16	33 ± 12 *	1.2 ± 0.2	0.054 ± 0.010 *	13.1 ± 0.6
Group 2 (*n*=9 patients)					
Remote segments (*n*=35)	92 ± 23	42 ± 20	1.3 ± 0.6	0.068 ± 0.020	13.4 ± 0.5
Collateralized segments (*n*=30)	68 ± 17 †	38 ± 16 †	1.9 ± 1.6 *	0.049 ± 0.015 ‡	12.1 ± 1.1 ‡

FDG/NH_3, ^{18}F-fluorodeoxyglucose to ^{13}N-ammonia relative uptake; k (min^{-1}), slope of ^{11}C-acetate clearance; MBF [$ml.(min.100g)^{-1}$], myocardial blood flow; rMGU [$\mu mol.(min.100g)^{-1}$], regional myocardial glucose uptake.
*p<0.05, †p<0.01, ‡p<0.001 vs. remote segments of group 2.

(33 ± 12 μmol.(min.100g)$^{-1}$). The ratio of metabolic rate for glucose utilization to myocardial blood flow, reflecting the extraction of glucose by the myocardium, was also higher in dysfunctional collateral dependent compared to normally contracting collateral dependent segments (0.60 ± 0.27 versus 0.42 ± 0.16 μmol/ml, $p < 0.004$). The relative ^{13}N-ammonia uptake in collateralized segments averaged 83 ± 10% (range 60 - 98% of maximum) in group 1 and 65 ± 17% (range 21 - 93%) in group 2 ($p < 0.001$). The ^{18}F-FDG uptake in collateral dependent segments relative to the flow profile was significantly higher in patients with compared to patients without wall motion abnormalities ("mismatch" ratio 1.9 ± 1.6 versus 1.2 ± 0.2, $p < 0.05$). A typical example of these findings is illustrated on Plate 3-2.

In patients with normal resting wall motion, the monoexponential slope of ^{11}C-acetate clearance, kmono, was comparable between remote and collateralized segments. At variance, in patients with resting wall motion abnormalities, ^{11}C-acetate clearance was faster in remote compared to collateral dependent segments (0.068 ± 0.020 versus 0.049 ± 0.015 min^{-1}, $p < 0.001$). Acetate kinetics did not differ, however, significantly among collateral dependent segments of patients with and without regional wall motion abnormalities. The venous plasma glucose, fatty acids, lactate and insulin plasma concentrations at the time of the tomographic study are listed in Table 3-8.

Collateral-dependent myocardial flow reserve. The absolute myocardial blood flow during dipyridamole infusion was determined in a subgroup of 11 patients with total occlusion of the left anterior descending coronary artery and normal circumflex coronary artery. Infusion of dipyridamole induced anginal pain and significant ST-segment depression (>0.1 mV in lateral leads) in all patients. In 3 patients with normal baseline anterior wall motion, transmural myocardial blood flow in collateral dependent segments increased from 78 ± 5 at rest to 238 ± 54 ml.(min.100g)$^{-1}$ during hyperemia. At variance, in 8 patients with dysfunctional collateral dependent myocardium, the flow increase was severely blunted from 88 ± 17 at rest to 112 ± 44 ml.(min.100g)$^{-1}$ during hyperemia. The maximal flow was not different

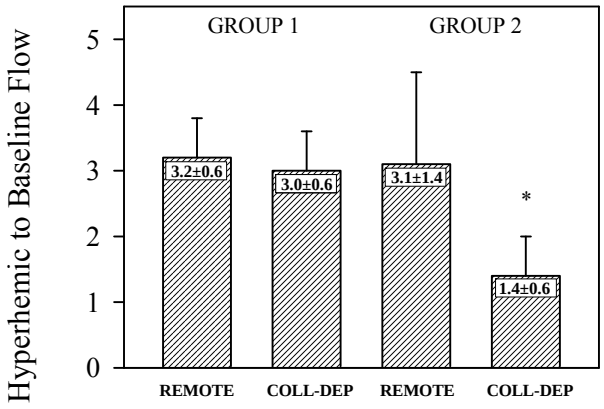

Figure 3-5. *The ratio of hyperemic/baseline absolute flow is shown as an index of "collateral flow reserve," which is significantly reduced in collateral dependent segments of group 2 patients. * p < 0.001. Adapted from Ref. 211.*

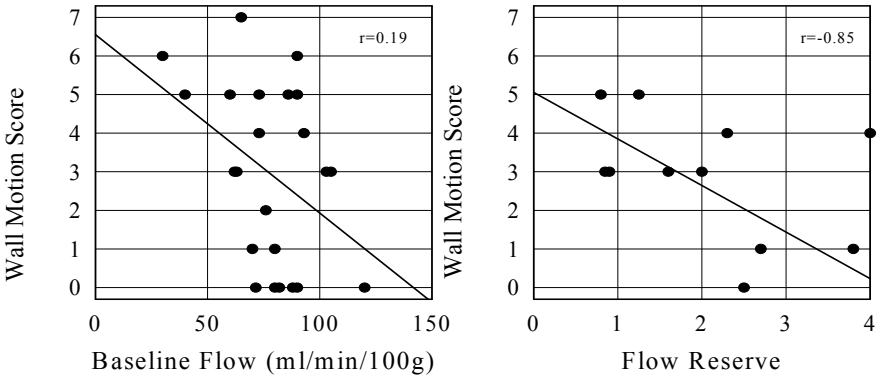

Figure 3-6. *Relationship between anterior wall motion score, baseline anterior wall myocardial blood flow (left) and anterior "flow reserve" (right). Correlation coefficients were obtained with the Spearman rank correlation. Adapted from Ref. 211*

in remote segments between group 1 (274 ± 44 ml.(min.100g)$^{-1}$) and group 2 (279 ± 125 ml.(min.100g)$^{-1}$) patients. The "collateral flow reserve", defined as the ratio of hyperemic over basal flow, is shown in Figure 3-5. A significant inverse relation ($r = -0.85$, $p < 0.001$) was found between the baseline anterior wall motion score and the ratio of hyperemic over basal flow in collateral dependent segments (Figure 3-6). There was, however, no relationship between the baseline wall motion score and the resting myocardial blood flow ($r = -0.19$) in these segments (Figure 3-6).

Functional follow-up. Coronary angiography and contrast left ventriculography 5 to 8 months following coronary revascularization were available in 12 patients from group 2. Among these, 8 patients underwent percutaneous transluminal coronary angioplasty of the occluded vessel and 4 had coronary artery bypass surgery. Adequate revascularization of the dysfunctional segments was achieved in 11 patients. In the remaining, reocclusion of the left anterior descending coronary artery had occurred following an initially successful angioplasty. Nevertheless, the regional wall motion score improved in all patients, including the one with reocclusion of the left anterior descending coronary artery (from 3.8 ± 1.3 to 0.8 ± 0.9, $p < 0.005$). Global ejection fraction improved (from 55 ± 7 to 65 ± 8%, $p < 0.001$) and the end-systolic volume decreased (from 47 ± 10 to 34 ± 11 ml/m², $p < 0.005$) in all patients.

Structural abnormalities in collateral dependent myocardium. Macroscopic scars were not detected during surgery in the anterior wall. With the exception of one patient (patient A in Table 3-9), little fibrosis was found in the biopsy specimens. Nonetheless, the cardiomyocytes of patients with anterior wall dysfunction showed characteristic morphological changes. Compared with cardiomyocytes in remote "normal" myocardium (Plate 3-3), about half the myocardial cells from dysfunctional segments showed various degrees of structural changes. One striking feature of these altered cardiomyocytes was the loss of contractile material. In some cells, this was limited to the vicinity of the nucleus, whereas in others it was very extended, leaving only few or no sarcomeres at the cell periphery (Plate 3-4). Myofibrillar loss was not accompanied by major cell volume changes, as the space previously

TABLE 3-8. Plasma Substrates Levels

	Glucose (mM)	Insulin (μU/ml)	Fatty acids (μM)	Lactate (mM)
All	6.2 ± 2.2	36 ± 14	739 ± 108	0.95 ± 0.24
Group 1	5.2 ± 1.2	37 ± 14	775 ± 478	1.18 ± 0.21
Group 2	7.2 ± 2.4	35 ± 14	713 ± 250	0.83 ± 0.19 *

* $p<0.05$ group 1 vs. group 2.

TABLE 3-9. Relation Among Anterior Wall Motion, Flow, Glucose Metabolism and Quantitative Morphological Data

					% Fibrosis		% AC	
Patient	AWMS	MBF	rMGU	FDG/NH_3	SE	TM	SE	TM
A*	4	96	37	1.45	50	-	90	-
B	3	57	30	1.03	1	1	40	35
C	3	110	40	1.34	11	8	67	59
D	3	72	42	1.50	5	4	27	19
E	1	74	38	1.33	10	6	39	30
F	1	78	12	1.69	2	2	15	15
G	1	89	26	1.00	3	3	5	4

AWMS, anterior wall motion score; MBF [$ml.(min.100g)^{-1}$], myocardial blood flow; rMGU [$\mu mol.(min.100g)^{-1}$], regional myocardial glucose uptake; FDG/NH_3, ratio of ^{18}F-deoxyglucose to ^{13}N-ammonia relative uptake; SE, subendocardial sample; TM, transmural data; %AC, percent abnormal cells.
* Subepicardial sample not available in this patient.

occupied by the myofilaments was filled with an amorphous, strongly PAS-positive material, typical of glycogen (Plate 3-5). In the electron microscope, the general organization pattern of the remaining peripherally located sarcomeres was well preserved. Mitochondria were small and scattered throughout the myolytic cytoplasm. Nuclei were tortuous, and showed uniformly dispersed heterochromatin. Sarcoplasmic reticulum was virtually absent, as were T-tubules. There were no signs of degeneration, such as cytoplasmic vacuolization, edema, mitochondrial swelling, membrane disruption, lipid droplets, suggestive of acute ischemic damage or cellular atrophy. The group data are shown in Table 3-9. The patients are ranked according to decreasing severity of anterior wall motion abnormalities.

Discussion

In this study, we attempted to elucidate the mechanisms by which ischemia may result in chronic but reversible regional dysfunction. We selected a human model in which myocardial perfusion depended entirely on collateral blood supply and in which regional dysfunction met the clinical criteria for chronic hibernation, as defined by Rahimtoola.[161] The findings of this study can be summarized as follows:

- dysfunctional collateral-dependent myocardium shows reduced myocardial blood flow and acetate clearance while exogenous glucose uptake is maintained, as compared to remote, normally perfused, myocardium in the same patient;

- there is no significant difference between normally contracting and dysfunctional collateral-dependent segments with respect to baseline blood flow and oxygen consumption;

- immature and/or insufficiently developed collaterals do not provide adequate flow reserve in the subgroup of patients with chronic regional dysfunction;

- marked morphological alterations, including a substantial loss of myofibrillar content, represent the structural correlate of the chronic dysfunction and of the metabolic changes.

Despite a marked reduction in external work, dysfunctional collateral dependent myocardium remains metabolically active as demonstrated by the nearly normal baseline flow and oxygen consumption and by the increased ^{18}F-FDG uptake relative to flow. Thus, the data in this model do not support the hypothesis that chronic dysfunction results from a chronic reduction in resting flow. The contention that flow is decreased in "hibernating" states has been based on clinical studies of the relative distribution of

flow tracers such as ^{201}Thallium or ^{82}Rubidium.[131] The interpretation of these scintigrams usually assumes that the segments with maximum tracer uptake have normal flow. However, perfusion scintigraphy only provides estimates of relative differences in tracer distribution. A seemingly decreased perfusion to a dysfunctional segment, as seen on Figure 3-4, may well result from an absolute increase in flow to the remote hyperfunctioning tissue, as shown in the present study by the quantitative measurements of transmural blood flow with ^{13}N-ammonia.

While a significant reduction in resting flow can be ruled out, some metabolic changes are nevertheless apparent in the patients from group 2. The glucose uptake is significantly increased in the remote areas, consistent with an increase in regional workload,[40] although slight differences in substrate supply might have contributed as well. In the dysfunctional collateral dependent areas, the absolute glucose uptake is preserved and the absolute glucose extraction is significantly increased, a pattern referred to as flow-metabolism "mismatch."[179] This pattern has been shown to identify reversible tissue injury after transient ischemic insults. Following adequate revascularization, improvement of regional wall motion is expected to occur in 78-92% of such areas, which indicates persistent tissue viability.[196,200]

The flow reserve of collateral dependent myocardium was evaluated using dipyridamole as the hyperemic agent.[155] A wide range of hyperemic transmural flow values, from a 4-fold increase to a 20% decrease in basal flow, was found. This is consistent with animal studies showing heterogeneity of the collateral vascular system early after total coronary occlusion induced by placement of an ameroid constrictor on a proximal coronary artery.[11,172,173] Whether the blunted collateral reserve in patients with regional dysfunction represents immaturity or insufficiency of the collateral system cannot be assessed from the present clinical data, since the exact time of the coronary occlusion, the delay between the occlusion and the study as well as the individual rate of collateral growth are unknown. The lack of correlation between the angiographic collateral score and the absolute tissue perfusion values is not surprising and probably relates to the limited resolution of angiography. Another explanation could be the presence of functional extracoronary collaterals in these patients.[203] While all patients had angina pectoris, the anginal symptoms were significantly more severe in patients with chronic dysfunction and reduced collateral flow reserve. Severe ischemia is likely to occur repeatedly in those patients during daily life caused by increased demand, reductions in blood pressure, spontaneous increases in microvascular constrictor tone,[158] or by a combination of any of these mechanisms. In patients with a significant increase in collateral dependent flow, angina and objective signs of ischemia during dipyridamole infusion still occurred. Similar findings were reported in a recent clinical study in which collateral flow reserve was assessed in patients with total occlusion of the left anterior descending coronary artery by use of thermodilution of the great cardiac vein.[51] In this study, collateral flow increased significantly in all patients during infusion of dipyridamole and collateral flow reserve was within normal limits. As shown by Schaper[172,173] and others[11] in animal studies, underperfusion in that case is usually limited to the subendocardium, because pharmacological vasodilation or moderate exercise can induce a transmural coronary steal.

The present findings challenge the currently accepted understanding of the pathophysiology of chronic dysfunction of noninfarcted myocardium. Several studies have documented the beneficial effects of coronary revascularization on survival and cardiac function in patients with coronary artery disease and left ventricular dysfunction.[1,61,151] These observations have led to the speculation that chronically hypoperfused myocardium, referred to as "hibernating," could maintain viability by simply reducing its metabolic demand to match the decreased supply, for as long as myocardial perfusion was inadequate.[113,161] The chronic impairment of contractile function in this setting was considered to represent a protective

mechanism, minimizing the energy requirements and preventing the appearance of irreversible tissue damage. This concept requires achievement of a new steady-state between reduced supply and decreased demand and implies the existence of chronic low-flow myocardial ischemia.[169] Recent studies in open-chest anesthetized pigs undergoing 1 to 5 hours partial coronary occlusion have partially come in support to this hypothesis.[3,62,134,150,167] Several investigators have indeed reported on the successful development of sustained low-flow perfusion-contraction matching in the pig heart (also called short-term hibernation).[3,62,134,150,167] Ischemia was produced by incomplete coronary occlusion leading to a 20 - 70% reduction of transmural myocardial blood flow. Although this resulted in a prompt and sustained decrease of segmental wall thickening, no myocardial necrosis ensued. Despite continuing low-flow and dysfunction, intriguing phenomena were observed, including the spontaneous resolution of the metabolic markers of ischemia and the regeneration of phosphocreatine back to nearly normal levels.[1,27,150] This condition was remarkably unstable, however, as superimposition of a chronotropic or inotropic stress invariably resulted in increased lactate production, decreased phosphocreatine and eventually myocardial necrosis.[182]

While these findings thus suggest that a precarious steady-state between reduced oxygen supply and decreased oxygen demand can be achieved and maintained for some time under particular experimental conditions, no data are presently available to indicate that such a perfusion-contraction matching can persist for weeks or months in chronic animal preparations, let alone in the intact individual. On the contrary, most investigators who have succeeded so far in reproducing chronic (>1 week) but reversible regional left ventricular ischemic dysfunction in the experimental lab have always ended up with models of perfusion-contraction mismatch. Canty and Klocke examined the temporal response of regional function after ameroid implantation in conscious dogs.[41] In their model, regional contraction was found to decrease progressively during the course of ameroid occlusion. Yet, measurements of regional endocardial blood flow suggested a dissociation between flow and function at the time of ameroid occlusion. Bolukoglu et al. achieved sustained reduction in segmental shortening without necrosis in swine undergoing a 50% reduction of the left anterior descending coronary artery flow velocity for 7 days.[22] In their experiments too, the decrease in segmental function was progressive over time and was not associated with reduced subendocardial blood flow by day 7. More recently, Shen et al. examined the time course of regional dysfunction after ameroid implantation in chronically instrumented pigs.[188] Here again, the resulting progressive segmental dysfunction was not associated with permanently reduced subendocardial blood flow but rather appeared to result from repeated transient episodes of acute ischemia followed by stunning. While the above studies do not entirely dismiss the possibility that chronic perfusion-contraction matching can be achieved in intact animals, they suggest that, rather than resulting from a state of decreased flow, chronic dysfunction most often results from to episodes of severe ischemia, the functional recovery being incomplete because of renewed ischemic and stunning episodes.[143] In this study, dysfunctional collateral dependent segments showed nearly normal baseline blood flow and oxygen consumption but severely limited flow reserve, which strongly supports such a scenario.

Finally, a definite answer was obtained from the analysis of tissue samples. Since experimental stunning is not associated with significant alterations in myocardial ultrastructure,[113] we performed a detailed morphological analysis of dysfunctional collateral-dependent human myocardium obtained during surgery in a limited number of patients. Profound abnormalities were found, much similar to those described earlier by Flameng et al.[64-66] The most striking features observed in chronically hypokinetic segments were the loss in myofibrillar content and the excessive accumulation of glycogen. We believe that this peculiar morphological pattern represents the structural correlate of myocardial "hibernation".

Whether these phenotypic changes are induced by ischemia per se or are the result of prolonged contractile unloading is unresolved at the present time.[45,187,189,199] It is likely that these phenotypic changes are reversible after revascularization, as can be inferred from the recovery of wall motion over time. However, for obvious reasons, direct evidence of structural reversibility in humans is lacking and will probably await the development of relevant animal models of chronic left ventricular ischemic dysfunction.

The comparison of the morphological data with the findings on metabolic imaging raises intriguing questions about the biochemical fate of exogenous glucose in "hibernating" cells. Although it was originally suggested that the increased glucose uptake resulted from stimulation of anaerobic metabolism by chronic ischemia,[179] this explanation now appears unlikely in view of the normal or nearly normal levels of absolute myocardial perfusion [50,77,207,211] and oxygen consumption [79-81,208,211] measured in these segments and in view of the accumulation of glycogen, a quite unusual finding in the setting of ongoing ischemia, rather expected to result in the opposite.[215,216] Glucose uptake by dysfunctional but metabolically active myocardium was shown to be relatively independent of the hormonal milieu and dietary conditions.[205] One possible explanation for this phenomenon could be a switch in the subtype of glucose transporters expressed at the surface of the cardiomyocytes. Although the insulin-responsive glucose transporter GLUT-4 is predominant in adult cardiac muscle,[38] it has been recently shown that ischemia could trigger the re-expression of the insulin-insensitive unidirectional glucose transporter GLUT-1.[31] GLUT-1 is expressed at only relatively low levels in adult cardiomyocytes, but is predominant in embryonic and neonatal cardiomyocytes.[223] Although this remains speculative, increased expression of GLUT-1 might just be one part of the many phenotypic changes shown to occur in chronically dysfunctional myocardium and be the molecular basis for both the increase in glucose uptake and the accumulation of glycogen. This view is supported by preliminary results showing a 2.5 fold relative increase in GLUT-1 compared to GLUT-4 messenger RNA content (by quantitative PCR) in dysfunctional segments of patients with hibernating myocardium.[185]

There is indeed accumulating evidence that the observed structural changes are the consequence of a dedifferentiation process, as the altered cells show many features of neonatal cardiomyocytes,24 including -1- depletion of contractile filaments, -2- presence of rough sarcoplasmic reticulum, -3- accumulation of glycogen, -4- occurrence of irregularly shaped nuclei with peculiar distribution of chromatin, -5- loss of organized sarcoplasmic reticulum, -6- lack of T-tubules, and -7- vesiculization of the sarcolemma. Not all the characteristics of altered cardiomyocytes resemble those of embryonic cells, however. For instance, the remaining sarcomeres in the altered cells often retain their orderly arrangement at the cell periphery, while they are randomly distributed in embryonic cells. Also, the amount of glycogen seen in altered cardiomyocytes far exceeds that reported in the embryo. The hypothesis of dedifferentiation is further substantiated by the demonstration by use of immunohistochemistry that these cells re-express contractile proteins that are specific to the fetal heart,[9,140] such as the α-smooth muscle cell actin (Plate 3-6), while at the same time, they exhibit the same organization pattern of structural proteins like titin as developing cardiomyocytes.[9] In addition, cardiotin, a recently described high molecular weight protein absent in fetal cells, seems also to be absent in the altered cells. These observations reinforce the thesis that altered cardiomyocytes undergo partial dedifferentiation.

This study has several potential limitations, which should be acknowledged. The study population was carefully selected in order to avoid inclusion of patients with previous infarction in the collateral dependent areas. It cannot be ruled out that small foci of subendocardial necrosis were present in some instances. Although histologic data are available in a limited number of patients, the fact that significant fibrosis was seen only in 1 out of 7

cases is reassuring. A weak relation was found between the presence of wall motion abnormalities and the severity of angina from carefully taken history. It would have been of interest to compare the total ischemic burden in both patient groups, since painless episodes may have contributed to the repeated stunning. It was not possible, however, to obtain Holter tape monitoring for quantitation of ST-T segment abnormalities. Finally, although special care was taken to obtain representative tissue samples from the center of the ischemic area at the appropriate level, we realize that a 15 mg biopsy probably is 5,000 times smaller than the entire anterior ischemic area. Obviously, such a small sample size is imposed by safety considerations.

In summary, this study demonstrates that in patients with noninfarcted collateral-dependent myocardium, in whom chronic regional dysfunction meets the clinical criteria for chronic hibernation (chronic dysfunction with hypoperfusion by relative perfusion imaging), absolute myocardial blood flow and oxygen consumption in the dysfunctional collateral dependent segments are nearly normal at rest, collateral flow reserve is markedly blunted and major structural changes are present on morphological analysis. In these patients, impaired function likely results from repetitive episodes of ischemia with a persistent stunning effect, which, at variance with experimental stunning, eventually results in structural alterations. We propose that these alterations represent the flow, metabolic, and morphologic correlates of chronic myocardial "hibernation."

3.5 Time Course of Recovery from Myocardial Hibernation after Coronary Revascularization

Among the many unresolved issues regarding myocardial hibernation, the time-course of recovery of contractile function after revascularization has received little attention. Given the severity of the structural changes seen in the hibernating myocardium,[24,50,211] one should expect that the recovery of function after revascularization would be delayed, and that the time course of recovery would be influenced by the severity of the underlying structural abnormalities. Surprisingly, few clinical studies have addressed this issue and their results have been varied.[84,124,144,201] Accordingly, we designed the following study to evaluate more comprehensively the time-course of functional improvement after successful revascularization and its potential determinants.

Methods

We studied 21 patients (18 men, mean age 55 ± 9 years, range 39 - 68 years) with ischemic heart disease undergoing successful coronary revascularization by either bypass surgery (n=15) or angioplasty (n=6). These patients were selected among a larger group of patients undergoing revascularization (*n*=40) based on the following criteria: -1- presence of severe regional dysfunction in the anatomical distribution of a significantly narrowed or occluded epicardial artery; -2- absence of peri-operative or peri-procedural myocardial infarction; -3- complete and successful revascularization of the dysfunctional segments; -4- significant improvement of both regional (improvement of wall motion score by at least one full grade in 2 adjacent a- or dyskinetic myocardial segments) and global (decreased end-systolic volume) left ventricular function at the 6th month follow-up examination. Eighteen patients had sustained at least one previous myocardial infarction, the most recent 28 days before inclusion into the study.

At coronary arteriography, performed in every patient before revascularization, 15 patients had complete occlusion of ≥ 1 major epicardial coronary segments, among whom 7 had occlusion of the left anterior descending coronary artery, 4 of the proximal circumflex artery and 11 of the right coronary artery. The remaining 6 patients had severe proximal stenoses on ≥ 1 major epicardial segment. Six patients had single vessel disease, 5 patients had two vessel disease, and 10 patients had three vessel disease. One patient also had left main stenosis.

2D-echocardiograms were obtained at rest, before revascularization, and again 10 days, 2 months and 6 months after revascularization. Images from the parasternal long- and short-axis and apical four- and two-chamber views were digitized in a quad screen, cineloop format and stored on 512 byte/sector rewritable optical disks. Images were interpreted qualitatively in accordance with previous guidelines by experienced observers who had no knowledge of the angiographic and clinical data. Regional function was interpreted in 16 myocardial segments (basal, midventricular and apical levels of the septum, lateral, anterior and inferior walls; and basal and midventricular levels of the anteroseptal and posterior walls) and defined as normal (1), hypokinetic (2), or akinetic (3) as described above. A global wall motion score was calculated for the baseline and all follow-up two-dimensional echocardiographic studies. A dysfunctional regional wall motion score was also obtained by summing the scores of all dysfunctional segments and dividing the sum by the number of dysfunctional segments. Left ventricular volumes at both end-diastole and end-systole and ejection fraction were computed from the apical 4- and 2- chamber views by use of a standard Simpson's method in each patient.

Positron emission tomography. Assessment of regional myocardial perfusion and metabolism by PET was performed in every patient at the time of the initial hospital stay. Data were acquired and analyzed as described in the introduction.

Results

The preoperative clinical and angiographic characteristics of the study population are summarized in Table 3-10. With PET, reversibly dysfunctional segments showed normal levels of resting myocardial blood flow (85 ± 34 $ml.(min.100g)^{-1}$, $114 \pm 36\%$ of remote) and maintained glucose uptake (28 ± 14 $\mu mol.(min.100g)^{-1}$, $72 \pm 24\%$ of remote). In 9 patients undergoing bypass surgery, a transmural biopsy was obtained from the center of the dysfunctional area. In all 9 patients, analysis of this biopsy sample demonstrated changes similar to those previously observed in patients with dysfunctional, albeit noninfarcted, collateral-dependent myocardium. In general, there was little fibrosis ($28 \pm 14\%$) and a large proportion of cardiomyocytes ($44 \pm 18\%$) showed structural signs of dedifferentiation

TABLE 3-10. Clinical and angiographic data before revascularization.

No. of patients	21
Age (years)	55 ± 10
Sex	18M, 3F
Anginal class	
CHA I + II	15/21
CHA III + IV	6/21
Functional class	
NYHA I + II	19/21
NYHA III + IV	2/21
Diseased vessels	
LAD	4/21
RCA	2/21
LAD + Cx	1/21
LAD + RCA	3/21
RCA + Cx	1/21
LAD + Cx + RCA	10/21

CHA, Canadian Heart Association; NYHA, New York Heart Association; LAD, left anterior descending artery; Cx, circumflex artery; RCA, right coronary artery

The time-course of recovery of regional contractile function is shown in Table 3-11 and Figure 3-7. The kinetics of functional improvement varied substantially from patient to patient. Some demonstrated significant improvements quite rapidly after revascularization, usually within the first week, while others showed a more progressive return of regional function. Monoexponential least square fitting routines were used to quantitate the time-course of functional recovery in individual patients. The time constant of the decrease in regional wall motion score averaged 39 ± 32 days, ranging from 9 to 120 days. The recovery of the left ventricular volumes and ejection fraction followed a similar time-course.

Factors associated with delayed improvement of function after revascularization. To define further the variables associated with the rate of

TABLE 3-11. Time course of hemodynamic and functional changes in 21 patients with hibernating myocardium

		Baseline	1 week	2 months	6 months
Heart rate	bpm	75 ± 13	84 ± 16	74 ± 15	75 ± 14
Mean blood pressure	mm Hg	102 ± 14	92 ± 8	102 ± 10	101 ± 12
Rate-pressure product	bpm x mmHg	10,031 ± 2,745	9,987 ± 2,143	9,973 ± 2,621	9,908 ± 2,706
LV EDV	ml	173 ± 67	160 ± 71	172 ± 51	155 ± 39*
LV ESV	ml	121 ± 49	103 ± 59*	97 ± 44**	81 ± 36**
LV EF	%	35 ± 9	39 ± 10**	46 ± 10**	49 ± 10**
WMS		2.6 ± 0.2	2.4 ± 0.1**	2.0 ± 0.3**	1.7 ± 0.3**

LV, left ventricle; EDV, end-diastolic volume; ESV, end-systolic volume; EF, ejection fraction; WMS, wall motion score.
* $p<0.05$, ** $p<0.01$ versus Baseline by ANOVA.

functional recovery after coronary revascularization, all prerevascularization clinical, angiographic, scintigraphic (PET flow and metabolism) and structural data available were proposed for inclusion into a multiple regression model. With univariate analysis, only the proportion of altered cardiomyocytes (r=0.95) and the relative surface of the biopsy covered by these cardiomyocytes (r=0.89) were found to correlate with the kinetics of recovery. Stepwise linear discriminant analysis selected the proportion of altered cardiomyocytes as the sole independent correlates of the time course of recovery (Figure 3-8).

Discussion

As shown in the preceding study, the most striking finding in tissue biopsies taken from hibernating myocardial segments is the presence of significant morphological abnormalities, which include dedifferentiation of the myocytes with loss of contractile material. Given the severity of these structural changes,[24,50,211] one would expect the return of function to these segments to be delayed despite adequate revascularization.

Surprisingly, few clinical studies have addressed this issue and results of those that have been performed and measured regional function early after revascularization have been controversial.[84,124,144,201] In a series of patients studied by transesophageal echocardiography within 15 minutes of discontinuation of cardiopulmonary bypass, Topol et al. reported that 57% of severely dysfunctional segments showed immediate improvement in wall thickening; no further improvement was observed 8 days later.[201] In contrast, in patients undergoing coronary angioplasty, Nienaber et al. found no significant improvement in regional wall motion 3 days after revascularization, although by 67 days, wall motion had significantly improved.[144] Another study found recovery from hibernation to be biphasic, with partial improvement within 15 minutes and further recovery after 13 weeks.[84] More recently, La Canna et al. reported immediate intraoperative improvement of wall motion in 33 carefully selected patients.[124]

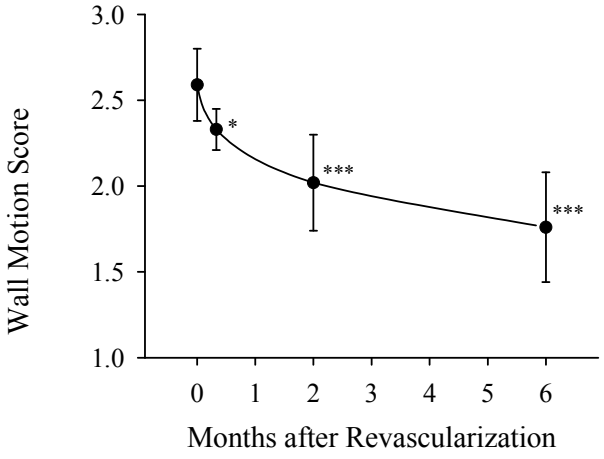

Figure 3-7. *Dot plot showing the time-course of recovery of regional wall motion after revascularization. The return of regional function was slowly progressive with a time constant of 39 days.* $p<0.05$; *** $p<0.001$ vs. baseline. Adapted from Ref. 219.*

The present study provides important new information on the time-course of recovery from myocardial hibernation. First, it shows that, on average, the recovery of function after revascularization is a rather slow and progressive phenomenon, with a time constant of about 40 days. Thus, in most patients, full recovery of function should not be expected before 4 to 6 months after revascularization. Our data also show that the rate of recovery varies substantially from patient to patient, some patients showing a very slow and delayed return of regional function, while others demonstrate an almost complete recovery by one week after revascularization. It is probable that, in these latter patients, significant changes would already have been noted in the operating room, had we performed an intraoperative assessment of function, as did Topol et al.[201] Perhaps the most important finding of this study is the observation that the rate of recovery of contractile function after revascularization is intimately related to the severity of the preexisting structural changes in the hibernating cardiomyocytes. This clearly suggests that these structural abnormalities are not simply the result of a mere coincidence but, to some extent, directly contribute to the contractile dysfunction of the hibernating myocardium.

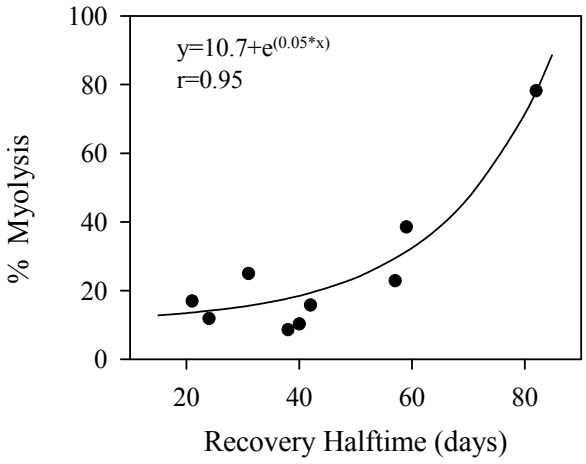

Figure 3-8. *Scatterplots of correlation between the proportion of myolytic cardiomyocytes and the recovery half-time. Adapted from Ref. 219.*

Although the present findings suggest that, like regional dysfunction, the structural changes are also reversible after revascularization, for obvious ethical reasons, we did not obtain direct evidence that it was indeed the case. This will probably await the development of relevant animal models of chronic left ventricular ischemic dysfunction.

Chapter 4 Implications for the Clinical Identification of Myocardial Viability

4.1 Introduction

Over the past 50 years, ischemic heart diseases have been a widespread cause of morbidity and the leading cause of mortality in the economically developed countries of the western world. Although the relative importance of coronary deaths has declined gradually during the last decade, "heart attacks" still account for approximately 25% of all deaths in the USA and in Europe. Mortality rates are higher in patients with severely depressed left ventricular function than in any other groups of patients, ranging from 15 to 60% per year.[61] Several studies have shown that surgical revascularization may improve survival and symptoms of heart failure in some of these patients.[1,151] The potential benefits of coronary revascularization should be balanced, however, with the higher surgical mortality of patients with left ventricular dysfunction, which ranges from 5 to 37%.

Presumably, the beneficial effects of revascularization result from improving blood supply to dysfunctional but viable regions with subsequent improvement in regional and global left ventricular function.[42] This scenario is supported by the results of several studies in patients with severe left ventricular dysfunction, showing that only patients with dysfunctional but "viable" myocardium invariably benefit from coronary revascularization.[53,59,126,197,232] Although these studies were retrospective and non-randomized, their results nevertheless suggest that, in addition to the evaluation of coronary anatomy, cardiac function and myocardial perfusion, the selection of patients with severe left ventricular dysfunction for coronary revascularization should also comprise a precise assessment of the presence of ischemi-cally compromised but viable myocardium.

Various approaches have been proposed to predict the reversibility of left ventricular dysfunction after coronary revascularization. Because regional contractile ischemic dysfunction reflects underlying alterations of myocardial perfusion and metabolism, flow and metabolic imaging with PET has focused much attention. As discussed in Chapter 3, PET is well suited for the delineation of the flow and metabolic patterns associated with the various causes of regional ischemic dysfunction. In theory thus, PET should permit an easy distinction between irreversible myocardial infarction and the reversible conditions of myocardial stunning and hibernation. Unfortunately, in daily clinical practice, patients seldom present with either purely stunned, hibernating or infarcted myocardium, but most often show an admixture of infarcted, potentially recoverable and normal myocardium, all coexisting within the same vascular territory.[184]

In this context, the identification of the potential for recovery after revascularization with PET may be far more complex than initially anticipated. In this chapter, I will review our approach to the evaluation of myocardial viability in unselected patients with coronary artery disease and left ventricular dysfunction and focus successively on:

1- the structural, flow and metabolic factors associated with the return of left ventricular contraction after revascularization in patients with chronic anterior wall dysfunction;[50]
2- the development of a multivariate approach to the identification of reversible dysfunction in patients with various degrees of left ventricular dysfunction;[77,217] and
3- the role of assessing residual inotropic reserve in the identification of reversible dysfunction after revascularization.[214,218]

The angiographic, echocardiographic and PET methodology is common to all studies and similar to that described in Chapter 3.

4.2. Flow, Metabolic and Structural Correlates of Reversible Left Ventricular Dysfunction after Revascularization

Because of the complex nature of the factors involved in the pathogenesis of chronic left ventricular ischemic dysfunction, a precise inventory of the factors associated with both the presence and extent of reversible injury is a necessary prerequisite to the development of a clinically relevant approach to the preoperative identification of reversible dysfunction. Accordingly, in this first study, we examined the structural, flow and metabolic factors associated with the return of left ventricular contraction after revascularization in patients with chronic anterior wall dysfunction. As in previous studies, we took advantage of the surgical procedure to obtain biopsies from the dysfunctional area, and correlated the flow, metabolic and morphometric findings with the presence and extent of functional recovery after revascularization.

Methods

We studied 24 nondiabetic patients (19 men, mean age 57 ± 13 years, range 27 - 72 years) with anterior wall dysfunction related to significant disease (> 75% diameter stenosis) on the left anterior descending coronary artery. Twelve patients had experienced a previous anterior myocardial infarction, the most recent 33 days before the study. All patients underwent successful coronary artery bypass surgery at an average of 54 days after the PET study, the left internal mammary artery being used to graft the left anterior descending coronary artery. The decision to revascularize was based on clinical criteria and not on the results of the PET study.

Selective coronary angiography and contrast cineventriculography were performed in every patient at an average of 34 days before the PET study. Complete occlusion of the proximal left anterior descending artery was found in 15 patients, and severe proximal stenosis in the remaining 9. There were 5 patients with single left anterior descending coronary artery disease, 9 patients with 2-vessel disease and 10 patients with 3-vessel disease. No patient showed significant left main stenosis.

Contrast cineventriculography (n=8) or two-dimensional echocardiography (n=16) were obtained at baseline and again 4.6 ± 2.7 months after surgery to assess the recovery of contractile function after revascularization. With both techniques, left ventricular volumes at end-diastole (r wave of the electrocardiogram) and end-systole (minimal volume) were calculated by use of the Simpson's method. With ventriculography, regional wall motion was assessed in 5 segments (antero-basal, antero-lateral, apical, inferior and postero-basal) by 2 experienced observers. Each segment was defined as: 0 - normal, 1 - hypokinetic, 2 - akinetic, 3 - dyskinetic. A wall motion score for the segments perfused by the left anterior descending coronary artery was calculated by summing up the scores of the antero-basal, antero-lateral and apical segments. With 2D-echocardiography, regional wall motion was assessed in 16 segments and defined as: 0 - normal, 1 - hypokinetic, 2 - akinetic, 3 - dyskinetic. A wall motion score for the segments perfused by the left anterior descending coronary artery was also calculated by summing up the scores of the mid anterior, antero-apical and latero-apical segments.

According to the changes in regional wall motion and global left ventricular function, patients were considered to have myocardium which improved function after revascularization if end-systolic volume decreased [83,226] and regional wall motion score improved by at least one full grade from baseline to the follow-up study.

Similarly, patients were considered to have persistently dysfunctional myocardium if end-systolic volume increased or if regional wall motion failed to improve at follow-up.

Results

Clinical and angiographic characteristics. Table 4-1 summarizes the individual clinical and

TABLE 4-1. Individual Clinical and Angiographic Characteristics before and after Revascularization

Patients	Age/sex (years)	Previous MI	% coronary stenosis LAD	LC	RCA	AWMS pre	AWMS post	EDV pre	EDV post	ESV pre	ESV post	EF pre	EF post
Patients with improved function													
# 1	47/M	No	90%	-	-	2	1	232	182	87	55	63	70
# 2	63/M	No	100%	75%	-	3	0	195	192	69	52	65	73
# 3	69/M	No	100%	-	-	2	1	260	204	107	97	59	53
# 4	31/M	Yes	100%	-	100%	3	1	187	220	85	81	56	61
# 5	70/M	No	100%	75%	-	4	2	213	138	93	38	56	73
# 6	27/F	No	100%	-	-	2	0	150	148	68	55	55	63
# 7	69/M	No	90%	90%	100%	3	0	189	186	131	108	31	42
# 8	68/M	No	100%	75%	75%	3	0	119	121	57	49	53	59
# 9	46/M	No	90%	90%	100%	5	3	200	182	135	107	33	41
# 10	58/F	No	90%	-	100%	5	4	154	100	100	55	35	45
# 11	41/M	Yes	100%	75%	100%	5	4	295	340	262	246	11	28
# 12	51/M	Yes	90%	100%	100%	5	1	211	206	151	110	28	47
# 13	66/M	Yes	100%	-	100%	6	4	161	112	99	51	39	54
# 14	67/F	Yes	100%	90%	100%	6	3	123	137	97	76	21	45
# 15	68/M	No	100%	-	100%	4	3	267	221	208	162	22	27
# 16	63/M	No	90%	90%	100%	6	4	157	143	105	83	33	42
Patients with persistent dysfunction													
# 17	67/F	Yes	90%	-	75%	5	5	201	260	121	152	40	41
# 18	39/M	Yes	100%	-	-	7	8	296	379	211	320	29	16
# 19	48/M	Yes	100%	90%	-	5	5	205	209	96	159	53	24
# 20	57/F	Yes	100%	90%	100%	5	5	173	198	112	173	35	13
# 21	71/M	No	90%	-	-	6	6	240	252	175	204	27	19
# 22	72/M	Yes	100%	90%	75%	6	6	178	224	122	175	31	22
# 23	54/M	Yes	90%	100%	100%	6	6	201	190	143	143	39	25
# 24	57/M	Yes	90%	75%	100%	5	5	305	315	208	235	32	25

MI, myocardial infarction; LAD, left anterior descending coronary artery; LC, circumflex artery; RCA, right coronary artery; AWMS, anterior wall motion score; EDV(ml), end-diastolic volume; ESV(ml), end-systolic volume; EF(%), ejection fraction; pre, before revascularization; post, after revascularization.

angiographic characteristics of the study population. Pre-revascularization ejection fraction averaged 39 ± 15% and mean anterior wall motion score was 4.5 ± 1.5. Ejection fraction was lower in patients with (34 ± 12%) than in those without (45 ± 16%, $p<0.01$) previous Q-wave infarction. Similarly, anterior wall motion score was worse (5.3 ± 1.0) in patients with than in those without (3.8 ± 1.5, $p<0.05$) previous Q-wave infarction.

As judged from the changes in regional wall motion and global left ventricular function before and after revascularization, 16 patients showed improved function following surgery while 8 patients showed persistent dysfunction despite revascularization. Table 4-2 shows the changes in global and regional left ventricular function in these 2 groups of patients. Before revascularization, ejection fraction was not significantly different among the 2 groups (43 ± 18% compared with 35 ± 9%, p=ns). After revascularization, patients with improved function increased ejection fraction and decreased left ventricular end-systolic volume (to 51 ± 14% and to 90 ± 52 ml, respectively, $p<0.001$ compared with preoperative values), whereas patients with persistent dysfunction

TABLE 4-2. Left Ventricular Volumes, Ejection Fraction and Regional Wall Motion Score before and after Revascularization.

		Improved (*n*=16)	Non-improved (*n*=8)
End-diastolic volume (ml)	before	195 ± 51	225 ± 51
	after	177 ± 58	253 ± 65
End-systolic volume (ml)	before	115 ± 54	149 ± 52
	after	90 ± 52	195 ± 59
Ejection fraction (%)	before	43 ± 18	35 ± 9
	after	51 ± 14	23 ± 9
AWMS	before	4.0 ± 1.5	5.6 ± 0.7
	after	1.9 ± 1.6	5.5 ± 0.9

There was no statistically significant difference in baseline left ventricular function between the 2 groups, except in anterior wall motion score ($p<0.01$). No statistical analysis was applied to the differences in left ventricular function after revascularization, which are built in by study design.

further deteriorated ejection fraction (to 23 ± 9%, p<0.01 compared with preoperative value) and increased end-systolic volume (to 195 ± 59 ml, p<0.01 compared with preoperative value).

Structural abnormalities in viable and nonviable myocardium. The individual morphological changes observed in biopsy specimens of patients with and without post-operative functional improvement are shown in Table 4-3. At the time of bypass surgery, gross macroscopic evidence of scar was seen in only one patient with persistent dysfunction and a previous Q-wave myocardial infarction. With light microscopy, patients with previous Q-wave infarction had a significantly larger surface of the biopsy occupied by fibrotic tissue (41 ± 21% compared with 24 ± 12%, p<0.05) than those without. Consequently, the relative surface actually covered by cardiomyocytes was significantly lower in patients with previous infarction. Typical examples of sections stained with toluidine-blue and PAS are illustrated in Plate 4-1. As shown in Figure 4-1, tissue samples from myocardium in which function improved following revascularization showed significantly less transmural (24 ± 13 compared with 49 ± 20%, p=0.002) and less subendocardial (20 ± 13 [n=9] compared with 53 ± 27% [n=5], p=0.008) fibrosis than tissue samples from persistently dysfunctional myocardium. A cut off value of 35% transmural fibrosis (from discriminant analysis) best differentiated patients with from those without post-operative functional improvement. By use of this cut off value, the severity of tissue fibrosis allowed to correctly identify 12/16 (75%) patients with and 7/8 (88%) without post-operative functional improvement. As illustrated in Figure 4-2, the percent of both transmural and subendocardial fibrosis correlated with both postoperative anterior wall motion score (r=0.74, p<0.001 and r=0.76, p<0.01, respectively) and the changes in anterior wall motion after revascularization (r=0.66, p<0.001 and r=0.62, p<0.05, respectively).

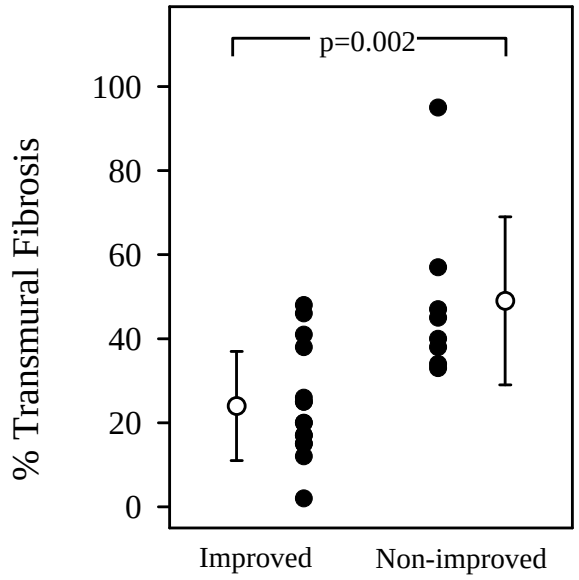

***Figure 4-1**. Dot plot showing individual percentages of the biopsy covered by fibrosis in patients with and without post-operative functional improvement. Note that patients who improved function post-operatively had significantly less tissue fibrosis than patients with persistent post-operative dysfunction. Adapted from Ref. 50.*

TABLE 4-3. Individual Flow, Metabolic and Structural Characteristics before Revascularization

Patients	MBF	rel NH_3	rMGU	rel FDG	rMGU/ MBF	FDG/NH_3	% AC SE	% AC TM	% fibrosis SE	% fibrosis TM
Patients with improved function										
# 1	98	83	38	120	1.45	0.39	51	38	16	17
# 2	78	81	31	87	1.08	0.40	21	22	26	26
# 3	98	82	41	111	1.35	0.42	34	30	12	12
# 4	73	73	42	76	1.04	0.58	47	18	10	41
# 5	100	78	37	113	1.45	0.37	NA	55	NA	38
# 6	75	61	24	73	1.19	0.32	NA	35	NA	17
# 7	97	80	82	90	1.13	0.85	82	71	0	2
# 8	104	80	75	98	1.22	0.72	31	36	28	20
# 9	54	64	96	67	1.05	1.78	15	23	43	25
# 10	67	47	64	84	1.79	0.96	NA	14	NA	48
# 11	60	70	44	97	1.38	0.73	46	37	20	15
# 12	100	78	35	90	1.15	0.35	NA	50	NA	15
# 13	59	58	46	58	1.00	0.78	NA	30	NA	46
# 14	118	75	57	60	0.80	0.48	28	30	29	25
# 15	85	92	60	83	0.90	0.71	NA	34	NA	20
# 16	135	80	22	96	1.20	0.16	NA	32	NA	23
Patients with persistent dysfunction										
# 17	46	49	28	106	2.17	0.61	40	34	43	33
# 18	43	47	4	50	1.06	0.06	3	2	95	95
# 19	86	69	31	52	0.76	0.36	NA	22	NA	45
# 20	66	41	28	42	1.03	0.42	7	4	62	57
# 21	61	64	37	76	1.19	0.61	16	12	37	35
# 22	50	76	26	98	1.29	0.52	53	45	28	38
# 23	52	54	46	38	0.70	0.88	NA	29	NA	47
# 24	63	60	40	66	1.10	0.63	NA	21	NA	40

MBF[ml.(min.100g)$^{-1}$], myocardial blood flow; rel NH_3(%), relative ammonia uptake; rMGU[µmol.(min.100g)$^{-1}$], regional myocardial glucose uptake; rel FDG(%), relative FDG uptake; FDG/NH_3, mismatch ratio; % AC, surface of the biopsy occupied by abnormal cardiomyocytes; SE, subendocardium; TM, transmural; % fibrosis, surface of the biopsy occupied by fibrosis; NA, not available. Units of rMGU/MBF are µmol/ml.

Compared with cardiomyocytes in remote "normal" myocardium, about half the myocardial cells from dysfunctional segments showed various degrees of dedifferentiation. Although structurally altered cardiomyocytes were present in both groups of patients, their relative amount and distribution differed significantly among the 2 groups. In myocardium whose function improved following surgery, altered cardiomyocytes occupied 35 ± 14% of the surface of the biopsy (Figure 4-3) and were mainly located in the subendocardium. By contrast, in persistently dysfunctional myocardium, altered cardiomyocytes occupied only 21 ± 15% of the surface of the biopsy ($p=0.04$ compared with myocardium which improved post-operatively). The changes in wall motion score following revascularization were inversely correlated with the amount of altered cardiomyocytes ($r=-0.48$, $p<0.05$).

Myocardial blood flow and metabolism in relation to post-operative functional outcome. Before revascularization, myocardium which improved functionally following revascularization had significantly higher ^{13}N-ammonia uptake (74 ± 11 versus 58 ± 12%,

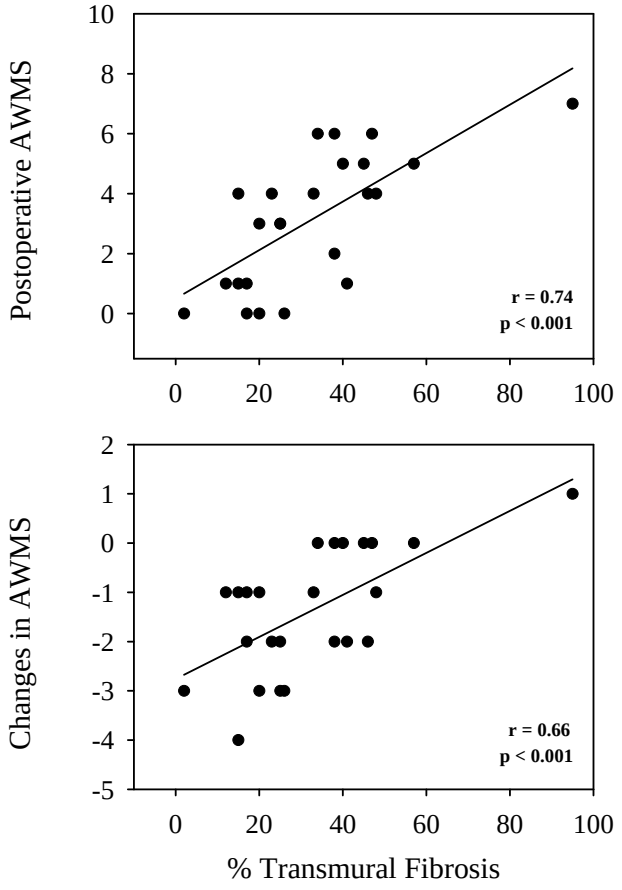

***Figure 4-2**. Top. Scatterplot showing the relationship between postoperative anterior wall motion score and the relative surface of the biopsy occupied by fibrosis. Bottom. Scatterplot showing the relationship between the changes in wall motion after revascularization and the relative surface of the biopsy occupied by fibrosis. Correlation coefficients were obtained with the Spearman rank correlation. Adapted from Ref. 50.*

p=0.003), absolute myocardial blood flow (88 ± 23 versus 61 ± 12 ml.(min.100g)$^{-1}$, p=0.005), relative FDG uptake (88 ± 18 versus 66 ± 26%, p=0.03) and absolute myocardial glucose uptake (50 ± 21 versus 30 ± 13 µmol.(min.100g)$^{-1}$, p=0.02) than myocardium with persistent post-operative dysfunction. By contrast, the relative FDG/ammonia ratio (1.20 ± 0.24 compared with 1.16 ± 0.45, p=ns), and both absolute (0.62 ± 0.38 compared with 0.51 ± 0.24 µmol/ml, p=ns) and normalized (% of remote) (136 ± 50 compared with 119 ± 35%, p=ns) glucose extraction was not significantly different among the 2 groups.

Both absolute myocardial blood flow (102 ± 14 vs. 98 ± 22 ml.(min.100g)$^{-1}$, p=ns) and glucose uptake (48 ± 24 compared with 42 ± 18 µmol.(min.100g)$^{-1}$, p=ns) were similar among remote regions of patients with and without post-operative functional improvement. Also, there was no significant difference in heart rate (71 ± 11 compared with 70 ± 15 beats.min^{-1}, p=ns) or rate-pressure product (9,454 ± 1,496 compared with 8,133 ± 1,889 mm Hg.beats.min^{-1}, p=ns) between the 2 groups at the time of the PET study.

As shown in Figure 4-4, a significant correlation was observed between the surface of the biopsy occupied by fibrosis and relative ammonia uptake (r=-0.73, p<0.001). The correlation was even stronger when subendocardial instead of transmural data were used (r=-0.82, p<0.001). Significant, though weaker, correlations were found between the surface of the biopsy occupied by fibrosis and both absolute and

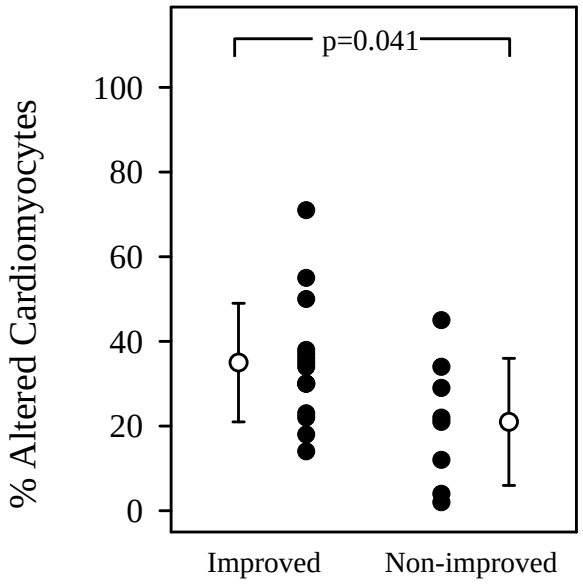

***Figure 4-3**. Dot plot showing individual percentages of the biopsy covered by cardiomyocytes with excess glycogen in patients with and without post-operative functional improvement. Note that patients who improved function post-operatively had significantly more cardiomyocytes with excess glycogen than patients with persistent post-operative dysfunction. Adapted from Ref. 50.*

normalized myocardial blood flow (r=-0.43, p<0.05 and -0.52, p<0.01, respectively). A correlation was also found between the percent surface of the biopsy occupied by abnormal cardiomyocytes and relative FDG uptake (r=0.63, p<0.01, Figure 4-4). The correlation was similar with the use of subendocardial data (r=0.64, p<0.01). A significant correlation was also found with absolute (r=0.49, p<0.05) but not with normalized levels of regional glucose uptake.

Multivariate analysis. To define further the variables associated with the return of regional ventricular function after coronary revascularization, all flow, metabolic and morphometric data available were proposed for inclusion into a multiple regression model. With univariate analysis, the improvement in wall motion score after revascularization was significantly associated with the severity of tissue fibrosis (r=0.64, p<0.001), absolute myocardial blood flow (r=-0.55, p=0.005), the relative surface of the biopsy occupied by altered cardiomyocytes (r=-0.55, p=0.005), baseline left ventricular end-diastolic volume (r=0.51, p=0.01) and absolute myocardial glucose uptake (r=-0.42, p<0.05). Stepwise multiple regression analysis selected the severity of tissue fibrosis, baseline left ventricular end-diastolic volume and absolute myocardial blood flow as independent correlates of the improvement of regional left ventricular function after revascularization. Of these 3 parameters, the severity of tissue fibrosis was the most significant.

Discussion

The results of this study indicate that functional improvement following revascularization is strongly associated with both the extent and the severity of tissue fibrosis, with the relative amount of metabolically active and morphologically viable, albeit often structurally remodeled, cardiomyocytes and with a normal or nearly normal resting myocardial perfusion.

The salient findings in this study relate to the structural differences in myocardium with and without functional improvement following revascularization. Myocardium which improved function following surgery showed significantly less transmural (24 ± 13 versus 49 ± 20%) and subendocardial (20 ± 13 versus 53 ± 27%) tissue fibrosis but contained significantly more metabolically active cardiomyocytes than myocardium with persistent post-operative dysfunction. This includes a larger proportion of altered cells (35 ± 14% versus 21 ± 15%). The threshold amount of tissue fibrosis that best differentiated myocardium with from that without post-operative functional improvement was 35%. This means that at least 65% of the

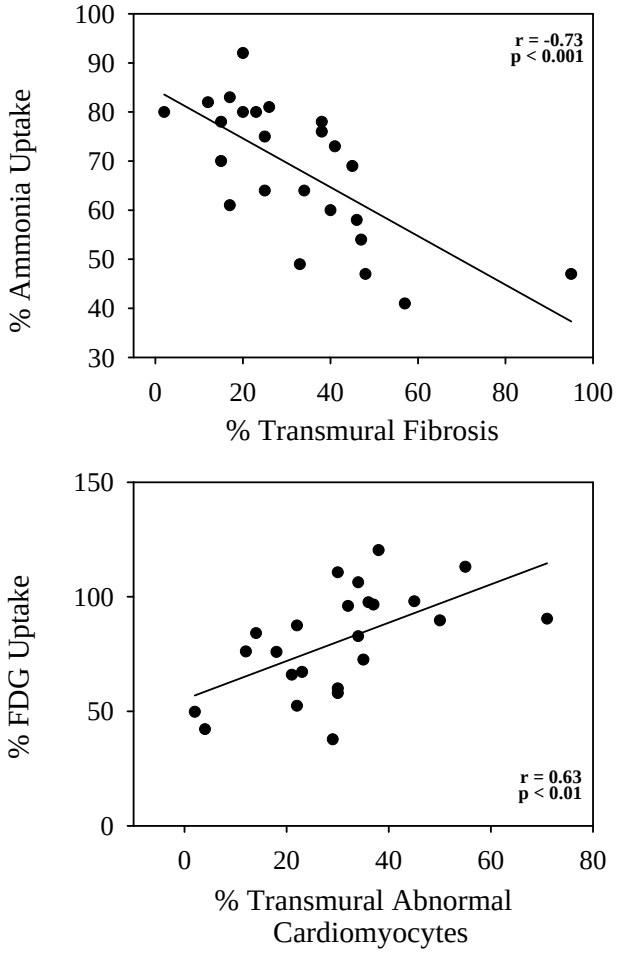

Figure 4-4*. Top. Scatterplot showing the relationship between relative anterior wall ammonia uptake and the relative surface of the biopsy occupied by fibrosis. Bottom. Scatterplot showing the relationship between relative anterior wall FDG uptake and the relative surface of biopsy occupied by abnormal cardiomyocytes. Correlation coefficients were obtained with the Spearman rank correlation. Adapted from Ref. 50.*

thickness of the dysfunctional wall needs to be occupied by potentially salvageable cardiomyocytes to portend functional recovery after revascularization. This value is similar to the threshold of relative ^{13}N-ammonia uptake (66%) that best differentiated "improved" from "non-improved" myocardium in our study, and to the minimal value of perfusable tissue index (70%) associated with viability.[52,231] These data thus suggest that the amount of tissue fibrosis is the structural basis underlying the ability to predict functional recovery by the measurement of residual tissue perfusion.

A second and equally important finding in this study relates to the levels of resting myocardial perfusion found in reversibly versus persistently dysfunctional myocardial segments. Resting myocardial blood flow was better preserved, and actually non significantly different from that in remote normal segments (88 ± 23 versus 102 ± 14 ml.(min.100g)$^{-1}$), in reversibly as opposed to persistently dysfunction segments. On an individual patient basis, all but 2 patients (87%) with reversible dysfunction after revascularization had normal levels (i.e., within the range of normal volunteers) of absolute myocardial blood flow to the dysfunctional area. These figures are quite similar to those previously reported by other investigators by use of either relative or quantitative PET imaging.[44,130,200,211]

Finally, this study confirms that myocardial glucose uptake is increased in reversibly as opposed to persistently dysfunctional myocardium.[36,37,196,200] In addition, the data show the uptake of glucose by the dysfunctional segments is intimately related to both the presence and amount of structurally altered cardiomyocytes.

This study has limitations, which should not be ignored. First, the interpretation of the relationship between the morphological changes seen in the microscope and the metabolic abnormalities observed with PET requires caution, mainly because of the small size of the biopsy samples. Indeed, for small samples, like the ones obtained in this study, to be representative of the underlying pathology, the morphological changes must be evenly distributed in the area of interest, which may not be the case in patients with previous myocardial infarction. As shown on Figure 4-2, however, the 2 groups of patients were reasonably well separated on the basis of tissue fibrosis, which suggests that despite potential sampling errors the 2 groups were quite homogenous. Second, subendocardial data were unavailable in 10 patients whose biopsy specimens were not separated immediately into an endocardial and an epicardial portion at the time of sampling. Since ischemic damage is always more severe in the subendocardium compared with the subepicardium, failure to obtain specific subendocardial samples in all patients may have influenced the results of the relationships between morphological and functional parameters. However, although consideration of subendocardial instead of transmural data in the subgroup of patients in whom they were available yielded slightly better correlation coefficients, these improvements were marginal and should not alter our conclusions. Finally, the fact that pre-operative studies occurred days to weeks before surgery raises the possibility that intervening events could have influenced the outcome in individual patients. Nonetheless, this possibility is unlikely since all patients were in stable condition and did not experience symptomatic deterioration during the interval preceding surgery.

In summary, we have described the structural, flow and metabolic correlates of the reversibility of left ventricular ischemic dysfunction in a group of patients with chronic coronary artery disease undergoing revascularization. In these patients, the recovery of contraction is associated with both the extent and the severity of tissue fibrosis, with the residual relative amount of metabolically active cardiomyocytes and with normal or nearly normal levels of resting myocardial perfusion.

4.3. Prediction of Reversible Left Ventricular Dysfunction after Revascularization by PET in Unselected Patients with Coronary Artery Disease

As shown in the preceding study, the flow and metabolic correlates of reversible myocardial ischemic dysfunction are quite multiple and complex, making it difficult to determine which of the variables has the best accuracy if the others are not considered simultaneously in a multivariate analysis. So far, results of such an integrated approach to the preoperative identification of reversible dysfunction have not been reported. Accordingly, we studied 2 different groups of patients with anterior wall dysfunction undergoing coronary revascularization. In the first group of patients, all preoperative PET flow and metabolic data generated were proposed for inclusion into a multivariate discriminant model to determine the best predictors of the return of function after revascularization. The accuracy of the discriminant function was tested in a separate group of patients with anterior wall dysfunction.

Methods

Initial study group. We studied 25 nondiabetic patients (20 men, mean age 57 ± 12 years, range 30 - 72 years) with chronic left anterior wall dysfunction and well defined coronary anatomy, whose individual clinical characteristics are summarized in Table 4-4. By reviewing all diagnostic coronary angiograms performed at 2 clinical sites, we selected prospectively patients having isolated severe anterior wall dysfunction due to proximal left anterior descending coronary artery disease. Fourteen patients had sustained at least one previous myocardial infarction, the most recent occurring 11 days before the tomographic study. Subsequent to the PET study, all patients underwent complete coronary revascularization. The decision to revascularize was based on clinical criteria and not on the results of the PET study. Bypass surgery was performed in 7 patients, with the use of the internal mammary artery to graft the left anterior descending coronary artery, and coronary angioplasty was performed in the remaining 18 patients. The adequacy of revascularization was based on the results of the follow-up angiographic study, performed prospectively in every patient 6 to 9 months after revascularization.

Selective coronary arteriography and left ventriculography were performed at an average of 17 days before the PET study (range 1 - 40 days) and again 6 to 9 months after revascularization. Significant disease was defined as a greater than 70% luminal diameter stenosis in any major coronary branch. Sixteen patients showed complete occlusion of the proximal left anterior descending coronary artery. The remaining 9 patients had severe proximal left anterior descending coronary artery stenosis (75 to 90 % percent luminal diameter stenosis). Fifteen patients had single left anterior descending coronary artery disease, 9 patients had two vessel disease, among whom 6 had a right coronary and 3 a left circumflex coronary artery disease. One patient had 3-vessel disease. None of the patients had left main stenosis. LV volumes and ejection fraction and regional wall motion score were calculated as above.

Patients with a left ventricular ejection fraction <35%. The flow and metabolic data obtained in the initial study group were used to generate an equation for prediction of reversible postoperative dysfunction. The accuracy of this function was tested in a separate group of 26 patients with an ejection fraction <35% (24 men, mean age 62 ± 8 years, range 40 to 74 years). Twenty-three patients had sustained a previous anterior Q-wave myocardial infarction, the most recent occurring 45 days before inclusion into the study. 7 patients had type II diabetes mellitus, among whom 6 were treated with oral sulfonamides and 1 with insulin (70 UI SC daily).

TABLE 4-4. Individual Clinical and Angiographic Characteristics before and after Revascularization

Patients	Age/sex (years)	Previous MI	% coronary stenosis LAD	LC	RCA	AWMS pre	AWMS post	EDV pre	EDV post	ESV pre	ESV post	EF pre	EF post
Patients with improved function													
# 1	63/F	No	100	-	-	4	3	97	72	45	26	54	64
# 2	63/F	Yes	100	-	-	5	1	NA	NA	NA	NA	53	69
# 3	72/M	No	100	-	70	5	3	104	96	50	39	52	59
# 4	51/F	No	100	-	-	4	1	NA	NA	NA	NA	59	75
# 5	64/M	Yes	100	-	-	5	3	120	112	60	46	50	59
# 6	46/M	No	100	-	-	4	2	101	114	42	41	58	64
# 7	63/F	Yes	100	-	-	5	3	123	156	81	66	34	58
# 8	62/M	No	100	70	-	3	0	113	111	40	30	65	73
# 9	46/F	No	100	-	-	3	1	134	105	50	32	63	70
# 10	68/M	No	85	-	-	3	2	150	118	62	56	59	53
# 11	62/M	No	100	-	-	5	2	NA	NA	NA	NA	38	63
# 12	51/M	No	100	-	-	4	0	NA	NA	NA	NA	60	75
# 13	69/M	No	100	75	-	4	2	123	80	54	22	56	73
# 14	62/M	Yes	90	60	-	7	5	100	100	71	50	29	50
# 15	42/M	No	100	-	-	4	1	70	56	38	16	46	71
# 16	30/M	Yes	100	-	100	3	1	108	127	47	49	56	61
# 17	49/M	Yes	100	75	100	5	4	142	107	102	69	28	36
Mean±SD						5±1	2±1	114±21	103±25	57±18	40±17	51±12	63±18
Patients with persistent dysfunction													
# 18	66/M	Yes	90	-	75	6	6	101	130	60	83	41	36
# 19	65/M	Yes	90	-	100	5	5	120	169	71	97	41	43
# 20	38/M	Yes	90	-	-	5	7	119	146	63	66	47	55
# 21	65/M	Yes	90	-	60	4	3	97	119	37	49	62	59
# 22	67/M	Yes	90	60	-	5	4	116	150	70	88	40	41
# 23	39/M	Yes	100	-	-	9	10	171	219	122	185	29	16
# 24	65/M	Yes	90	-	-	5	7	118	87	51	57	57	34
# 25	62/M	Yes	90	-	-	4	4	120	114	60	46	50	60
Mean±SD						6±2	6±3	120±22	142±40	67±25	84±45	46±11	43±15

MI, myocardial infarction; LAD, left anterior descending coronary artery; LC, circumflex artery; RCA, right coronary artery; AWMS, anterior wall motion score; EDV(ml), end-diastolic volume; ESV(ml), end-systolic volume; EF(%), ejection fraction; pre, before revascularization; post, after revascularization.

Selective coronary arteriography was also performed in every patient. Ten patients showed complete occlusion of the proximal left anterior ascending coronary artery. The remaining 16 patients had severe proximal stenosis of the same vessel. One patient had isolated left anterior descending coronary artery disease, 6 patients had 2-vessel disease, among whom 4 had a right coronary artery disease and 2 a left circumflex coronary artery disease; 19 patients had 3-vessel disease.

In both study groups, patients were considered to have myocardium which improved functionally after revascularization if end-systolic volume decreased [83,226] and regional wall motion score improved by at least one full grade from baseline to the follow-up study. Similarly, patients were considered to have persistently dysfunctional

TABLE 4-5. Individual Flow and Metabolic Characteristics before Revascularization

Patients	MBF [ml.(min.100g)$^{-1}$]	rel NH3 (%)	rMGU [µmol.(min.100g)$^{-1}$]	rel FDG (%)	FDG-to-ammonia ratio	rMGU/MBF (µmol.ml^{-1})
Patients with improved function						
# 1	99	91	19	135	1.49	0.19
# 2	67	57	41	138	2.46	0.61
# 3	75	80	63	98	1.17	0.84
# 4	45	34	26	182	6.07	0.58
# 5	49	69	30	61	0.90	0.61
# 6	102	80	47	86	1.10	0.46
# 7	93	58	14	101	1.53	0.15
# 8	57	88	32	91	1.03	0.56
# 9	72	67	41	101	1.50	0.57
# 10	110	81	41	109	1.34	0.37
# 11	90	89	30	82	0.91	0.33
# 12	62	69	57	100	1.47	0.92
# 13	96	82	37	119	1.45	0.39
# 14	73	50	22	107	2.26	0.30
# 15	89	85	51	96	1.13	0.57
# 16	87	75	41	91	1.20	0.47
# 17	49	57	23	96	1.75	0.47
Mean±SD	77±20	71±16	36±14	105±27	1.69±1.21	0.49±0.20
Patients with persistent dysfunction						
# 18	37	39	32	42	1.11	0.86
# 19	50	71	27	77	1.08	0.54
# 20	45	71	15	81	1.16	0.33
# 21	56	61	23	149	2.45	0.41
# 22	56	52	28	112	2.17	0.50
# 23	48	46	3	137	3.01	0.06
# 24	68	55	37	33	0.60	0.39
# 25	47	50	25	98	1.92	0.53
Mean±SD	51±9	56±11	24±11	91±41	1.69±0.83	0.45±0.23

MBF, myocardial blood flow; rel NH3, relative ammonia uptake; rMGU, regional myocardial glucose uptake; rel FDG, relative FDG uptake.

myocardium if end-systolic volume increased or if regional wall motion failed to improve at follow-up.

Statistical analysis. Values are expressed as mean ± one standard deviation. An exact Fisher test was used to assess differences in categorical variables. A Mann-Whitney rank-sum test was used to assess differences in continuous variables between patients with and without evidence of myocardial viability. All tests were two-tailed and a probability value greater than 0.05 was considered indicative of a statistically nonsignificant difference. The 9 previously defined PET variables were submitted to a stepwise linear discriminant analysis with a forward selection procedure. Variables were entered until no F-to-enter statistics were significant at the 5% level and until the mean squared error reached a minimum. The power of the discriminant function was assessed by the canonical correlation. Based on the results of the

TABLE 4-6. Myocardial blood flow and regional glucose uptake in 25 patients classified according to changes in regional wall motion score and end-systolic volume before and after revascularization.

			Improved (*n*=17)	Non-improved (*n*=8)
Myocardial blood flow	[ml.(min.100g)-1]	remote	97 ± 18	87 ± 18
		anterior	77 ± 20 ***	51 ± 9 *** ‡
Myocardial glucose uptake	[µmol.(min.100g)-1]	remote	36 ± 18	37 ± 28
		anterior	36 ± 14	24 ± 11 †
Glucose extraction	(µmol.ml-1)	remote	0.39 ± 0.22	0.42 ± 0.31
		anterior	0.49 ± 0.20 **	0.45 ± 0.23
FDG/ammonia		anterior	1.69 ± 1.21	1.69 ± 0.83
Rate-pressure product	(bpm x mm Hg)		9,944 ± 1,976	7,516 ± 890 †

* $p<0.05$, ** $p<0.01$, *** $p<0.001$ versus remote from the same group
† $p<0.05$, ‡ $p<0.01$ versus anterior from the improved group

discriminant analysis, an equation was built that provided maximal separation between patients with and without viable myocardium. A jackknife-validation procedure was performed to reduce the bias in the evaluation of the number of patients correctly classified into each group. The predictive accuracy of the discriminant function was determined by the Cohen's kappa coefficient.

Results in the initial study group

Clinical and angiographic characteristics. Bypass surgery was performed in 7 patients, with the use of the internal mammary artery to graft the LAD, and coronary angioplasty was performed in the remaining 18 patients. None of the patients suffered from perioperative or post-angioplasty myocardial infarction. As judged from the results of the follow-up angiographic study, performed prospectively in every patient 6 to 9 months after revascularization, complete revascularization was achieved in all patients undergoing bypass surgery and in 8 of 18 patients undergoing angioplasty. In the remaining 10 patients, a restenosis had occurred at the site of the initially successful angioplasty. In 8 of these patients, the restenosis was moderate (50-75% luminal diameter stenosis), while in 2 other patients, reocclusion or severe restenosis (75-95% luminal diameter stenosis) of the left anterior descending coronary artery had occurred. Regional wall motion score and global left ventricular function improved in 8 patients despite restenosis, including the 2 patients with reocclusion or severe restenosis.

According to the changes in resting anterior wall motion and end-systolic volume before and after revascularization, the patients were categorized into two groups: group 1 (*improved*) 17 patients (15 men, mean age 56 ± 12 years, range 30 - 72) with improved anterior wall motion score (-2.47 ± 0.94 grade) and end-systolic volume (-15 ± 11 ml/m²); group 2 (*non-improved*) 8 patients (7 men, mean age 58 ± 12 years, range 38 - 67) with an increase in end-systolic volume (+ 17 ± 22 ml/m²) and variable changes in anterior wall motion score (3 patients with no changes, 2 patients with improvement by only 1 grade and 3 patients with deterioration). Before revascularization, anterior wall motion score, left ventricular volumes, left ventricular ejection fraction and coronary anatomy were similar among the 2 patient groups (p=ns, Table 4-4). There was, however, a significantly greater proportion of patients with previous myocardial infarction in the group with persistent postoperative dysfunction (100 versus 35%, p<0.01). As shown in Figure 4-5, an inverse correlation was observed between the changes in global ejection fraction and the improvement in

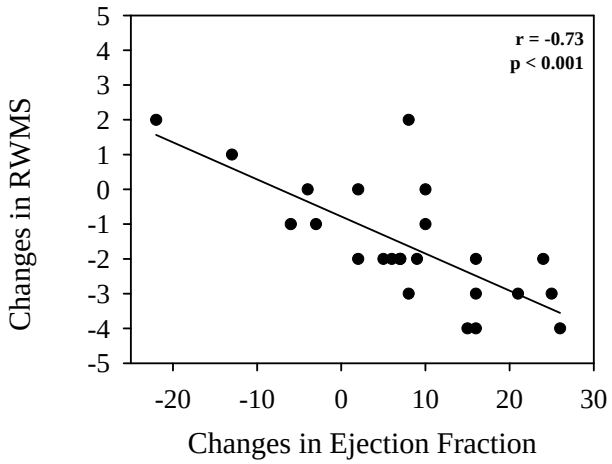

Figure 4-5. *Scatterplot showing the relation between the changes in regional wall motion score and the changes in global left ventricular ejection fraction following revascularization. Correlation coefficients were obtained with the Spearman rank correlation. Adapted from Ref. 77.*

regional wall motion score after revascularization (r=-0.73, p<0.001).

Estimates of myocardial perfusion and metabolism before revascularization. The individual tomographic measurements of myocardial perfusion and metabolism before revascularization are shown in Table 4-5. Mean values for these measurements in remote normal and ischemic regions in groups of patients with and without reversible dysfunction are presented in Table 4-6. Before revascularization, reversibly dysfunctional myocardium exhibited significantly higher absolute myocardial blood flow (77 ± 20 versus 51 ± 9 ml.(min.100g)$^{-1}$, p=0.004, Figure 4-6) than myocardium with persistent postoperative dysfunction. Absolute regional myocardial glucose uptake (36 ± 14 versus 24 ± 11 μmol.(min.100g)$^{-1}$, p=0.04, Figure 4-7) was also slightly higher in reversibly compared with persistently dysfunctional myocardium.

To explore possible reasons for interpatient variability in blood flow in normal remote myocardium, absolute levels of perfusion were compared with rate-pressure product as an index of myocardial oxygen demand. A linear relation

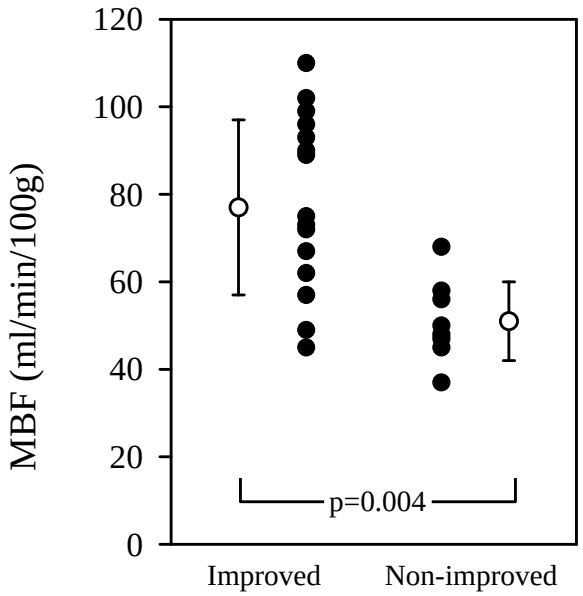

Figure 4-6. *Dot plot showing individual absolute myocardial blood flow (MBF) in patients with and without post-operative functional improvement. Adapted from Ref. 77.*

was observed between rate-pressure product and myocardial blood flow (r=0.56, p<0.01). In contrast, blood flow (r=0.35, p=ns) was unrelated to rate-pressure product in dysfunctional segments.

As shown in Figure 4-8, the FDG over ammonia ratio did not differ among patients with and without reversible dysfunction. A flow-metabolism mismatch pattern was present in 11 of 17 patients with reversible dysfunction (sensitivity 65%) and 4 of 8 patients with persistent postoperative dysfunction (specificity 50%). The overall accuracy was 60%. It should be pointed out, however, that 8 of 17 (47%) patients with reversible dysfunction and no patient with persistent postoperative dysfunction had normal perfusion at rest, defined as >80% of maximal perfusion (p=0.05). If only patients with relative hypoperfusion in anterior regions (<80% of maximal perfusion) are considered, 8 patients with reversible (sensitivity 89%) and 4 patients with persistent dysfunction (specificity 50%) showed a flow-metabolism mismatch pattern in the anterior region. Overall accuracy was 77%.

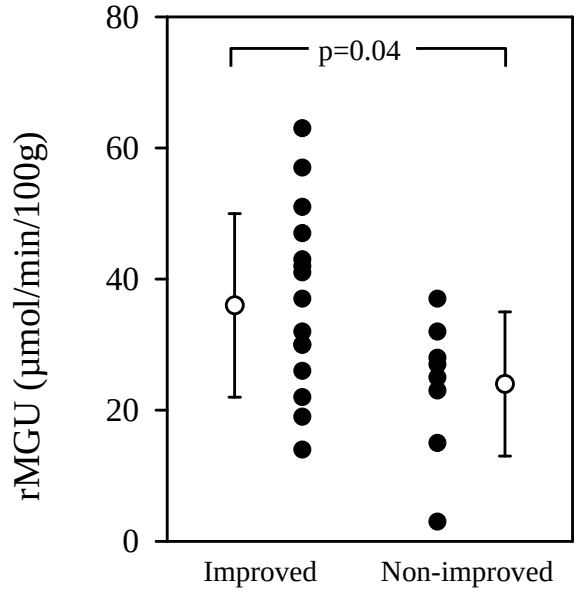

Figure 4-7*. Dot plot showing individual absolute regional myocardial glucose uptake (rMGU) in patients with and without post-operative functional improvement. Note that patients who improved functionally had significantly higher levels of absolute regional myocardial glucose uptake than those who did not. Adapted from Ref. 77.*

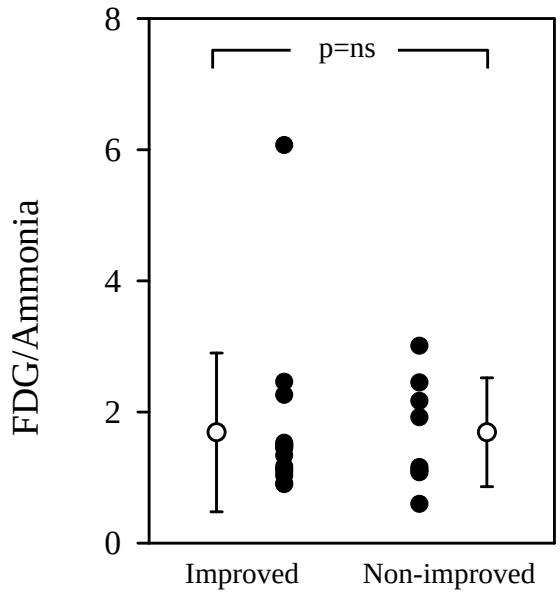

Figure 4-8*. Dot plot showing individual FDG over ammonia activity ratio (mismatch ratio) in patients with and without post-operative functional improvement. Note that there was no difference in the matching between flow and metabolism among the two groups of patients. Adapted from Ref. 77.*

Analysis of factors associated with improved global and regional left ventricular function after coronary revascularization. To define further the variables associated with the return of global and regional ventricular function after coronary revascularization, all pre-revascularization PET flow and metabolic data available were proposed for inclusion into a multivariate discriminant model. Among the 9 PET variables analyzed, both absolute and normalized (% of absolute remote values) levels of resting myocardial perfusion, absolute regional myocardial glucose uptake and normalized glucose extraction were related to the presence of reversible dysfunction (Table 4-7).

Among the PET variables, stepwise linear discriminant analysis selected absolute resting myocardial blood flow and normalized glucose extraction as independent predictors of the reversibility of left ventricular ischemic dysfunction (Table 4-7). Of these 2 factors, myocardial perfusion was the most significant (p=0.004). According to myocardial blood flow alone and by use of a cut off value of 64 ml.(min.100g)$^{-1}$ (from discriminant analysis), 12 of 17 patients with reversible dysfunction (sensitivity 70%) and 7 of 8 patients with persistent postoperative dysfunction (specificity 88%) were correctly categorized by PET. Overall accuracy of absolute myocardial blood flow measurements was 76%.

As shown on Figure 4-9, the discriminant function improved the ability to identify patients in whom ventricular function is likely to recover following revascularization. Consideration of normalized glucose extraction in addition to absolute myocardial blood flow allowed correct classification in 14 of 17 patients with (sensitivity 82%) and 7 of 8 patients without reversible dysfunction (specificity 88%). Overall accuracy improved to 84%. To refine further our ability to classify an individual patient into groups with and without reversible dysfunction, the 95% confidence interval on the discriminant line was determined. Accordingly, 16 of 25

TABLE 4-7. Stepwise Linear Discriminant Analysis of the Factors Associated with Improvement in Global and Regiona after Coronary Revascularization.

	Step	F-to-enter	*p* value
PET Variables in Univariate Analysis			
Absolute myocardial blood flow		12.21	< 0.01
Normalized myocardial blood flow		11.09	< 0.01
Relative ^{13}N-ammonia uptake		6.20	< 0.05
Normalized absolute glucose extraction		5.97	< 0.05
Absolute regional glucose uptake		5.19	< 0.05
Normalized absolute glucose uptake		4.39	< 0.05
PET Variables in Discriminant Analysis			
Absolute myocardial blood flow	1	12.21	< 0.01
Normalized absolute glucose extraction	2	6.36	< 0.05

Normalized, % of remote absolute values.

patients (64%) were correctly classified, 2 of 25 were incorrectly classified and 7 of 25 were unclassified (28%). Thus, in patients outside the 95% confidence bands, correct classification was achieved with 89% accuracy.

Results in patients with <35% ejection fraction

Clinical and angiographic characteristics. The baseline clinical and angiographic characteristics of the study population are summarized in Table 4-8. Subsequent to the echocardiographic and PET studies, but independent of their results, all patients underwent successful coronary revascularization. The interval from these studies to coronary revascularization averaged 61 days (range 6 - 118 days). Bypass surgery was performed in 25 patients, with the use of the left internal mammary artery to graft the left anterior descending coronary artery, and coronary angioplasty was performed in the remaining patient.

Effects of coronary revascularization on segmental and global left ventricular function. Follow-up echocardiograms were obtained 5.0 ± 1.9 months after the revascularization procedure. Anterior wall motion improved after revascularization in 13 patients (from 7.8 ± 1.1 to 6.1 ± 1.6) and did nor change in the other 13 patients (from 8.2 ± 0.8 to 8.4 ± 0.7). All but one patients with improved anterior wall motion after revascularization also improved global left ventricular function (defined as a >5% increase in left ventricular ejection fraction). In these patients, ejection fraction increased from 27 ± 6 to 40 ± 6% (p<0.001). By contrast, no significant changes were noted in patients with persistent regional dysfunction (from 27 ± 5 to 25 ± 5%, p=ns). Left ventricular volumes at both end-diastole (from 217 ± 57 to 202 ± 68 ml) and end-systole (from 159 ± 49 to 124 ± 53 ml) decreased in patients with improved wall

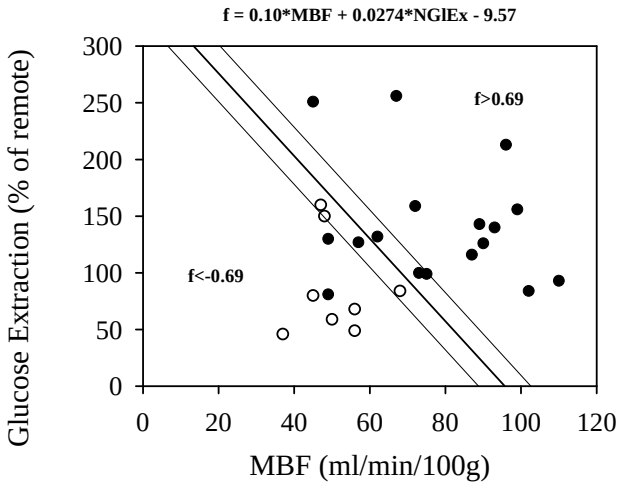

Figure 4-9. *Scatterplot of the relation between normalized glucose extraction and myocardial blood flow and superimposition of the discriminant function and its 95% confidence limits. Patients with and without post-operative functional improvement are reflected by ● and ○ respectively.*

TABLE 4-8. Clinical and angiographic data before and after revascularization.

	Improved	Non-improved
No. of patients	13	13
Age (years)	62 ± 9	64 ± 6
Sex	11 M, 2 F	13 M
Anginal class		
CHA I + II	10/13	11/13
CHA III + IV	3/13	2/13
Functional class		
NYHA I + II	10/13	9/13
NYHA III + IV	3/13	4/13
Diseased vessels		
LAD	0/13	1/13
LAD + Cx	1/13	1/13
LAD + RCA	2/13	2/13
LAD + Cx + RCA	10/13	9/13

CHA, Canadian Heart Association; NYHA, New York Heart Association; LAD, left anterior descending artery; Cx, circumflex artery; RCA, right coronary artery.

motion, but were unchanged in those with persistent dysfunction.

Estimates of myocardial perfusion and metabolism before revascularization. Before revascularization, reversibly dysfunctional myocardium exhibited significantly higher absolute myocardial blood flow (96 ± 27 versus 63 ± 26 ml.(min.100g)$^{-1}$, p<0.005) than persistently dysfunctional myocardium. In segments with reversible dysfunction, values of absolute myocardial blood flow were not significantly different from those measured in the remote normal segments of the same patients (85 ± 18 ml.(min.100g)$^{-1}$) or in anterior and lateral segments of 6 normal volunteers (88 ± 22 ml.(min.100g)$^{-1}$). None of the dysfunctional segments that improved after revascularization had baseline levels of absolute myocardial blood flow below the lowest value of the normal volunteers, i.e. 60 ml.(min.100g)$^{-1}$.

As shown in Table 4-9, estimates of regional myocardial glucose uptake in remote segments reached values similar to those found in the normal volunteers (50 ± 18 versus 53 ± 11 µmol.(min.100g)$^{-1}$). In dysfunctional anterior segments, regional myocardial glucose uptake was slightly, albeit non significantly, higher in reversibly compared with persistently dysfunctional segments (45 ± 17 versus 31 ± 19 µmol.(min.100g)$^{-1}$, p=0.07). There was a significant difference in normalized myocardial glucose uptake (expressed as % of remote) between the 2 types of segments (anterior/remote ratio 0.89 ± 0.22 versus 0.62 ± 0.23, p<0.003). Yet, normalized glucose extraction was similar among the 2 groups. A 'viable' pattern (normal flow and FDG or a flow-metabolism mismatch pattern) was present in 11/13 dysfunctional regions that improved functionally after revascularization, but absent in 5/13 regions that remained dysfunctional despite revascularization.

Diagnostic accuracy of the discriminant function. To evaluate whether the discriminant function would allow correct identification of which patients with a low ejection fraction will benefit from coronary revascularization, its diagnostic accuracy was tested in the subgroup of patients with an ejection fraction <35%. According to myocardial blood flow alone and by use of the cut off value of 64 ml.(min.100g)$^{-1}$ obtained in the preceding study, 12 of 13 patients with reversible dysfunction (sensitivity 91%) and 8 of 13 patients with persistent postoperative dysfunction (specificity 62%) were correctly categorized by PET. Overall accuracy of absolute myocardial blood flow measurements was 77%. Consideration of normalized glucose extraction in addition to absolute myocardial blood flow allowed correct classification in 12 of 13 patients with (sensitivity 91%) and 9 of 13 patients without reversible dysfunction (specificity 70%). Overall accuracy improved to 80%.

TABLE 4-9. Myocardial blood flow and regional glucose uptake in 26 patients with an ejection fraction <35% classified according to the changes in regional wall motion score before and after revascularization.

			Improved (n=13)	Non-improved (n=13)
Myocardial blood flow	[ml.(min.100g)$^{-1}$]	remote	85 ± 18	78 ± 18
		anterior	96 ± 27 ***	63 ± 26 *** ‡
Myocardial glucose uptake	[μmol.(min.100g)$^{-1}$]	remote	51 ± 18	49 ± 18
		anterior	45 ± 17	31 ± 19
Glucose extraction	(μmol.ml^{-1})	remote	0.63 ± 0.25	0.42 ± 0.31
		anterior	0.51 ± 0.26 *	0.51 ± 0.25 *

* p<0.05, ** p<0.01, *** p<0.001 versus remote from the same group
† p<0.05, ‡ p<0.01 versus anterior from the improved group

Discussion

The present study indicates that, in patients with left anterior descending coronary artery disease and sustained anterior wall dysfunction, postoperative improvement in both regional and global left ventricular function was best predicted by a discriminant function that combines preoperative measurements of absolute levels of myocardial blood flow and normalized myocardial glucose extraction in the area of dysfunction. The discriminant function identified the presence of viable myocardium with a sensitivity of 82%, a specificity of 88% and an overall accuracy of 84%.

Myocardial glucose metabolism to predict the presence of viable myocardium. Because glucose is the main substrate under ischemic conditions, PET with ^{18}F-fluorodeoxyglucose has been proposed to delineate the presence of residual metabolic activity within dysfunctional myocardial segments of patients with coronary artery disease. Results of studies using PET with FDG showed that the persistence of residual glucose utilization in hypoperfused segments (the relative flow-metabolism mismatch) identified those likely to resume satisfactory contractile function following revascularization.[196,200] Using this approach, myocardial viability could be detected with sensitivity in the range of 75 to 85% and specificity of 78 to 92%.[196,200] At first glance, the results of the present study (sensitivity of 65% and specificity of 50%) might thus appear in contradiction with those of these earlier reports. They are, however, in agreement with those of previous studies indicating that, in patients studied both early and later after myocardial infarction, PET with FDG may overestimate both the amount and extent of viable myocardium. In a study aimed at examining the natural history of the return of function after acute myocardial infarction, Schwaiger et al. observed that the functional outcome of infarcted segments with a flow-metabolism mismatch pattern was quite variable.[183] Similarly, Piérard et al. demonstrated that the presence of a flow-metabolism mismatch pattern in recently infarcted segments was of limited value to predict the recovery of contractile function after successful revascularization.[156] Gropler et al. reached very similar conclusions.[79] It must be emphasized that these 3 studies dealt mainly with patients studied early (usually within 1 week) after infarction. Their findings might therefore not be applicable to those in the current study, which was more targeted towards patients with chronic coronary artery disease. Nonetheless, our findings are also in agreement with data recently reported by vom Dahl et al. in patients with chronic left ventricular ischemic dysfunction,[221] thus suggesting that overestimation of the capacity for recovery with PET and FDG is not limited to the immediate postinfarction period and may extend into the first weeks after the initial event. In the present study, 20 of 25 (80%) patients with chronic ischemic regional dysfunction had either normal perfusion at rest or a flow-metabolism mismatch pattern in the anterior wall. Thus, only 4 patients (instead of 8) would have been considered to

have nonviable myocardium, had we used the concept of flow-metabolism mismatch as the reference standard to delineate myocardial viability. Although it is possible that the suboptimal results of FDG imaging in some earlier reports reflected inadequate revascularization, poor myocardial protection, coronary artery graft closure or restenosis, we feel they are more likely the manifestation of the exquisite sensitivity of FDG imaging which could allow to detect even small, perhaps subepicardial, portions of myocardium not materially contributing to contraction when revascularized.

Myocardial blood flow to predict the presence of viable myocardium. Previous studies assessing relative perfusion with 201Thallium have indicated that tracer uptake was maintained to levels close to normal in dysfunctional but metabolically active myocardium.[23,55,56,133,137,146,159] Studies with PET and 15O-water demonstrated that at least 70% of the wall thickness had to be normally perfused before revascularization for normal function to resume following revascularization.[52,231] Few studies, however, evaluated the accuracy of absolute myocardial blood flow measurements for predicting the reversibility of dysfunction in patients undergoing coronary revascularization. Gewirtz et al.[74] recently showed that the presence of viable myocardium was very unlikely if basal myocardial blood flow was less than 25 ml.(min.100g)$^{-1}$. In the present study, none of the patients with persistent postoperative dysfunction exhibited such a large flow deficit. Our data indicate, however, that assessment of myocardial blood flow in absolute terms is also valuable in segments with blood flow >25 ml.(min.100g)$^{-1}$. Indeed, among all absolute and relative PET variables investigated in our study, absolute myocardial blood flow was the single most powerful predictor of the return of left ventricular function after revascularization. Twelve of the 17 patients with viable myocardium and only 1 of the 8 patients with nonviable myocardium had flow values within the 95% confidence limits of normality for our laboratory. Thus, the predictive value of a normal flow value for identification of viable myocardium in our population was >93%. Additional information is thus required only in patients with reduced absolute blood flow values. In these patients assessment of regional glucose extraction appears to be the most useful.

Study limitations. This study also has some limitations. As with previous studies from our laboratory, data were acquired with a single slice PET camera. Although static images from several other levels of the left ventricle were usually obtained, only one tomographic level was used for dynamic imaging. It is therefore assumed that this tomographic level was representative of the entire anterior ischemic area. Only patients having stable coronary artery disease and left ventricular dysfunction were enrolled in this study. Although 14 patients had sustained at least one previous myocardial infarction, the most recent occurring 11 days before the PET study, none was studied during the acute phase of infarction (less than 3 days). Therefore, the conclusions of the present study can only be applied to patients with chronic coronary artery disease and presumably not to patients with recent (< 3 days) infarction. Finally, because of the necessarily aerobic nature of cardiac contraction, some authors have proposed to assess myocardial oxidative metabolism with PET and ^{11}C-acetate as an alternative to FDG. Studies in both experimental animals[225] and in humans[79-81] have recently shown that maintenance of oxidative metabolism in dysfunctional myocardium portended its functional recovery after revascularization. In the present study, we did not systematically assess oxidative metabolism. Definite conclusions regarding the relative power of flow measurements compared with measurements of oxidative metabolism in differentiating "viable" from "nonviable" myocardium can therefore not be drawn from our data. Nonetheless, because myocardial blood flow and oxygen consumption are closely coupled in both viable and nonviable myocardium,[48,210] it is likely that both measurements will have a similar accuracy in the identification of myocardial viability.

In summary, this study identified absolute myocardial blood flow and normalized glucose

extraction as the most powerful predictors of the return of contractile function after coronary revascularization in patients with ischemic anterior wall dysfunction, many of whom had a previous infarction. In this population, assessment of flow and metabolism in absolute terms appears to be superior to relative flow-metabolism mismatch for identification of viable myocardium.

4.4. Residual Inotropic Reserve to Identify Reversible Left Ventricular Dysfunction after Revascularization

Although it is clear from the preceding studies that flow and metabolic imaging with PET allows precise and accurate identification of dysfunctional but viable myocardium, PET is an expensive technology which, until now, has not been widely available. Alternative ways to identify reversible left ventricular ischemic dysfunction should therefore be actively sought.

In experimental models of myocardial stunning, dysfunctional but viable and non-ischemic myocardium retains the ability to improve function temporarily upon stimulation with catecholamines or calcium.[7,13,60,103,136] Recent observations in humans indicate that, in the early post-infarction period, dysfunctional but viable myocardium also responds to infusion of catecholamines by increasing function.[12,156,157,190] This has led some investigators to propose and use successfully dobutamine, a synthetic catecholamine, in combination with two-dimensional echocardiography, to delineate the presence of viable myocardium in patients recovering from acute myocardial infarction.

While existing data suggest that augmentation of regional function in response to dobutamine may identify viable myocardium after myocardial infarction, few data are available to support the efficacy of the dobutamine test to predict the return of contractile function after revascularization in patients with chronic left ventricular ischemic dysfunction.[43,124,214] Accordingly, the present study was designed to evaluate whether dobutamine echocardiography could provide clinicians with valuable information as to the potential for reversibility of chronic left ventricular ischemic dysfunction.

Methods

We studied 64 patients (56 men, mean age 59 ± 9 years; range 35 - 72 years) with ischemic heart disease and well-defined coronary anatomy. By reviewing all diagnostic coronary angiograms performed at our institution between October 1991 and September 1993, we selected prospectively patients with severe regional dysfunction in the anatomical distribution of a significantly narrowed or occluded epicardial artery. Fifty-six patients had sustained at least one previous myocardial infarction, the most recent occurring 33 days before inclusion into the study. Subsequent to the echocardiographic and scintigraphic studies, all patients underwent coronary revascularization by bypass surgery or angioplasty. The decision to revascularize was always based on clinical considerations and not on the results of the viability studies. Of the 64 patients initially considered for inclusion into the study, 7 were excluded from final analysis because of death (n=2) or perioperative myocardial infarction (n=5, see below).

Selective coronary arteriography and contrast left ventriculography were performed in every patient before the echocardiographic study. Fifty-one patients had complete occlusion of one or more major epicardial coronary segments, among whom 25 had occlusion of the left anterior descending coronary artery, 7 of the proximal circumflex artery and 32 of the right coronary artery. The remaining thirteen patients had severe proximal stenoses on at least one major epicardial segment. Eleven patients had single vessel disease, 22 patients had two vessel disease, and 31 patients had three vessel disease. Three patients also had left main stenosis.

Dobutamine stress.[132] All patients underwent dobutamine echocardiography during the hospital admission for cardiac catheterization. All patients were allowed to take their prescribed medications with an exception for ß-blockers, which were withdrawn for at least 24 hours

before the investigation. Before the test was started, a clinical history was recorded, a rest ECG and echocardiogram were obtained and a venous line was secured. Dobutamine was then infused in 3-min dose increments from 5 to 40 µg.(kg.min)$^{-1}$ under continuous ECG and echocardiographic monitoring. For safety reasons, in the first 20 patients of the study, peak dose was limited to 20 µg.(kg.min)$^{-1}$. Later on, as the safety profile of the test in patients with poor left ventricular ejection fraction became better appreciated, doses up to 40 µg/kg/min were commonly used. The test was concluded after achievement of the peak dose or earlier if the patient developed severe ischemia (either angina or impairment of left ventricular function) or experienced intolerable side-effects including hypertension (systolic blood pressure >250 mm Hg), or hypotension (fall in systolic blood pressure >50 mm Hg compared with peak pressure or systolic blood pressure <100 mm Hg), ventricular arrhythmias (>3 consecutive premature ventricular contractions or constant bigeminy) or sustained supraventricular tachyarrhythmias. Clinical signs and the ECG and echocardiographic images were recorded at the beginning of the study and every 3 min thereafter until completion of the stress.

Follow-up study. Subsequent to the echocardiographic and scintigraphic studies, but independent of their results, all patients underwent successful coronary revascularization. The interval from the viability studies to coronary revascularization averaged 48 days (range 1 - 174 days). Coronary artery bypass surgery (CABG) was performed in 44 patients, with the use of the left internal mammary artery to graft the left anterior descending coronary artery, and percutaneous transluminal coronary angioplasty (PTCA) was performed in the remaining 20 patients. During the revascularization procedure, an attempt was made to revascularize all major branches with >70 % luminal diameter stenosis, independent of the presence or absence of residual viability by either tests. Five patients undergoing bypass surgery had evidence of peri-operative myocardial infarction, defined as new onset Q-wave on the electrocardiogram and/or a postoperative increase in plasma enzymes activity (creatine kinase activity > 1500 U/l with > 100 U/l MB isoform activity, or in plasma SGOT activity > 90 U/l). Follow-up echocardiograms were obtained 5.3 ± 2.7 months after surgery.

***Data analysis*.**

2D-echocardiograms were obtained and analyzed as described above. Images were interpreted qualitatively in accordance with previous guidelines by experienced observers who had no knowledge of the angiographic and clinical data. Regional function was interpreted in 16 myocardial segments (basal, midventricular and apical levels of the septum, lateral, anterior and inferior walls; and basal and midventricular levels of the anteroseptal and posterior walls) and defined as normal (1), hypokinetic (2), or akinetic (3).[2,171] Normal wall motion was defined as ≥5 mm of endocardial excursion and obvious systolic wall thickening. Hypokinesis was defined as <5 mm of endocardial excursion and reduced wall thickening. Akinesis was defined as near absence of endocardial excursion or thickening. A global wall motion score was calculated for all stages of the dobutamine stress and for the follow-up two-dimensional echocardiographic study. Left ventricular volumes and ejection fraction were obtained in each patient before revascularization, at rest, 10 µg.(kg.min)$^{-1}$ and peak dose of dobutamine, and again at the follow-up echo study. Left ventricular volumes at both end-diastole and end-systole were computed from the apical 4- and 2-chamber views by use of a standard Simpson's method.

Dobutamine echocardiography. A normal segmental response to dobutamine was defined as a progressive enhancement in contractility during stress. Ischemia was identified by a stress-induced wall motion abnormality. Akinetic or dyskinetic myocardium at baseline was considered as *responsive* to dobutamine if, *on a segmental basis*, wall motion improved by at least 1 full grade or as *non responsive* if regional wall motion did not improve with low-dose dobutamine. The diagnostic performance of the

test was also investigated *on an individual patient basis*. Individual patients were considered to have dobutamine responsive dysfunctional myocardium if wall motion score improved by at least 1 full grade in 2 adjacent a- or dyskinetic segments from the same vascular territory during infusion of 5 - 10 µg.(kg.min)$^{-1}$ dobutamine.

Follow-up echocardiography. As judged from the comparison of resting regional wall motion before and after revascularization, dysfunctional myocardium was considered as *viable* if, *on a segmental basis*, wall motion improved by at least one full grade after revascularization or as *nonviable* if regional wall motion did not improve after revascularization. Because indexes of global left ventricular function, such as ejection fraction and end-systolic volume are important prognostic indicators in patients with ischemic left ventricular dysfunction, myocardial viability was also defined *on an individual patient basis*. Patients were considered to have viable myocardium if wall motion score improved post-operatively by at least one full grade in 2 adjacent akinetic or dyskinetic myocardial segments and if end-systolic volume decreased .

Statistical analysis. The sensitivity, specificity, and accuracy of dobutamine echocardiography was obtained in the usual fashion. The ability of the tests to predict viability in the different coronary vascular territories was assessed by ascribing the interventricular septum, the anteroseptal and anterior walls to the left anterior descending coronary artery, the lateral wall to the circumflex artery, and the inferior wall to the right coronary artery. Because of the varying vascular supply of the apex, this was allocated to any other involved territory. If the apex alone was involved, the left anterior descending coronary artery was imputed. Likewise, the posterior wall was ascribed to either the right or the circumflex territory if either was involved. If the posterior wall alone was involved, it was ascribed to the circumflex artery.

Results

Clinical and angiographic characteristics.

TABLE 4-10. Clinical and angiographic data before revascularization.

	Improved	Non-improved
No. of patients	33	24
Age (years)	58 ± 9	59 ± 9
Sex	30 M, 3 F	19 M, 5 F
Anginal class		
CHA I + II	26/33	19/24
CHA III + IV	7/33	5/24
Functional class		
NYHA I + II	28/33	19/24
NYHA III + IV	5/33	5/24
Diseased vessels		
LAD	4/33	3/24
Cx or RCA	4/33	0/24
LAD + Cx	4/33	2/24
LAD + RCA	9/33	5/24
Cx + RCA	2/33	0/24
LAD + Cx + RCA	10/33	14/24

CHA, Canadian Heart Association; NYHA, New York Heart Association; LAD, left anterior descending artery; Cx, circumflex artery; RCA, right coronary artery.

Three patients died during the follow-up period, one from bleeding complications immediately after bypass surgery, one suddenly 3 weeks after surgery and another one 5 months after surgery from pulmonary infection. Follow-up studies were unavailable in the first 2 patients. Five other patients sustained a peri-operative myocardial infarction and were therefore excluded from further analysis. Adequate follow-up studies were thus available in 57 patients (49 men, mean age 59 ± 9 years, range 35 - 72 years).

According to the changes in resting wall motion and end-systolic volume before and after revascularization, the patients were categorized into two groups: group 1 (*viable*) 33 patients (30 men, mean age 58 ± 9 years, range 40 - 71 years) with improved regional wall motion score (-5.6 ± 3.3 grade) and end-systolic volume (-26 ± 22 ml); group 2 (*nonviable*) 24 patients (19 men, mean age 59 ± 9 years, range 35 - 72 years) with increased end-systolic volume (+ 27 ± 20 ml) and variable changes in regional wall motion score (4 patients with no changes, 6

TABLE 4-11. Left Ventricular Volumes, Ejection Fraction and Regional Wall Motion Score before and after Revascularization.

		Improved (n=33)	Non-improved (n=24)
End-diastolic volume (ml)	before	177 ± 51	227 ± 51 ***
	after	162 ± 50	245 ± 45
End-systolic volume (ml)	before	114 ± 51	150 ± 52 **
	after	88 ± 45	177 ± 47
Ejection fraction (%)	before	37 ± 13	35 ± 12
	after	48 ± 13	29 ± 12
AWMS	before	30 ± 6	34 ± 6 *
	after	25 ± 6	36 ± 5

* p<0.05, ** p<0.01, *** p<0.001 viable versus nonviable. No statistical analysis was applied to the differences in left ventricular function after revascularization, which are inherent in the study design.
WMS: global wall motion score.

patients with improvement by only 1 grade and 14 patients with deterioration). Before revascularization, clinical and angiographic data were similar among the 2 groups of patients (Table 4-10). Although left ventricular ejection fraction was similar among patients with and without viable myocardium, regional wall motion score (30 ± 6 versus 34 ± 6, p=0.03), and left ventricular volumes at both end-diastole (177 ± 51 versus 227 ± 51 ml, p<0.001) and end-systole (114 ± 51 versus 150 ± 52 ml, p=0.01) were significantly lower in patients with than in those without viable myocardium. The changes in left ventricular function resulting from coronary revascularization are shown in Table 4-11. There was an significant correlation between the changes in regional wall motion score and those in global ejection fraction and end-systolic volume after revascularization.

Hemodynamics and segmental response to dobutamine infusion. For safety reasons, in the first 20 patients, peak dose was limited to 20 µg.(kg.min)-1. In the remaining 37 patients, mean dose at peak stage or stress portion of the protocol was 32 ± 8 µg.(kg.min)$^{-1}$ (range 10 - 40 µg.(kg.min)$^{-1}$). End-points for this stage were achievement of maximal dose in 16, arrhythmias

TABLE 4-12. Hemodynamic and Segmental Response to Infusion of Dobutamine.

		Baseline	Low-dose Dobutamine 10 µg.(kg.min)$^{-1}$	Peak dose Dobutamine 27±11 µg.(kg.min)$^{-1}$
Heart rate (bpm)	Improved	75 ± 12	84 ± 22	111 ± 25
	Non-improved	77 ± 14	84 ± 19	103 ± 23
Mean blood pressure (mmHg)	Improved	107 ± 14	110 ± 13	104 ± 18
	Non-improved	104 ± 13	106 ± 14	101 ± 16
Rate-pressure product (mm Hg.bpm)	Improved	10,333 ± 2,407	12,272 ± 4,225	15,822 ± 4,980
	Non-improved	10,316 ± 2,296	12,067 ± 3,315	13,926 ± 3,733
End-diastolic volume (ml)	Improved	177 ± 51	161 ± 52	156 ± 51
	Non-improved	227 ± 51 ***	216 ± 58***	213 ± 62**
End-systolic volume (ml)	Improved	114 ± 51	82 ± 42	87 ± 45
	Non-improved	150 ± 52**	137 ± 58***	137 ± 58**
Ejection fraction (%)	Improved	37 ± 13	51 ± 11	47 ± 15
	Non-improved	35 ± 12	39 ± 15**	38 ± 14*
Wall motion score	Improved	30 ± 6	25 ± 6	30 ± 8
	Non-improved	34 ± 6*	33 ± 6***	34 ± 6*

* p<0.05; ** p<0.01; *** p<0.001 improved versus non improved.

in 7, chest pain in 3, induction of wall motion abnormalities in a remote area in 3, hypotension in 6, hypertension in one, and dyspnea in one. The mean peak dose was not different among patients with (27 ± 10 µg.(kg.min)$^{-1}$) and without (26 ± 11 µg.(kg.min)$^{-1}$) viable myocardium.

The effects of incremental doses of dobutamine on hemodynamics and regional and global left ventricular function in the 2 groups of patients are shown in Table 4-12. Infusion of low-dose dobutamine (10 µg.(kg.min)$^{-1}$) resulted in minor changes in heart rate and mean blood pressure. Rate-pressure product increased by an average of 15%. With further dose increments, heart rate, blood pressure and rate-pressure product continued to increase. At peak dose, rate-pressure product averaged 15,093 mm Hg.(beats.min)$^{-1}$ (146% of baseline). There was no difference in the evolution of these parameters among the 2 groups of patients.

With low-dose dobutamine, regional wall motion score improved in both groups, albeit significantly more in patients with viable myocardium (by 5.4 ± 4.3 compared with 0.9 ± 3.3 in patients without, $p<0.001$). Improvement in regional wall motion in patients with nonviable myocardium almost exclusively involved previously hypokinetic segments, while it involved both akinetic or dyskinetic and hypokinetic segments in patients with viable myocardium. With higher doses, no further improvement in wall motion was observed. Thirty patients even showed deterioration of wall motion at higher doses. In 18 patients, functional deterioration occurred in remote, initially normally contracting, segments (ischemia at distance). In 21 patients, it occurred in previously dysfunctional segments that were improved at low-dose dobutamine. A biphasic contractile pattern (improvement followed by deterioration) was only observed in patients with viable myocardium. As shown in Figure 4-10, a significant correlation was found between the changes in regional wall motion score with low-dose dobutamine and those after revascularization.

Diagnostic accuracy of dobutamine echo in delineating myocardial viability. As shown in Figure 4-11, of the 912 segments analyzed, 354 showed akinesis or dyskinesis preoperatively and 191 showed hypokinesis. Of the 354 initially akinetic or dyskinetic segments, 115 recovered satisfactory contractile function following revascularization and were therefore considered as viable. Ninety-three of the 115 viable segments, or 81%, responded to preoperative dobutamine infusion by increasing function. Of the 239 dysfunctional segments that remained abnormal after revascularization, 205 (or 86%) failed to improve function during the preoperative dobutamine stress. Figure 4-12 shows the response of hypokinetic segments. Of the 191 initially hypokinetic segments, 68 recovered satisfactory contractile function following revascularization. Fifty-six of these segments, or 82%, responded to preoperative dobutamine infusion by increasing function. Of the 123 dysfunctional segments that remained abnormal after revascularization, 68 (or 55%) failed to improve function during the preoperative dobutamine stress. The overall diagnostic accuracy of the test did not improve with further dose increases. On the contrary, sensitivity decreased in a dose-dependent manner as the number of segments deteriorating increased. The test was equally effective in delineating viable from nonviable myocardium in the different vascular territories.

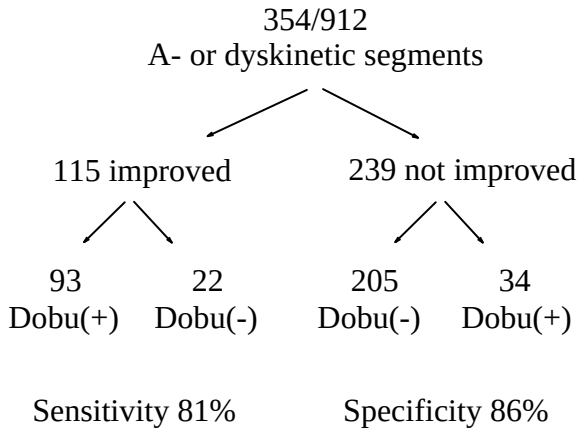

Figure 4-11*. Flow diagram displaying the changes in regional wall motion after coronary revascularization in akinetic segments and their response to infusion of a low-dose of dobutamine.*

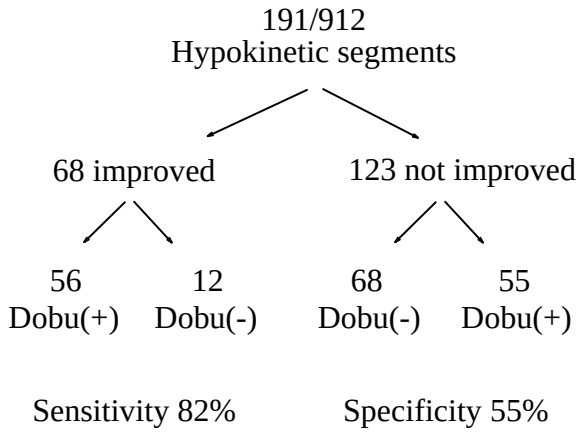

Figure 4-12. *Flow diagram displaying the changes in regional wall motion after coronary revascularization in hypokinetic segments and their response to infusion of a low-dose of dobutamine.*

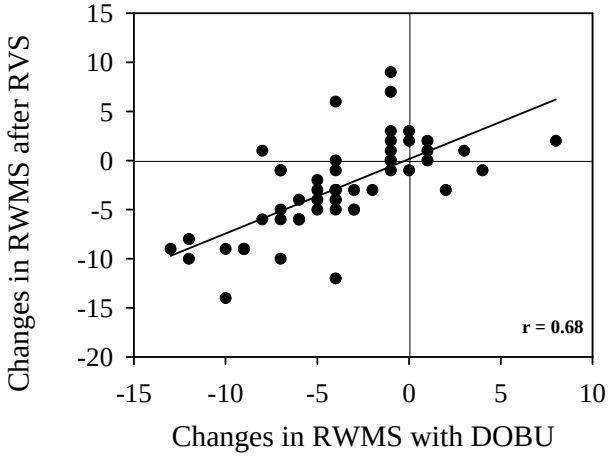

Figure 4-10. *Scatterplot showing the relationship between the changes in regional wall motion score (RWMS) during low-dose dobutamine (DOBU) and those observed after revascularization (RVS).*

Because indexes of global left ventricular function, such as ejection fraction and end-systolic volume are important prognostic indicators in patients with ischemic left ventricular dysfunction, the diagnostic performance of the dobutamine test was also investigated on an individual patient basis. As mentioned above, individual patients were considered to have dobutamine responsive dysfunctional myocardium if wall motion score improved by at least one full grade in 2 adjacent akinetic or dyskinetic segments during infusion of dobutamine. Dobutamine echocardiography correctly identified 88% of the patients with and 75% of the patients without viable myocardium. Overall accuracy was 82%. The preoperative predictive value of a + dobutamine test for postoperative recovery was 83%, while that of a negative test for persistent dysfunction was 82%.

Discussion

The results of this study indicates that low-dose dobutamine echocardiography is an accurate method for the clinical prediction of the reversibility of left ventricular dysfunction after coronary revascularization.

Delineation of myocardial viability with low-dose dobutamine echocardiography. Conventional dobutamine echocardiographic protocols has been recently proposed for identification of residual myocardial viability early (<2 weeks) after myocardial infarction. Comparing the results of low-dose dobutamine echocardiography with those of positron emission tomography in 17 patients recovering from acute myocardial infarction, Piérard et al. found both techniques to be concordant in 79% of the dysfunctional segments.156 In a selected group of patients with incomplete infarction, Barilla et al. observed that most dobutamine-responsive regions improved after revascularization.[12] Nonrevascularized segments also responded to dobutamine, but showed less improvement at follow-up. In 51 patients treated with thrombolytic therapy for acute myocardial infarction, Smart et al. reported that improvement in wall motion score index during low-dose (4 µg.(kg.min)$^{-1}$) dobutamine had a sensitivity of 86% for functional recovery at follow-up, while the absence of an improvement had a specificity of 90% for failure to improve at follow-up.190 These authors also showed that the sensitivity of the test was inversely related to the dose of dobutamine infused, the number of segments with persistent dysfunction increasing in a dose-dependent manner. Previtali et al. reported very similar results.[157]

While existing data suggest that augmentation of regional function in response to low-dose

dobutamine infusion accurately reflects myocardial viability early after infarction, fewer data are available to support the efficacy of this technique in patients with chronic left ventricular ischemic dysfunction, the so-called "chronic myocardial hibernation." In contrast to the early post-infarction period, where stunned myocardium is probably predominant, chronic myocardial hibernation likely involves both postischemic dysfunction and ongoing reduction of myocardial blood flow. It is known to be associated with marked structural alterations of the myocytes,[24,211] including a loss of myofilaments and contractile material, and with no or a very limited residual coronary flow reserve.[211] It would therefore not be surprising if chronically dysfunctional but hibernating myocardium was less responsive to inotropic stimulation than purely stunned myocardium. Yet, there is increasing evidence that low-dose dobutamine echocardiography permits accurate prediction of the reversibility of dysfunction in chronically hibernating myocardium as well. In 25 patients undergoing coronary revascularization, Cigarroa et al. showed that a >20% improvement of the systolic wall thickening score during dobutamine had sensitivity of 82% and a specificity of 86% for recovery at follow-up.[43] Similar results (87% sensitivity and 82% specificity) were recently reported by La Canna et al., in 33 selected patients undergoing CABG.[124]

The present findings confirm and extend these 2 previous reports. Of the 115 initially akinetic or dyskinetic segments resuming satisfactory contractile function following revascularization, 93 (or 81%) responded to preoperative dobutamine infusion by increasing function. Similarly, of the 239 dysfunctional segments that remained abnormal after revascularization, 205 (or 86%) failed to improve function during low-dose dobutamine infusion. The specificity of the test was less, however, in hypokinetic segments, as only 68 (55%) of the 123 segments with persistent postoperative dysfunction were correctly identified by the preoperative low-dose dobutamine test. There are several potential reasons for the poor specificity of the dobutamine test in hypokinetic segments. Segmental hypokinesis may reflect the presence of a subendocardial scar and be unaffected by revascularization. Nonetheless, if enough noninfarcted myocardium remains in mid and epicardial layers, such segments could still manifest improvement with dobutamine. Tethering by adjacent akinetic segments could also be an explanation. In this case, the segmental response to revascularization will largely depend on the recovery of the adjacent segments, while that to dobutamine will also reflect the changes in segmental contractility, cavity size and afterload.

We also considered the accuracy of the test for prediction of reversible dysfunction in individual patients. Of the 57 patients finally included in our study, 33 showed improvement in 2 akinetic or dyskinetic adjacent segments or more and did not deteriorate global left ventricular function after revascularization. The remaining 24 patients had no or minimally viable tissue and experienced further increases in both end-diastolic and end-systolic volumes after revascularization. Thus, an improvement in regional wall motion by at least one full grade in 2 adjacent akinetic or dyskinetic segments during low-dose dobutamine infusion correctly identified 88% of the patients with and 75% of the patients without viable myocardium. Overall accuracy was 82%, regardless of the vascular territories involved.

Study limitations. The present study has some limitations. First, we did not obtain follow-up angiograms in every patient to ascertain that complete revascularization of the dysfunctional segments had indeed been achieved. We cannot therefore rule out the possibility that incomplete revascularization, graft closure or restenosis contributed to the lack of functional improvement in patients with persistent dysfunction. It is also possible that, in some patients, the revascularization procedure was harmful and precipitated functional deterioration. This would imply, however, that either the hibernating myocardium, the remodeled remote myocardium or both are prone to greater injury during sequences of ischemia-reperfusion. Although we cannot dismiss this

possibility, our previous observations on the relationship between the extent of recovery and the severity of the tissue fibrosis suggest that the capacity for recovery after revascularization is largely determined by factors unrelated to the revascularization procedure. In addition, the magnitude of changes in left ventricular volumes seen in patients with persistent dysfunction is compatible with the natural history of left ventricular remodeling as delineated in several large scale multicenter trials.

In summary, this study demonstrates that dysfunctional but viable myocardium conserves a significant degree of inotropic reserve and that this property can be used clinically for the delineation of reversible from irreversible ischemic injury. Accordingly, dobutamine echocardiography is a promising new method to assess the potential for recovery of left ventricular function after revascularization in patients with coronary artery disease and left ventricular dysfunction. However, its relative place in the large armamentarium of techniques currently available to address the issue of viability in patients with LV ischemic dysfunction needs to be better defined. Further studies should therefore aim at directly comparing, in the same patients, the relative diagnostic accuracy of the currently available methods (dobutamine echocardiography, thallium SPECT and PET) and, ideally, should come up with clinically sounded and economically viable strategies that can be applied to most patients in whom the issue of viability needs to be addressed.

Chapter 5 Summary and future directions

Due to its inherent truly quantitative capabilities, its noninvasive nature and its nondestructive characteristics, PET has emerged as a unique investigative tool for the assessment and quantification of myocardial blood flow and metabolism in man. The present thesis reviews some of the insights gained with the use of PET into the pathophysiology of regional left ventricular ischemic dysfunction.

Chapters 1 and 2 dealt with definitions and specific issues pertinent to the pathophysiological background of our studies and to the PET technology that was used to assess myocardial blood flow and metabolism.

In Chapter 3, I have concentrated on the study of the flow and metabolic correlates of myocardial infarction, myocardial stunning and myocardial hibernation in humans as well as on the structural changes shown to occur in the hibernating myocardium. *In reperfused myocardial infarction*, studied at an average of 40 days after the acute event, flow and function were found to be significantly reduced and appropriately matched (chronic perfusion-contraction matching). Regional myocardial oxidative metabolism was also reduced, in proportion to the reduction in myocardial blood flow, while glucose metabolism was highly variable. In subsequent studies, the severity of flow reduction was found to be dependent on the severity of tissue fibrosis, providing an anatomical substrate for the noninvasive evaluation of the transmural extension of the fibrotic scar across the left ventricular wall. *In the stunned myocardium*, our results confirmed those previously demonstrated in the experimental lab, namely that regional perfusion and oxygen consumption were largely restored despite the continuing loss of regional contraction. The most unexpected observations were made *in the hibernating myocardium*. It had been initially postulated that myocardial hibernation resulted from the spontaneous adaptation of the ischemic myocardium to chronic underperfusion, whereby the heart downgrades its myocardial function to the extent that flow and function are once again matched and, as a consequence, no myocardial necrosis ensues. Surprisingly, quantification of myocardial perfusion and metabolism in absolute terms by the use of PET in patients with chronic hibernation failed to demonstrate any significant reduction of resting blood flow to the dysfunctional segments. Reduced blood flow values could only be measured in less than 25% of the patients with myocardial hibernation, the remaining patients showing normal levels of resting perfusion. Obviously, in these latter patients, the dysfunction could not be explained on the basis of a permanent, chronic reduction of transmural perfusion. The observation that regional dysfunction correlated closely with the severity of impairment of the coronary vasodilatory reserve raised the possibility that frequent, repeated and incompletely resolutive episodes of ischemia followed by stunning could be the primary mechanisms. Accordingly, myocardial hibernation would rather be the result of repetitive ischemia and stunning than the consequence of chronic and permanent underperfusion. It is therefore an unstable condition, which, in the absence of coronary recanalization, could eventually lead to tissue necrosis. Although such instability had not been anticipated in earlier studies, recent retrospective studies have confirmed that patients with hibernating myocardium indeed had a poor outcome if given only medical treatment. Although suggestive evidence thus indicates that repetitive ischemia with a persistent stunning effect probably sets the stage to chronic hibernation, definite proof that more frequent, more prolonged and more severe episodes of ischemia do indeed occur in patients with chronic dysfunction is still lacking. Future research should therefore aim at evaluating the

total ischemic burden in these patients, for instance by use of quantitative Holter monitoring. The study of myocardial structure provided important clues as to the pathophysiology of the hibernating myocardium. Although stunning does not usually result in significant structural changes, marked alterations were noted in about half the cardiomyocytes in hibernating segments, including the loss of myofibrillar content and the accumulation of glycogen. Interestingly, these structural changes were accompanied by qualitative changes in the isoform expression of various contractile and cytoskeleton proteins, including the re-expression of the α-smooth-muscle actin and of the GLUT-1 glucose transporter, or changes in the organization pattern of titin and cardiotin towards a fetal phenotype. These observations, which are reminiscent of cell dedifferentiation, will likely stimulate the study of the molecular mechanisms underlying hibernation, and promote the development of relevant animal models for hibernation. Finally, definite proof that the structural changes directly contribute to the pathophysiology of myocardial hibernation was provided by studies on the time course of recovery of contractile function following revascularization, which showed that the rate of functional return after revascularization was intimately related to the severity of the preexisting structural changes. The finding that abnormal glucose uptake by previously hibernating myocardium can persist for prolonged periods of time after successful coronary recanalization further supports this contention. Unfortunately, for obvious ethical reason, confirmation of structural reversibility has not been possible, although it can be inferred from the return of function over time. Obviously, a better understanding of the genetic mechanisms controlling the processes of dedifferentiation and redifferentiation in the setting of hibernation is needed to develop appropriate pharmacological or genetic tools to hasten the recovery of function in these patients.

In Chapter 4, we have attempted to apply the concepts derived from our previous studies to the clinical identification of which patient is most likely to resume satisfactory contractile function and thus benefit from coronary revascularization. We first characterized the flow, metabolic and structural factors associated with the return of regional contraction after revascularization, in patients with left ventricular dysfunction and a previous myocardial infarction. These studies largely confirmed our previous observations, namely that functional reversibility only occurs in segments with preserved flow, further supporting the concept that a permanent reduction of coronary blood flow is not needed to explain the dysfunction. These studies further indicated that the extent of recovery of regional contraction after revascularization was linked to both the extent and severity of tissue fibrosis, and thus irreversible injury. The ability to identify reversible dysfunction before revascularization by use of PET flow-metabolic imaging was then evaluated in 2 cohorts of patients with varying degrees of left ventricular ischemic dysfunction. By use of a multivariate approach, an equation which combined flow and normalized glucose extraction was generated that allowed prediction of functional recovery in 80 - 85% of the patients, irrespective of the severity of the underlying dysfunction. Finally, we examined the potential role of assessing residual inotropic reserve in dysfunctional segment to predict the reversibility of LV ischemic dysfunction after revascularization. We used the ß1-receptor agonist dobutamine as the inotropic agent and evaluated the diagnostic significance of an enhancement of regional function at echocardio-graphy during infusion of a low-dose of dobutamine for the prediction of functional recovery after revascularization. The results showed that dobutamine-echocardiography provides a potentially useful alternative to the use of PET to delineate myocardial viability in most patients with LV ischemic dysfunction.

REFERENCES

1. Alderman EL, Fisher LD, Litwin P, Kaiser GC, Myers WO, Maynard C, Levine F, Schloss M. Results of coronary artery bypass surgery in patients with poor left ventricular function (CASS). *Circulation* 1983;68:785-795.
2. American Society of Echocardiography Committee on standards, Subcommittee on Quantitation of Two-dimensional Echocardiograms. Recommendations for quantitation of the left ventricle by two-dimensional echocardiography. *J Am Soc Echocardiogr* 1989;2:358-367.
3. Arai AE, Pantely GA, Anselone CG, Bristow J, Bristow JD. Active downregulation of myocardial energy requirements during prolonged moderate ischemia in swine. *Circ Res* 1991;69:1458-1469.
4. Araujo L, Lammertsma A, Rhodes C, McFalls E, Iida H, Rechavia E, Galassi A, De Silva R, Jones T, Maseri A. Non invasive quantification of regional myocardial blood flow in coronary artery disease with oxygen-15-labeled carbon dioxide inhalation and positron emission tomography. *Circulation* 1991;83:875-885.
5. Armbrecht JJ, Buxton DB, Brunken RC, Phelps ME, Schelbert HR. Regional myocardial oxygen consumption determined noninvasively in humans with [1-^{11}C] acetate and dynamic positron tomography. *Circulation* 1989; 80:863-872.
6. Armbrecht JJ, Buxton D, Schelbert HR. Validation of [1-^{11}C] acetate as a tracer for noninvasive assessment of oxidative metabolism with positron emission tomography in normal, ischemic, postischemic, and hyperemic canine myocardium. *Circulation* 1990;81:1594-1605.
7. Arnold JMO, Braunwald E, Sandor T, Kloner RA. Inotropic stimulation of reperfused myocardium with dopamine: effects on infarct size and myocardial function. *J Am Coll Cardiol* 1985, 6:1026-1034.
8. Atar A, Gao WD, Backx PH, Murphy Am, Marban E. Immunoblot analysis of stunned myocardium reveals structural alterations of the myofilaments predicted by modelling of cross-bridge kinetics. *Circulation* 1994;90(Part2):I-646.
9. Ausma J, Schaart G, Thoné F, Shivalkar B, Flameng W, Depré C, Vanoverschelde J-L, Ramaekers F, Borgers M. Chronic ischemic viable myocardium in man: aspects of dedifferentiation. *Cardiovasc Pathol* 1995;4:29-37.
10. Bacharach SL, Bonow RO, Cuocolo A, Perrone-Filardi P, Voipio-Pulkki L-M, Carson RE, Frank JA, Maurea S, Scheffknecht B. Myocardial blood flow by PET: correction for spillover and partial volume. In: Computers in Cardiology, Chicago, USA, IEEE Computer Society Press, Los Alamitos, California, 1991, 53-56.
11. Bache RJ, Schwartz JS. Myocardial blood flow during exercise after gradual coronary occlusion in the dog. *Am J Physiol* 1983;245:H131-H138
12. Barilla F, Gheorghiade M, Alam M, Khaja F, Goldstein S. Low-dose dobutamine in patients with acute myocardial infarction identifies viable but not contractile myocardium and predicts the magnitude of improvement in wall motion abnormalities in response to coronary revascularization. *Am Heart J* 1991;122:1522-1531.
13. Becker LC, Levine JH, DiPaula AF, Guarnieri T, Aversano T. Reversal of dysfunction in postischemic stunned myocardium by epinephrine and postextrasystolic potentiation. *J Am Coll Cardiol* 1986;7:580-589.

14. Bergmann SR, Hack S, Tewson T, Welch MJ, Sobel BE. The dependence of accumulation of $^{13}NH_3$ by myocardium on metabolic factors and its implication for quantitative assessment of perfusion. *Circulation* 1980;61:34-43.
15. Bergmann SR, Fox KAA, Rand AL, McElvany KD, Welch MJ, Markham J, Sobel BE. Quantification of regional myocardial blood flow in vivo with $H_2{}^{15}O$. *Circulation* 1984;70:724-733.
16. Bergmann SR, Herrero P, Markham J, Walsh MN. Noninvasive quantitation of myocardial blood flow in human subjects with oxygen-15-labeled water and positron emission tomography. *J Am Coll Cardiol* 1989; 14:639-652.
17. Bol A, Michel C, Melin JA, Wijns W: Requisites to modeling of tracer kinetics in the heart using Positron Emission Tomography; In C Beckers, A Goffinet & A Bol. Positron Emission Tomography in Clinical Research and Clinical Diagnosis, Kluwer Academic Publishers, 1989, pp 249-262.
18. Bol A, Iida H, Essamri B, Vanbutsele R, Labar D, Grandin C, Wijns W, Melin JA. Assessment of myocardial oxidative reserve with PET: comparison of C-11 acetate kinetics with quantitation of metabolic rate of oxygen (MRO2) using O-15 O2. *J Nucl Med* 1991;32(abstract): 988-989.
19. Bol A, Melin JA, Vanoverschelde JL, Baudhuin T, Vogelaers D, De Pauw M, Michel C, Luxen A, Labar D, Cogneau M, Robert A, Heyndrickx GR, Wijns W. Direct comparison of N-13 ammonia and O-15 water estimates of perfusion for quantitation of regional myocardial blood flow by microspheres. *Circulation* 1993;87:512-525.
20. Bolli R. Mechanism of myocardial "stunning". *Circulation* 1990, 82:723-738.
21. Bolli R. Myocardial "stunning" in man. *Circulation* 1992; 86:1671-1691.
22. Bolukoglu H, Liedtke J, Nellis S, Eggleston A, Subramanian R, Renstrom B. An animal model of chronic coronary stenosis resulting in hibernating myocardium. *Am J Physiol* 1992;263:H20-H29.
23. Bonow RO, Dilsizian V, Cuocolo A, Bacharach SL. Identification of viable myocardium in patients with chronic coronary artery disease and left ventricular dysfunction. Comparison of Thallium scintigraphy with reinjection and PET imaging with F-18 deoxyglucose. *Circulation* 1991;83:26-37.
24. Borgers M, Thoné F, Wouters L, Ausma J, Shivalkar B, Flameng W. Structural correlates of regional myocardial dysfunction in patients with critical coronary artery stenosis: Chronic hibernation? *Cardiovasc Pathol* 1993; 2:237-245.
25. Braunwald E, Kloner R. The stunned myocardium: Prolonged, postischemic ventricular dysfunction. *Circulation* 1982;66:1146-1149.
26. Braunwald E, Rutherford JD. Reversible ischemic left ventricular dysfunction: evidence for "hibernating myocardium." *J Am Coll Cardiol* 1986;8:1467-1470.
27. Bristow JD, Arai AE, Anselone CG, Pantely GA. Response to myocardial ischemia as a regulated process. *Circulation* 1991;84:2580-2587.
28. Brown M, Marshall DR, Sobel BE, Bergmann SR. Delineation of myocardial oxygen utilization with carbon-11-labeled acetate. *Circulation* 1987;76:687-696.
29. Brown M, Myears DW, Bergmann SR. Noninvasive assessment of canine myocardial oxidative metabolism with carbon-11 acetate and positron emission tomography. *J Am Coll Cardiol* 1988;12:1054-1063.

30. Brown MA, Myears DW, Bergmann SR. Validity of estimates of myocardial oxidative metabolism with carbon-11 acetate and positron emission tomography despite altered patterns of substrate utilization. *J Nucl Med* 1989;30:187-193.
31. Brosius FC, Sun DQ, England R, Nguyen N, Schwaiger M. Altered glucose transporter mRNA levels in cardiac ischemia. *Circulation* 1993;88(suppl I):I-542.
32. Buck A, Wolpers HG, Hutchins GD, Savas V, Mangner TJ, Ngyen N, Schwaiger M. Effects of carbon-11-acetate recirculation on estimates of myocardial oxygen consumption by PET. *J Nucl Med* 1991;32:1950-1957.
33. Buxton DB, Schwaiger M, Nguyen A, Phelps ME, Schelbert HR. Radiolabeled acetate as a tracer of myocardial tricarboxylic acid cycle flux. *Circ Res* 1988; 63:628-634.
34. Buxton DB, Nienaber CA, Luxen A, Ratib O, Hansen H, Phelps, Schelbert HR. Noninvasive quantitation of regional myocardial oxygen consumption in vivo with [1-^{11}C] acetate and dynamic positron emission tomography. *Circulation* 1989;79:134-142.
35. Buxton DB, Schwaiger M, Vaghaiwalla Mody F, Krivokapitch J, Nienaber C, Armbrecht J, Luxen A, Ratib O, Phelps ME, Schelbert HR. Regional abnormality of oxygen consumption in reperfusion assessed with [1-^{11}C] acetate and positron emission tomography. *Am J Cardiac Imaging* 1989;3:276-287.
36. Buxton DB, Schelbert HR. Measurement of regional glucose metabolic rates in reperfused myocardium. *Am J Physiol* 1991;262:H2058-H2068.
37. Buxton DB, Vaghaiwalla Mody F, Krivokapitch J, Phelps ME, Schelbert HR. Quantitative assessment of prolonged metabolic abnormalities in reperfused canine myocardium. *Circulation* 1992;85:1842-1856.
38. Calderhead DM, Kitagawa K, Lienhard GE, Gould GW. Translocation of the brain-type glucose transporter largely accounts for insulin stimulation of glucose transport in BC3H-1 myocytes. *Biochem J* 1990;269:597-601.
39. Camici P, Ferrannini E, Opie LH. Myocardial metabolism in ischemic heart disease: basic principles and application to imaging with positron emission tomography. *Prog Cardiovasc Dis* 1989;32:217-238.
40. Camici P, Marracini P, Marzilli M, Lorenzoni R, Buzzigoli G, Puntoni R, Boni C, Bellina CR, Klassen GA, L'Abbate A, Ferrannini E. Coronary hemodynamics and myocardial metabolism during and after pacing stress in normal subjects. *Am J Physiol* 1989;257:E309-E317.
41. Canty JM, Klocke FJ. Reductions in regional myocardial function at rest in conscious dogs with chronically reduced regional coronary artery pressure. *Circ Res* 1987;61(suppl II):II-107-II-116.
42. Chatterjee K, Swan CJ, Parmley W, Sustaita N, Marcus HS, Matloff M. Influence of direct myocardial revascularization on left ventricular asynergy and function in patients with coronary heart disease, with and without previous myocardial infarction. *Circulation* 1973;47:276-286.
43. Cigarroa CG, deFilippi CR, Brickner E, Alvarez LG, Wait MA, Grayburn PA. Dobutamine stress echocardiography identifies hibernating myocardium and predicts recovery of left ventricular function after coronary revascularization. *Circulation* 1993;88:430-436.

44. Conversano A, Herrero P, Geltman EM, Pérez JE, Bergmann SR, Gropler RJ. Differentiation of stunned from hibernating myocardium by positron emission tomography. *Circulation* 1992;86(Suppl I):I-107.
45. Cooper G, Tomanek RJ. Load regulation of structure, composition, and function of mammalian myocardium. *Circ Res* 1982;50:788-798.
46. Corretti MC, Koretsune Y, Chacko VP, Zweier JL, Marban E. Glycolytic inhibition and calcium overload as consequences of exogenously-generated free radicals in rabbit hearts. *J Clin Invest* 1991, 88:1014-1025.
47. Czernin J, Muller P, Chan S, Brunken RC, Porenta G, Krivokapitch J, Chen K, Chan A, Phelps ME, Schelbert HR. Influence of age and hemodynamics on myocardial blood flow and flow reserve. *Circulation* 1993;88:62-69.
48. Czernin J, Porenta G, Brunken R, Krivokapitch J, Chen K, Bennet R, Hage A, Fung C, Tillisch J, Phelps ME, Schelbert HR. Regional blood flow, oxidative metabolism, and glucose utilization in patients with recent myocardial infarction. *Circulation* 1993;88:884-895.
49. DeFronzo RA, Tobin JD, Andres R. Glucose clamp technique: a method for quantifying insulin secretion and resistance. *Am J Physiol* 1979;237:E214-E223.
50. Depré C, Vanoverschelde J-L, Melin JA, Borgers M, Bol A, Ausma J, Dion R, Wijns W. Structural and metabolic correlates of the reversibility of chronic left ventricular ischemic dysfunction in humans. *Am J Physiol* 1995;268: in press
51. DeServi S, Ferrario M, Ghio S, Angoli L, Bramucci E, Ardissino D, Specchia G. Effects of atrial pacing and dipyridamole administration on coronary hemodynamics of collateralized myocardial regions in stable angina pectoris. *Am J Cardiol* 1990;65:703-708.
52. de Silva R, Yamomoto Y, Rhodes CG, Iida H, Nihoyannopoulos P, Davies GJ, Lammertsma AA, Jones T, Maseri A. Preoperative prediction of the outcome of coronary revascularization using positron emission tomography. *Circulation* 1992;86:1738-1742.
53. Di Carli MF, Davidson M, Little R, Khanna S, Mody FV, Brunken RC, Czernin J, Rokhsar S, Stevenson LW, Laks H, Hawkins R, Schelbert HR, Phelps ME, Maddahi J. Value of metabolic imaging with positron emission tomography for evaluating prognosis in patients with coronary artery disease and left ventricular dysfunction. *Am J Cardiol* 1994;73:527-533.
54 Di Carli M, Sherman T, Khanna S, Davidson M, Rokhsar S, Hawkins R, Phelps M, Schelbert H, Maddahi J. Myocardial viability in asynergic regions subtended by occluded coronary arteries: relation to the status of collateral flow in patients with chronic coronary artery disease. *J Am Coll Cardiol* 1994;23:860-868.
55. Dilsizian V, Rocco TP, Freedman NM, Leon MB, Bonow RO. Enhanced detection of ischemic but viable myocardium by the reinjection of thallium after stress redistribution imaging. *N Engl J Med* 1990; 323:141-146.
56. Dilsizian V, Freedman NMT, Bacharach SL, Perrone-Filardi P, Bonow RO. Regional Thallium uptake in irreversible defects: magnitude of change in Thallium activity after reinjection distinguishes viable from nonviable myocardium. *Circulation* 1992;85:627-634.
57. du Toit EF, Opie LH. Modulation of severity of reperfusion stunning in the isolated rat heart by agents altering calcium flux at onset of reperfusion. *Circ Res* 1992;70:960-967.

58. Duwel CMB, Visser FC, van Eenige MJ, Roos JP. Variables of myocardial backdiffusion, determined with 17-IODO-131 heptadecanoic acid in the normal dog heart. *Mol Cell Biochem* 1989;88:191-194.
59. Eitzman D, Al-Aouar Z, Kanter HL, vom Dahl J, Kirsh M, Deeb GM, Schwaiger M. Clinical outcome of patients with advanced coronary artery disease after viability studies with positron emission tomography. *J Am Coll Cardiol* 1992, 20:559-565.
60. Ellis SG, Wynne J, Braunwald E, Henschke CI, Sandor T, Kloner RA. Response of reperfusion-salvaged, stunned myocardium to inotropic stimulation. *Am Heart J* 1984, 107:13-19.
61. Emond M, Mock MB, Davis KB, Fisher LD, Holmes DR, Chaitman BR, Kaiser GC, Alderman E, Killip III T, and Participants in the Coronary Artery Surgery Study (CASS). Long-term survival of medically-treated patients in the Coronary Artery Surgery Study (CASS) registry. *Circulation* 1994;90:2645-2657.
62. Fedele FA, Gewirtz H, Capone RJ, Sharaf B, Most AS. Metabolic response to prolonged reduction of myocardial blood flow distal to a severe coronary artery stenosis. *Circulation* 1988;78:729-735.
63. Feng TP. The effect of length on the resting metabolism of muscle. *J Physiol (London)* 1932;74:441-454.
64 Flameng W, Suy R, Schwartz F, Borgers M, Piessens J, Thone F, Van Ermen H, De Geest H. Ultrastructural correlates of left ventricular contraction abnormalities in patients with chronic ischemic heart disease: determinants of reversible segmental asynergy post-revascularization surgery. Am Heart J 1981;102:846-857.
65. Flameng W, Wouters L, Sergeant P, Lewi P, Borgers M, Thone F, Suy R. Multivariate analysis of angiographic histologic and electrocardiographic data in patients with coronary disease. *Circulation* 1984;70:7-17.
66. Flameng W, Vanhaecke J, Van Belle H, Borgers M, De Beer L, Minten J. Relation between coronary artery stenosis and myocardial purine metabolism, histology and regional function in humans. *J Am Coll Cardiol* 1987;9: 1235-1242.
67. Fox KA, Abendschein DR, Ambos HD, Sobel SE, Bergmann SR. Efflux of metabolized and non-metabolized fatty acid from canine myocardium: implications for quantifying myocardial metabolism tomographically. *Circ Res* 1985;57:232-243.
68. Gallagher KP, Kumada T, Koziol JA, Mc Kown MD, Kemper WS, Ross Jr. Significance of regional wall thickening abnormalities relative to transmural myocardial perfusion in anesthetized dogs. C*irculation* 1980;62:1266-1274.
69. Gallagher KP, Matsuzaki M, Koziol JA, Kemper WS, Ross Jr. Regional myocardial perfusion and wall thickening during ischemia in conscious dogs. *Am J Physiol* 1984;16:H727-H738.
70. Gallagher KP, Matsuzaki M, Osakada Kemper WS, Ross Jr. Effects of exercise on the relationship between myocardial blood flow and systolic wall thickening in dogs with acute coronary stenosis. *Circ Res* 1983;52:716-729.
71. Gambhir SS, Schwaiger M, Huang SC, Krivokapitch J, Schelbert HR, Nienaber CA, Phelps ME: A simple noninvasive quantification method for measuring myocardial glucose utilization in humans employing positron emission tomography and F-18 deoxyglucose. *J Nucl Med* 1989;30:359-366.

72. Gao WD, Atar D, Backx PH, Marban E. Direct measurement of the calcium responsiveness of the contractile proteins in intact stunned myocardium. *Circulation* 1994;90(part 2):I-646.
73. Gayheart PA, Vinten-Johansen J, Johnston WE, Hester TO, Robert Corderll A. Oxygen requirements of the dyskinetic myocardial segment. *Am J Physiol* 1989; 257:H1184-H1191.
74. Gewirtz H, Fischman AJ, Abraham S, Gilson M, Strauss HW, Alpert NM. Positron emission tomographic measurements of absolute myocardial blood flow permits identification of nonviable myocardium in patients with chronic myocardial infarction. *J Am Coll Cardiol* 1994; 23:851-859.
75. Gould KL, Schelbert HR, Phelps ME, Hoffman EJ. Non invasive assessment of coronary stenoses with myocardial perfusion imaging during pharmacologic coronary vasodilatation. V. Detection of 47 percent diameter coronary stenosis with intravenous nitrogen-13 ammonia and emission computed tomography in intact dogs. *Am J Cardiol* 1979; 3:200-208.
76. Grandin C, Bol A, Coppens A, Essamri B, Demeure R, Hammer F, Wijns W, Melin J. MRI determination of myocardial contours for partial volume and spillover corrections of PET data. *Eur J Nucl Med* 1991;18:647.
77. Grandin C, Wijns W, Melin JA, Bol A, Robert A, Heyndrickx GR, Michel C, Vanoverschelde J-L. Delineation of myocardial viability with positron emission tomography: Incremental value of quantitative flow and metabolic assessment for identification of reversible dysfunction after coronary revascularization. *J Nucl Med* 1995, in press.
78. Gropler RJ, Siegel BA, Lee KJ, Moerlein SM, Perry DJ, Bergmann SR, Geltman EM. Nonuniformity in myocardial accumulation of fluorine-18-fluorodeoxyglucose in normal fasted humans. *J Nucl Med* 1990;31:1749-1756.
79. Gropler RJ, Siegel BA, Sampathkumaran K, Pérez JE, Sobel BE, Bergmann SR, Geltman EM. Dependence of recovery of contractile function on maintenance of oxidative metabolism after myocardial infarction. *J Am Coll Cardiol* 1992;19:989-997.
80. Gropler RL, Geltman EM, Sampathkumaran K, Pérez JE, Moerlein SM, Sobel BE, Bergmann SR, Siegel BA. Functional recovery after coronary revascularization for chronic coronary artery disease is dependent on maintenance of oxidative metabolism. *J Am Coll Cardiol* 1992;20:569-577.
81. Gropler RJ, Geltman EM, Sampathkumaran K, Pérez JE, Schechtman KB, Conversano A, Sobel BE, Bergmann SR, Siegel BA. Comparison of carbon-11-acetate with fluorine-18-fluorodeoxyglucose for delineating viable myocardium by positron emission tomography. *J Am Coll Cardiol* 1993;22:1587-1597.
82. The GUSTO Angiographic Investigators. The effects of tissue plasminogen activator, streptokinase or both on coronary artery patency, ventricular function, and survival after acute myocardial infarction. *N Engl J Med* 1993; 329:1615-1622.
83. Hamer AW, Takayama M, Abraham KA, Roche AHG, Kerr AR, Williams BF, Ramage C, White HD. End-systolic volume and long-term survival after coronary artery bypass graft surgery in patients with impaired left ventricular function. *Circulation* 1994;90:2899-2904.

84. Hamm CW, Weber PW, Reimers J, Markworth P, Hinrichs A. Biphasic recovery of left ventricular dysfunction in hibernating myocardium. *Circulation* 1992;86(suppl I):I-190.
85. Harris P, Gloster J. The effects of acute hypoxia on lipid synthesis in the rat heart. *Cardiology* 1971;56:43-47.
86. Hearse DJ, Humphrey SM, Chain EB: Abrupt reoxygenation of the anoxic potassium-arrested perfused rat heart: a study of myocardial enzyme release. *J Mol Cell Cardiol* 1973;5:395-407.
87. Hearse DJ, Humphrey SM, Nayler WG: Ultrastructural changes associated with reoxygenation in the anoxic myocardium. *J Mol Cell Cardiol* 1975;7:315-324.
88. Hearse DJ: Reperfusion of the ischemic myocardium. *J Mol Cell Cardiol* 1977;9:605-616.
89. Hearse DJ, Garlick PB, Humphrey SM: Ischaemic contracture of myocardium. Mechanisms and prevention. *Am J Cardiol* 1977;39:926-933.
90. Henes CG, Bergmann SR, Walsh MN, Sobel BE, Geltman EM. Assessment of myocardial oxidative metabolic reserve with positron emission tomography and carbon-11 acetate. *J Nucl Med* 1989;30:1489-1499.
91. Henes CG, Bergmann SR, Pérez JE, Sobel BE, Geltman EM. The time course of restoration of nutritive perfusion, myocardial oxygen consumption, and regional function after coronary thrombolysis. *Coronary Artery Disease*. 1990;1:687-696.
92. Herrero P, Markham J, Bergmann, SR. Quantitation of myocardial blood flow with $H_2{}^{15}O$ and positron emission tomography: assessment and error analysis of a mathematical approach. *J Comput Assist Tomogr* 1989; 13:862-873.
93. Herrero P, Bergmann SR. Recent developments in quantification of myocardial perfusion with positron emission tomography. *Coronary Artery Disease* 1990;1: 518-525.
94. Herrero P, Staudenherz A, Walsh JF, Gropler RJ, Bergmann, SR. Heterogeneity of myocardial perfusion provides the physiological basis of "perfusable tissue index." *J Nucl Med* 1995;36:320-327.
95 Heyndrickx GR, Millard RW, Mc Ritchie RJ, Maroko PR, Vatner SF. Regional myocardial functional and electrophysiological alterations after brief coronary occlusions in conscious dogs. *J Clin Invest* 1975;56:978-985
96. Heyndrickx GH, Wijns W, Vogelaers D, Degrieck Y, Bol A, Vandeplassche G, Melin JA. Recovery of regional contractile function and oxidative metabolism in stunned myocardium induced by 1-hour circumflex coronary artery stenosis in chronically instrumented dogs. *Circ Res* 1993; 72:901-913.
97. Hicks RJ, Herman WH, Kalff V, Molina E, Wolfe ER, Hutchins G, Schwaiger M. Quantitative evaluation of regional substrate metabolism in the human heart by positron emission tomography. *J Am Coll Cardiol* 1991; 18:101-111.
98. Hoffman EJ, Huang Sc, Phelps ME. Quantitation in positron emission computed tomography: 1. effect of object size. *J Comput Assist Tomogr* 1979;3:299-308.
99. Hoffman EJ, Phelps ME, Huang S-C, Schelbert HR. Dynamic, gated and high resolution imaging with the ECAT III. *IEEE Trans Nucl Sci* 1986;33:452-455.
100. Hutchins GD, Schwaiger M, Rosenspire KC, Krivokapitch J, Schelbert H, Kuhl DE. Noninvasive quantification of regional blood flow in the human heart using N-13 ammonia and dynamic positron emission tomographic imaging. *J Am Coll Cardiol* 1990;15:1032-1042.

101. Iida H, Kanno I, Takahashi A. Measurement of absolute myocardial blood flow with $H_2{}^{15}O$ and dynamic positron emission tomography. *Circulation* 1988;78:104-115.
102. Iida H, Rhodes C, de Silva R, Yamamoto Y, Araujo L, Maseri A, Jones T. Myocardial tissue fraction - Correction for partial volume effects and measure of tissue viability. *J Nucl Med* 1991;32:2169-2175.
103. Ito BR, Tate H, Kobayashi M, Schaper W. Reversibly injured, postischemic canine myocardium retains normal contractile reserve. *Circ Res* 1987, 61:834-846.
104. Janier MF, Vanoverschelde J-L, Bergmann SR. Protection of ischemic and reperfused myocardium by adenosine involves different receptor-mediated mechanisms. *Am J Physiol* 1993,264:H163-H170.
105. Janier MF, Vanoverschelde J-L, Bergmann SR: Ischemic preconditioning stimulates anaerobic glycolysis in the isolated rabbit heart *Am J Physiol* 1994;267:H1353-H1360.
106. Jennings RB, Sommers HM, Smyth GA, Flack HH, Linn H: Myocardial necrosis induced by temporary occlusion of a coronary artery in the dog. *Arch Pathol* 1960;70:68-78.
107. Jeremy RW, Koretsune Y, Marban E, Becker LC. Relation between glycolysis and calcium homeostasis in postischemic myocardium. *Circ Res* 1992, 70:1180-1190.
108. Kalff V, Hicks R, Hutchins G, Topol E, Schwaiger M. Use of carbon-11 acetate and dynamic positron emission tomography to assess regional myocardial oxygen consumption in patients with acute myocardial infarction receiving thrombolysis or coronary angioplasty. *Am J Cardiol* 1993;71:529-535.
109. Kety SS. The theory and applications of the exchange of inert gas at the lungs and tissues. *Pharmacol Rev* 1951;3: 1-41.
110. Kety SS. Theory of blood-tissue exchange and its application to measurement of blood flow. *Meth Med Res* 1960;8:223-227.
111. Kety SS. Measurement of local blood flow by the exchange of an inert, diffusible substance. *Meth Med Res* 1960;8:228-236.
112. Kloner RA, Ganote CE, Jennings RB: The 'no-reflow' phenomenon after temporary coronary occlusion in the dog. *J Clin Invest* 1974, 54:1496-1508.
113. Kloner RA, Przyklenk K, Patal B. Altered myocardial states. The stunned and hibernating myocardium. *Am J Med* 1989;86(suppl 1A):14-22.
114. Knuuti MJ, Nuutila P, Ruotsalainen U, Saraste M, Härkönen R, Ahonen A, Teras M, Haaparanta M, Wegelius U, Haapanen A, Hartiala J, Voipio-Pulkki LM: Euglycemic hyperinsulinemic clamp and oral glucose load in stimulating myocardial glucose utilization during positron emission tomography. *J Nucl Med* 1992;33:1255-1262.
115. Knuuti MJ, Yki-Jarvinen H, Voipio-Pulkki LM, Maki M, Ruotsalainen U, Härkönen R, Teras M, Haaparanta M, Bergman J, Hartiala J, Wegelius U, Nuutila P. Enhancement of myocardial [fluorine-18]-fluoro-deoxyglucose uptake by a nicotinic acid derivative. *J Nucl Med* 1994;35:989-998.
116. Khouri EM, Gregg DE, Rauford CR. Effect of exercise on cardiac output, left coronary flow and myocardial metabolism in the unanesthetized dog. *Circ Res* 1965;17: 427-437.
117. Kitakaze M, Weisman HF, Marban E. Contractile dysfunction and ATP depletion after transient calcium overload in perfused ferret hearts. *Circulation* 1988, 77:685-695.
118. Krivokapitch J, Huang SC, Phelps ME, MacDonald NS, Shine KI. Dependence of $^{13}NH_3$ myocardial extraction and clearance on flow and metabolism. *Am J Physiol* 1982; 242:H536-542.

119. Krivokapitch J, Huang SC, Selin CE, Phelps ME: Fluorodeoxyglucose rate constants, lumped constant, and glucose metabolic rate in rabbit heart. *Am J Physiol* 1987; 252:H777-H787.
120. Krivokapitch J, Smith GT, Huang SC, Hoffman EJ, Ratib O, Phelps ME, Schelbert HR. N-13 ammonia myocardial imaging at rest and with exercise in normal volunteers. Quantification of absolute myocardial perfusion with dynamic positron emission tomography. *Circulation* 1989;80:1328-1337.
121. Krivokapitch J, Huang SC, Schelbert HR. Assessment of the effects of dobutamine on myocardial blood flow and oxidative metabolism in normal human subjects using nitrogen-13 ammonia and carbon-11 acetate. *Am J Cardiol* 1993;71:1351-1356.
122. Kusuoka H, Porterfield JK, Weisman HF, Weisfeldt ML, Marban E. Pathophysiology and pathogenesis of stunned myocardium: Depressed Ca^{++} activation of contraction as a consequence of reperfusion-induced cellular calcium overload in ferret hearts. *J Clin Invest* 1987;79:950-961.
123. Kusuoka H, Koretsune Y, Chacko VP, Weisfelt ML, Marban E. Excitation-contraction coupling in postischemic myocardium: Does failure of activator Ca^{2+} transients underlie "stunning"? *Circ Res* 1990;66:1268-1276.
124. La Canna G, Alfieri O, Giubbini R, Gargano M, Ferrari R, Visioli O. Echocardiography during infusion of dobutamine for identification of reversible dysfunction in patients with coronary artery disease. *J Am Coll Cardiol* 1994;23:617-626.
125. Laxson DD, Homans DC, Dai XZ, Sublett E, Bache RJ. Oxygen consumption and coronary reactivity in postischemic myocardium. *Circ Res* 1989;64:9-20.
126. Lee KS, Marwick TH, Cook SA, Go RT, Fix JS, James KB, Sapp SK, MacIntyre WJ, Thomas JD. Prognosis of patients with left ventricular dysfunction, with and without viable myocardium after myocardial infarction. Relative efficacy of medical therapy and revascularization. *Circulation* 1994;90:2687-2694.
127. Liedtke AJ. Alterations of carbohydrate and lipid metabolism in the acutely ischemic heart. *Prog Cardiovasc Dis* 1981;23:321-336.
128. Marban E. Myocardial stunning and hibernation. The physiology behind the colloquialisms. *Circulation* 1991; 83:681-688.
129. Marcus ML, Harrison DG, White CW, McPherson DD, Wilson RF, Kerber RE. Assessing the physiologic significance of coronary obstructions in patients. Importance of diffuse undetected atherosclerosis. *Prog Cardiovasc Dis* 1988;31:39-56.
130. Marinho NVS. Keogh BE, Costa DC, Ell PJ, Lammertsma AA, Camici PG. Hibernating myocardium: is it really due to chronic underperfusion? *Circulation* 1994;90(part 2):I-314.
131. Marwick TH, MacIntyre WJ, Lafont A, Nemec JJ, Salcedo EE. Metabolic responses of hibernating and infarcted myocardium to revascularization. A follow-up study of regional perfusion, function and metabolism. *Circulation* 1992;85:1347-1353.
132. Marwick T, Vanoverschelde JLJ: Echocardiographic Determination of Myocardial Viability. In Marwick TH (Ed): *Stress Echocardiography: its Role in the Diagnosis and Evaluation of Coronary Artery Disease.* Dordrecht. Kluwer Academic Publishers, 1994, pp163-178.
133. Marzullo P, Parodi O, Reisenhofer B, Sambuceti G, Picano E, Distante A, Gimelli A, L'Abbate A. Value of rest Thallium-201 / technetium-99m sestamibi scans and

dobutamine echocardiography for detecting myocardial viability. *Am J Cardiol* 1993;71:166-172.
134. Matsuzaki M, Gallagher KP, White F, Ross J Jr. Sustained regional dysfunction produced by prolonged coronary stenosis: gradual recovery after reperfusion. *Circulation* 1983;68:170-182.
135. Melin JA, Vanoverschelde J-L, Bol A, Heyndrickx G, Wijns W: The use of ^{11}C-acetate for assessment of aerobic metabolism. *J Nucl Cardiol* 1994; 1:S48-S57.
136. Mercier JC, Lando U, Kanmatsuse K, Ninomiya K, Meerbaum S, Fishbein MC, Swan HJC, Ganz W. Divergent effects of inotropic stimulation on the ischemic and severely depressed reperfused myocardium. *Circulation* 1982, 66:397-400.
137. Mori T, Minamiji K, Kurogane H, Ogawa K, Yoshida Y. Rest-injected Thallium-201 imaging for assessing viability of severe asynergic regions. *J Nucl Med* 1991; 32,9:1718-1724.
138. Muzik O, Beanlands R, Hutchins G, Mangner TJ, Nguyen N, Schwaiger M. Validation of nitrogen-13 ammonia tracer kinetic model for quantification of myocardial blood flow using PET. *J Nucl Med* 1993;34:83-91.
139. Myears DW, Sobel BE, Bergmann SR. Substrate use in ischemic and reperfused canine myocardium: quantitative considerations. *Am J Physiol* 1987;253:H107-H114.
140. Nakao K, Yasue H, Fujimoto K, Jougasaki M, Yamamoto H, Hitoshi Y, Takatsu K, Miyamoto E. Increased expression and regional differences of atrial myosin light chain 1 in human ventricles with old myocardial infarction: Analyses using two monoclonal antibodies. *Circulation* 1992;86:1727-1737.
141. Neely JR, Morgan HE. Relationship between carbohydrate and lipid metabolism and the energy balance of the heart muscle. *Annu rev Physiol* 1974;36:412-459.
142. Ng CK, Holden JE, DeGrado TR, Raffel DM, Kornguth ML, Gatley J: Sensitivity of myocardial fluoro-deoxyglucose lumped constant to glucose and insulin. *Am J Physiol* 1991:260:H593-H603.
143. Nicklas JM, Becker LC, Bulkley BH. Effects of repeated brief coronary occlusion on regional left ventricular function and dimensions in dogs. *Am J Cardiol* 1985;56:473-478.
144. Nienaber CA, Brunken RC, Sherman CT, Yeatman LA, Gambhir SS, Krivokapitch J, Demer LL, Ratib O, Child JS, Phelps ME, Schelbert HR. Metabolic and functional recovery of ischemic myocardium after coronary angioplasty. *J Am Coll Cardiol* 1991;18:966-978.
145. Nixon JV, Brown CN, Smitherman TC. Identification of transient and persistent segmental wall motion abnormalities in patients with unstable angina by two-dimensional echocardiography. *Circulation* 1982;65:1497-1503.
146. Ohtani H, Tamaki N, Yonekura Y, Mohiuddin I, Hirata K, Ban T, Konishi J. Value of Thallium-201 reinjection after delayed SPECT imaging for predicting reversible ischemia after coronary artery bypass graft. *Am J Cardiol* 1990; 66:394-399.
147. Opie LH. Reperfusion injury and its pharmacologic manipulation. *Circulation* 1989, 80:1049-1062.
148. Opie LH. Cardiac metabolism - emergence, decline, and resurgence. Part I. *Cardiovasc Res* 1992;26:721-733.
149. Opie LH. Cardiac metabolism - emergence, decline, and resurgence. Part II. *Cardiovasc Res* 1992;26:817-830.

150. Pantely GA, Malone SA, Rhen WS, Anselone CG, Arai A, Bristow J, Bristow JD. Regeneration of myocardial phosphocreatine in pigs despite continued moderate ischemia. *Circ Res* 1990;67:1481-1493.
151. Passamani E, Davis BD, Gillespie MJ, Killip T and the CASS principal investigators and their associates. A randomized trial of coronary artery bypass surgery. Survival of patients with low ejection fraction. *N Engl J Med* 1985;312:1665-1671.
152. Patlak CS, Blasberg RG, Fenstermacher JD. Graphical evaluation of blood-to-brain transfer constants from multiple-time uptake data. *J Cereb Blood Flow Metab* 1983;3:1-7.
153. Phelps ME, Hoffman EJ, Huang SC, Ter-Pogossian NM. Effect of positron range on spatial resolution. *J Nucl Med* 1975;16:649-652.
154. Phelps ME, Huang SC, Hoffman EJ, Selin C, Sokoloff L, Kuhl DE. Tomographic measurement of local glucose metabolic rates in humans with [18-F]-2-fluoro 2-deoxy-D-glucose: validation of the method. *Ann Neurol* 1979;6:371-388.
155. Picano E, Simonetti I, Masini M, Marzilli M, Lattanzi F, Distante A, DeNes M, L'Abbate A. Transient myocardial dysfunction during pharmacologic vasodilation as an index of reduced coronary reserve: a coronary hemodynamic and echocardiographic study. *J Am Coll Cardiol* 1986;8:84-90.
156. Piérard LA, DeLandsheere CM, Berthe C, Rigo P, Kulbertus HE. Identification of viable myocardium by echocardiography during dobutamine infusion in patients with myocardial infarction after thrombolytic therapy: comparison with positron emission tomography. *J Am Coll Cardiol* 1990;15:1021-1031.
157. Previtali M, Poli A, Lanzarini L, Fetiveau R, Mussini A, Ferrario M. Dobutamine stress echocardiography for assessment of myocardial viability and ischemia in acute myocardial infarction treated with thrombolysis. *Am J Cardiol* 1993;72:124G-130G.
158. Pupita G, Masuri A, Kaski JC, Galassi AR, Gavrielides S, Davies G, Crea F. Myocardial ischemia caused by distal coronary artery constriction in stable angina pectoris. N Engl J Med 1990;323:514-520.
159. Ragosta M, Beller GA, Watson DD, Kaul S, Gimple LW. Quantitative planar rest-redistribution ^{201}Tl imaging in detection of myocardial viability and prediction of improvement in left ventricular function after coronary bypass surgery in patients with severely depressed left ventricular function. *Circulation* 1993;87:1630-1641.
160. Rahimtoola S. A perspective on the three large multicenter randomized clinical trial of coronary bypass surgery for stable angina. *Circulation* 1985;72(suppl V):V-123-V-135.
161. Rahimtoola SH. The hibernating myocardium. *Am Heart J* 1989;117:211-221.
162. Randle PJ, England PJ, Denton RM. Control of tricarboxylic cycle and its interaction with glycolysis during acetate utilization in rat heart. *Biochem J* 1970; 117:667-695.
163. Ratib O, Phelps ME, Huang SC, Henze E, Selin CE, Schelbert HR. Positron tomography with deoxyglucose for estimating local myocardial glucose metabolism. *J Nucl Med* 1982;23:577-586.
164. Rauch B, Helus F, Grunze M, Braunwell E, Mall G, Hasselbach W, Kubler W. Kinetics of ^{13}N-ammonia uptake in myocardial single cells indicating potential limitations in its applicability as a marker of myocardial blood flow. *Circulation* 1985;71:387-393.
165. Renkin J, Wijns W, Ladha Z, Col J. Reversal of segmental hypokinesis by coronary angioplasty in patients with unstable angina, persistent T wave inversion, and left

anterior descending coronary artery stenosis. Additional evidence for myocardial stunning in humans. *Circulation* 1990;82:913-921.
166. Renstrom B, Liedtke AJ, Nellis SH. Mechanisms of substrate preference for oxidative metabolism during early myocardial reperfusion. *Am J Physiol* 1990;259:H317-H323.
167. Rose J, Schultz R, Martin C, Heusch G. Post-ejection wall thickening as a marker of successful short-term hibernation. *Cardiovascular Research* 1993;27:1306-1311.
168. Rosenspire KC, Schwaiger M, Mangner TJ, Hutchins GD, Sutorik A, Kuhl DE. Metabolic fate of [^{13}N] ammonia in human and canine blood. *J Nucl Med* 1990;31:163-167.
169. Ross J Jr. Myocardial perfusion-contraction matching. *Circulation* 1991;83:1076-1083.
170. Russel III RR, Mrus JM, Mommessin JI, Taegtmeyer H. Compartmentation of hexokinase in rat heart: a critical factor for tracer kinetic analysis of myocardial glucose metabolism. *J Clin Invest* 1992;90:1972-1977.
171. Sawada SG, Segar DS, Ryan T, Brown SE, Dohan AM, Williams R, Fineberg NS, Armstrong WF, Feigenbaum H. Echocardiographic detection of coronary artery disease during dobutamine infusion. *Circulation* 1991;83:1605-1614.
172. Schaper W, Lewi P, Flameng W, Gijpen L. Myocardial steal produced by coronary vasodilation in chronic coronary occlusion. *Basic Res Cardiol* 1973;68:3-20.
173. Schaper W, Görge G, Winkler B, Schaper J. The collateral circulation of the heart. *Prog Cardiovasc Dis* 1988;31:57-77.
174. Schaper W, Schott RJ, Kobayashi M. Reperfused myocardium: stunning, preconditioning and reperfusion injury, in Heusch G (ed): *Pathophysiology and rational pharmacotherapy of myocardial ischemia.* Darmstadt, FRG, Steinkopff Verlag, 1990:pp175-pp197.
175. Schelbert HR, Phelps ME, Hoffman EJ, Huang SC, Selin CE, Kuhl DE. Regional myocardial perfusion assessed with N-13 labeled ammonia and positron emission computerized axial tomography. *Am J Cardiol* 1979; 43:209-218.
176. Schelbert HR, Phelps ME, Huang SC, MacDonald NS, Hansen H, Selin C, Kuhl DE. N-13 ammonia as an indicator of myocardial blood flow. *Circulation* 1981; 63:1259-1272.
177. Schelbert HR, Henze E, Schon HR, Keen R, Hansen H, Selin C, Huang SC, Barrio JR, Phelps ME. C-11 palmitate for the non-invasive evaluation of regional fatty acid metabolism with positron computed tomography. III. In vivo demonstration of the effects of substrate availability on myocardial metabolism. *Am Heart J* 1983;105:492-504.
178. Schelbert HR, Henze E, Keen R, Schon HR, Hansen H, Selin C, Huang SC, Barrio JR, Phelps ME. C-11 labeled palmitic acid for the non-invasive evaluation of regional myocardial fatty acid metabolism with positron-computed tomography. IV. In vivo evaluation of acute demand-induced ischemia in dogs. *Am Heart J* 1983;106:736-750.
179. Schelbert HR, Buxton D. Insights into coronary artery disease gained from metabolic imaging. *Circulation* 1988; 78:496-505
180. Schon HR, Schelbert HR, Robinson GD, Najafi A, Huang SC, Hansen H, Barrio JR, Phelps ME, Kuhl DE. C-11 labeled palmitic acid for the non-invasive evaluation of regional myocardial fatty acid metabolism with positron-computed tomography : I Kinetics of C-11 palmitic acid in normal myocardium. *Am Heart J* 1982;103:532-547.
181. Schon HR, Schelbert HR, Najafi A, Hansen H, Robinson GD, Huang SC, Barrio JR, Phelps ME. C-11 labeled palmitic acid for the non-invasive evaluation of regional myocardial fatty acid metabolism with positron-computed tomography. II. Kinetics of C-11 palmitic acid in acutely ischemic myocardium. *Am Heart J* 1982;103:548-561.

182. Schulz R, Rose J, Martin C, Brodde OE, Heusch G. Development of short-term hibernation. Its limitation by the severity of ischemia and inotropic stimulation. *Circulation* 1993;88:684-695.
183. Schwaiger M, Brunken R, Grover-McKay M, Krivokapitch J, Child J, Tillisch JH, Phelps ME, Schelbert HR. Regional myocardial metabolism in patients with acute myocardial infarction assessed by positron emission tomography. *J Am Coll Cardiol* 1986;8:800-808.
184. Schwaiger M, Neese RA, Araujo L, Wyns W, Wisneski JA, Sochor H, Swank S, Kulber D, Selin C, Phelps M, Schelbert HR, Fishbein MC, Gertz EW: Sustained nonoxidative glucose utilization and depletion of glycogen in reperfused canine myocardium. *J Am Coll Cardiol* 1989;13:745-754.
185. Schwaiger M, Sun D, Deeb GM, Nguyen N, Haas F, Sebening F, Brosius III FC. Expression of myocardial glucose transporter (GLUT) mRNA's in patients with advanced coronary artery disease (CAD). *Circulation* 1994;90(part 2):I-113.
186. Shah A, Schelbert HR, Schwaiger M, Henze E, Hansen H, Selin C, Huang SC. Measurement of regional myocardial blood flow with N-13 ammonia and positron emission tomography in intact dogs. *J Am Coll Cardiol* 1985;5:92-100.
187. Sharp WW, Terracio L, Borg TK, Samarel AM. Contractile activity modulates actin synthesis and turnover in cultured neonatal rat heart cells. *Circ Res* 1993;73:172-183.
188. Shen YT, Vatner SF. Mechanism of impaired myocardial function during progressive coronary stenosis in conscious pigs: hibernation versus stunning ? *Circ Res* 1995;76:479-488.
189. Simpson P, Savion S. Differentiation of rat myocytes in single cell cultures with and without proliferating non myocardial cells: cross-striations, ultrastructure, and chronotropic response to isoproterenol. *Circ Res* 1982;50: 101-116.
190. Smart SC, Sawada S, Ryan T, Segar D, Atherton L, Berkovitz K, Bourdillon PDV, Feigenbaum H. Low-dose dobutamine echocardiography detects reversible dysfunction after thrombolytic therapy of acute myocardial infarction. *Circulation* 1993;88:405-415.
191. Sokoloff L, Reivich M, Kennedy C, DesRosiers MH, Patlak S, Pettigrew KD, Sakurada O, Shinohara M. The C-14 deoxyglucose method for the measurement of local cerebral glucose utilization: theory, procedure and normal values in the conscious and anesthetized albino rat. *J Neurochem* 1977;28:897-916.
192. Stahl LD, Weiss HR, Becker LC. Myocardial oxygen consumption, oxygen supply/demand heterogeneity, and microvascular patency in regionally stunned myocardium. *Circulation* 1988;77:865-872.
193. Stanley WC, Hall JL, Stone CK, Hacker TA. Acute myocardial ischemia causes a transmural gradient in glucose extraction but not glucose uptake. *Am J Physiol* 1992;262:H91-H96.
194. Taegtmeyer H, Hems R, Krebs HA. Utilization of energy providing substrates by the isolated rat heart. *Biochem J* 1980;186:701-711.
195. Taegtmeyer H, Roberts AFC, Raine AEG. Energy metabolism in reperfused hearts muscle: metabolic correlate to return of function. *J Am Coll Cardiol* 1985; 6:864-870.
196. Tamaki N, Yonekura Y, Yamashita K, Saji H, Mazata Y, Senda M, Konishi Y, Hiratu K, Ban T, Kowishi J. Positron Emission Tomography using fluorine-18 deoxyglucose in evaluation of coronary artery bypass grafting. *Am J Cardiol* 1989;64:860-865.

197. Tamaki N, Kawamoto M, Takahashi N, Yonekura Y, Magata Y, Nohara R, Kambara H, Sasayama S, Hirata K, Ban T, Konishi J. prognostic value of an increase in fluorine-18-deoxyglucose uptake in patients with myocardial infarction: comparison with stress-thallium imaging. *J Am Coll Cardiol* 1993;22:1621-1627.
198. Tennant R, Wiggers CJ. The effects of coronary occlusion on myocardial contraction. *Am J Physiol* 1935;112:351-361.
199. Thompson EW, Marino TA, Uboh CE, Kent RL, Cooper G. Atrophy reversal and cardiocyte redifferentiation in reloaded cat myocardium. *Circ Res* 1984;54:367-377.
200. Tillisch J, Brunken R, Marshall R, Schwaiger M, Mandelkern M, Phelps ME, Schelbert HR. Reversibility of cardiac wall motion abnormalities predicted by Positron Tomography. *N Engl J Med* 1986;314:884-888.
201. Topol EJ, Weiss JL, Guzman PA, Dorsey-Lima S, Blank T, Humphrey L, Baumgartner W, Flaherty J, Reitz B. Immediate improvement of dysfunctional myocardial segments after coronary revascularization: detection by intraoperative transesophageal echocardiography. *J Am Coll Cardiol* 1984;4:1123-1134.
202. Tripp MR, Meyer MW, Einzig S, Leonard JJ, Swayze CR, Fox IJ. Simultaneous regional myocardial blood flows by tritiated water and microspheres. *Am J Physiol* 1977; 232:H173-H190.
203. Unger EF, Sheffield CD, Epstein SE. Creation of anastomoses between an extracardiac artery and the coronary circulation. *Circulation* 1990;82:1449-1466.
204. Uren N, Melin JA, DeBruyne B, Wijns W, Baudhuin T, Camici PG. Relation between myocardial blood flow and the severity of coronary artery stenosis. *New Engl J Med* 1994;330:1782-1788.
205. Vaghaiwalla Mody F, Buxton DB, Krivokapitch J, Hansen HA, Selin CE, Schelbert HR. Attenuated response of glucose metabolism in reperfused canine myocardium to changes in substrate levels. *J Am Coll Cardiol* 1990;31(Suppl A):80A.
206. Vanoverschelde J-L, Heyndrickx G, Wijns W, Vogelaers D, Vanbutsele R, Bol A, Melin JA. Assessment of myocardial oxidative metabolism with Carbon-11 acetate: relation to regional work. *Circulation* 1989, 80 (suppl II):II-515
207. Vanoverschelde J-L, Wijns W, Bol A, Essamri B, Melin JA: Regional oxidative metabolism remains coupled to myocardial blood flow in patients with reperfused myocardial infarction. *Eur Heart J* 1990, 11 (Abstr Suppl):26.
208. Vanoverschelde J-L, Melin JA, Essamri B, Heyndrickx G, Wijns W: Resting oxidative metabolism in collateral dependent myocardium. *Circulation* 1990, 82 (suppl III):III-479.
209. Vanoverschelde JLJ, Wijns W, Kolanowski J, Bol A, DeCoster P, Michel C, Cogneau M, Heyndrickx GR, Essamri B, Melin J.A. Competition between palmitate and ketone bodies for the human heart: a study with Positron Emission Tomography. *Am J Physiol* 1993, 264:H701-H707.
210. Vanoverschelde JLJ, Melin JA, Bol A, Vanbutsele R, Cogneau M, Labar D, Robert A, Michel C, Wijns W. Regional oxidative metabolism in patients after recovery from reperfused anterior myocardial infarction: relation to regional blood flow and glucose uptake. *Circulation* 1992;85:9-21.
211. Vanoverschelde JLJ, Wijns W, Depré C, Essamri B, Heyndrickx GR, Borgers M, Bol A, Melin JA. Mechanisms of chronic regional postischemic dysfunction in humans: New

insights from the study of non-infarcted collateral dependent myocardium. *Circulation* 1993;87:1513-1523.

212. Vanoverschelde JLJ, Wijns W, Essamri B, Bol A, Robert A, Labar D, Cogneau M, Michel C, Melin JA. Hemodynamic and mechanical determinants of myocardial oxygen consumption in the normal human heart: Effects of dobutamine. *Am J Physiol* 1993, 265:H1884-H1892.
213. Vanoverschelde JLJ, Bergmann SR. Myocardial reperfusion injury: Concepts, mechanisms, and therapeutic strategies. In Sobel BE and Collen D (eds): *Coronary Thrombolysis in Perspective: Principles Underlying Conjunctive and Adjunctive Therapy*. New-York, Marcel Dekker Inc., 1993, pp271-301.
214. Vanoverschelde J-L, Marwick T, d'Hondt A-M, Baudhuin T, Wijns W, Melin JA: Delineation of myocardial viability with low-dose dobutamine stress-echocardiography in patients with chronic ischemic left ventricular dysfunction. *Circulation* 1993, 88(suppl I):I-111.
215. Vanoverschelde JLJ, Janier MF, Bergmann SR. The relative importance of myocardial energy metabolism compared with ischemic contracture in the determination of ischemic injury in isolated perfused rabbit hearts. *Circ Res* 1994; 74:817-828.
216. Vanoverschelde JLJ, Janier MF, Bakke JE, Marshall DR, Bergmann SR: The rate of anaerobic glycolysis during ischemia determines ischemic injury and functional recovery following reperfusion in the isolated perfused rabbit heart. *Am J Physiol* 1994;267:H1785-H1794.
217. Vanoverschelde J-L, Grandin C, Bol A, Robert A, Wijns W, Melin JA. Preoperative prediction of the return of left ventricular function after revascularization: role of dynamic PET imaging. *Eur Heart J* 1994 (abstract suppl);15:555.
218. Vanoverschelde J-L, Gerber BL, D'Hondt A-M, De Kock M, Dion R, Wijns W, Melin JA. How to select coronary patients with poor left ventricular ejection fraction who should undergo coronary revascularization ? *Circulation* 1994;90(part 2):I-252.
219. Vanoverschelde J-L, Melin JA, Depré C, Borgers M, Dion R, Wijns W. Time-course of functional recovery of hibernating myocardium after coronary revascularization. *Circulation* 1994;90(part 2):I-378.
220. vom Dahl J, Herman WH, Hicks RJ, Ortiz-Alonso FJ, Lee KS, Allman KC, Wilfe ER, Kalff V, Schwaiger M: Myocardial glucose uptake in patients with insulin-dependent diabetes mellitus assessed quantitatively by dynamic positron emission tomography. *Circulation* 1993;88:395-404.
221. vom Dahl J, Eitzman DT, Al-Aouar ZR, Kanter L, Hicks RJ, Deeb GM, Kirsh MM, Schwaiger M. Relation of regional function, perfusion, and metabolism in patients with advanced coronary artery disease undergoing surgical revascularization. *Circulation* 1994;90:2356-2366.
222. Walsh MN, Geltman EM, Brown MA, Henes CG, Weinheimer CJ, Sobel BE, Bergmann SR. Noninvasive estimation of regional myocardial oxygen consumption by positron emission tomography with carbon-11-acetate in patients with myocardial infarction. *J Nucl Med* 1989;30:1798-1808.
223. Wang C, Hu SM. Developmental regulation in the expression of rat heart glucose transporters. *Biochem Biophys Res Commun* 1991;177:1095-1100.

224. Weinberg IN, Huang SC, Hoffman EJ, Araujo L, Nienaber C, Grover-McKay M, Dahlbom M, Schelbert H. Validation of PET-acquired input functions for cardiac studies. *J Nucl Med* 1988;29:241-247.
225. Weinheimer CJ, Brown MA, Nohara R, Pérez JE, Bergmann SR. Functional recovery after reperfusion is predicated on recovery of myocardial oxidative metabolism. *Am Heart J* 1993;125:939-949.
226. White HD, Norris RM, Brown MA, Brandt PWT, Whitlock RML, Wild CJ. Left ventricular end-systolic volume as the major determinant of survival after recovery from myocardial infarction. *Circulation* 1987;76:44-51.
227. Wijns W, Schwaiger M, Huang SC, Buxton DB, Hansen H, Selin C, Keen R, Phelps ME, Schelbert HR. Effects of inhibition of fatty acid oxidation on myocardial kinetics of C-11 labeled palmitate. *Circ Res* 1989;65:1787-1797.
228. Wijns W, Heyndrickx GR, Vogelaers D, Vanoverschelde JLJ, Bol A, Essamri B, Grandin C, Melin JA: Metabolic imaging in postischemic canine myocardium. In Zaret BL and Beller GA (eds): *Nuclear Cardiology: State of the Art and Future Directions*. St Louis, Mosby, 1993, pp284-293.
229. Wijns W, Vanoverschelde J-L, Gerber B, Bartunek J, De Bruyne B, Heyndrickx GR, Melin JA. Evidence that myocardial stunning occurs in humans following unstable angina. *J Am Coll Cardiol* 1995, in press.
230. Williamson JR. Glycolytic control mechanisms: I. Inhibition of glycolysis by acetate and pyruvate in the isolated rat heart. *J Biol Chem* 1965;240:2308-2321.
231. Yamamoto Y, de Silva R, Rhodes CG, Araujo LI, Iida H, Rechavia E, Nihoyannopoulos P, Hacket D, Galassi AR, Taylor CJV, Lammertsma AA, Jones T, Maseri A. A new strategy for the assessment of viable myocardium and regional myocardial blood flow using ^{15}O-water and dynamic positron emission tomography. *Circulation* 1992;86:167-178.
232. Yoshida K, Gould KL. Quantitative relation of infarct size and myocardial viability by positron emission tomography to left ventricular ejection fraction and 3-year mortality with and without revascularization. *J Am Coll Cardiol* 1993;22:984-997.

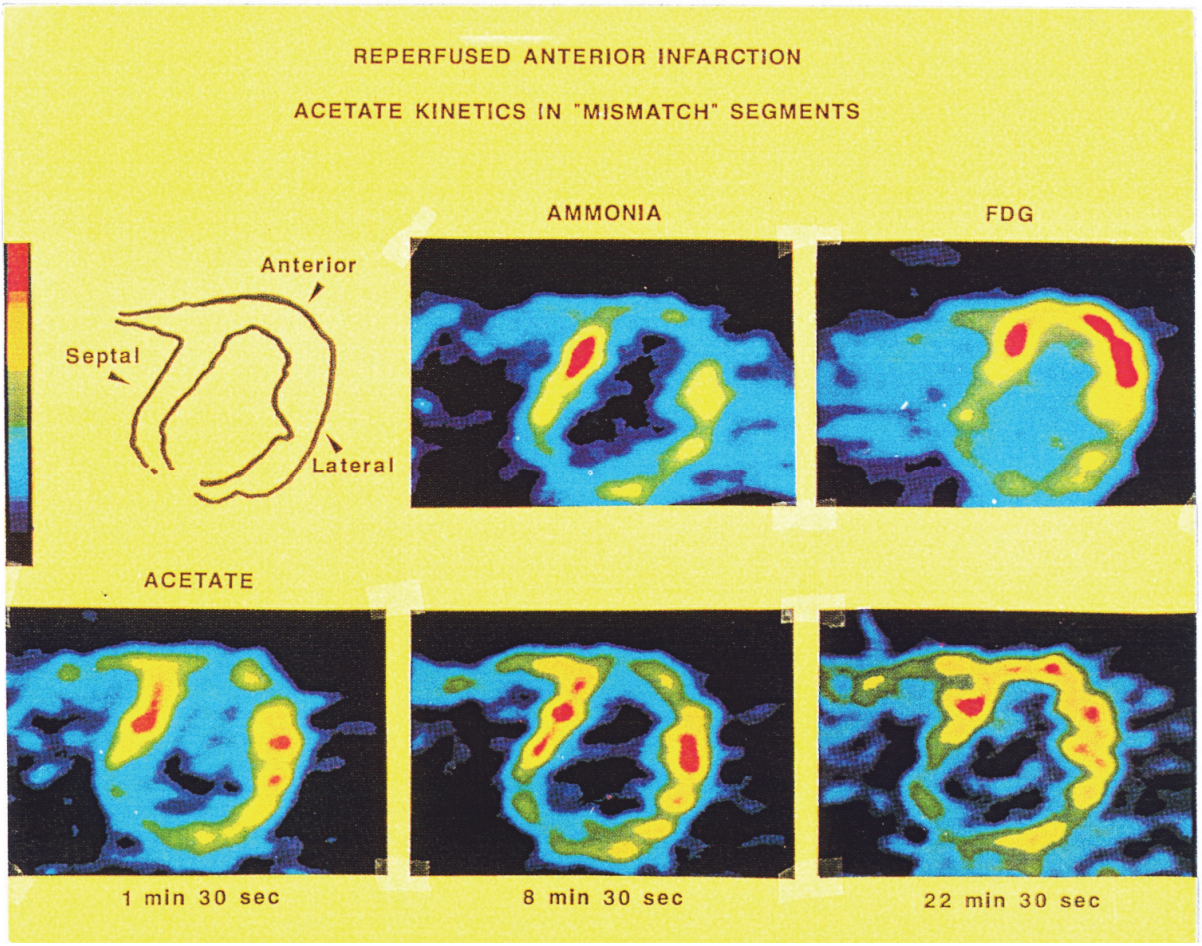

Plate 3-1 *Upper panels:* Schematic representation of patient P669's anatomic cross section (left) and corresponding images obtained after administration of ^{13}N-ammonia (middle) and ^{18}F-FDG (right) 20 days after reperfused acute anterior myocardial infarction. Uptake of ^{13}N-ammonia is decreased in anterior wall (area of infarction), whereas ^{18}F-FDG uptake is increased, relative to flow (flow-metabolism mismatch) in the same territory. *Lower panels:* Serial cross-sectional images obtained after administration of ^{11}C-acetate. Times below images represent mid-acquisition times. Initial images (left) show tracer uptake by myocardium, which is proportional to flow. Note the reduced uptake in hypoperfused anterior segments. Later images (middle and right) allow an appreciation of the clearance of the tracer. Note delayed ^{11}C clearance from the anterior segments.

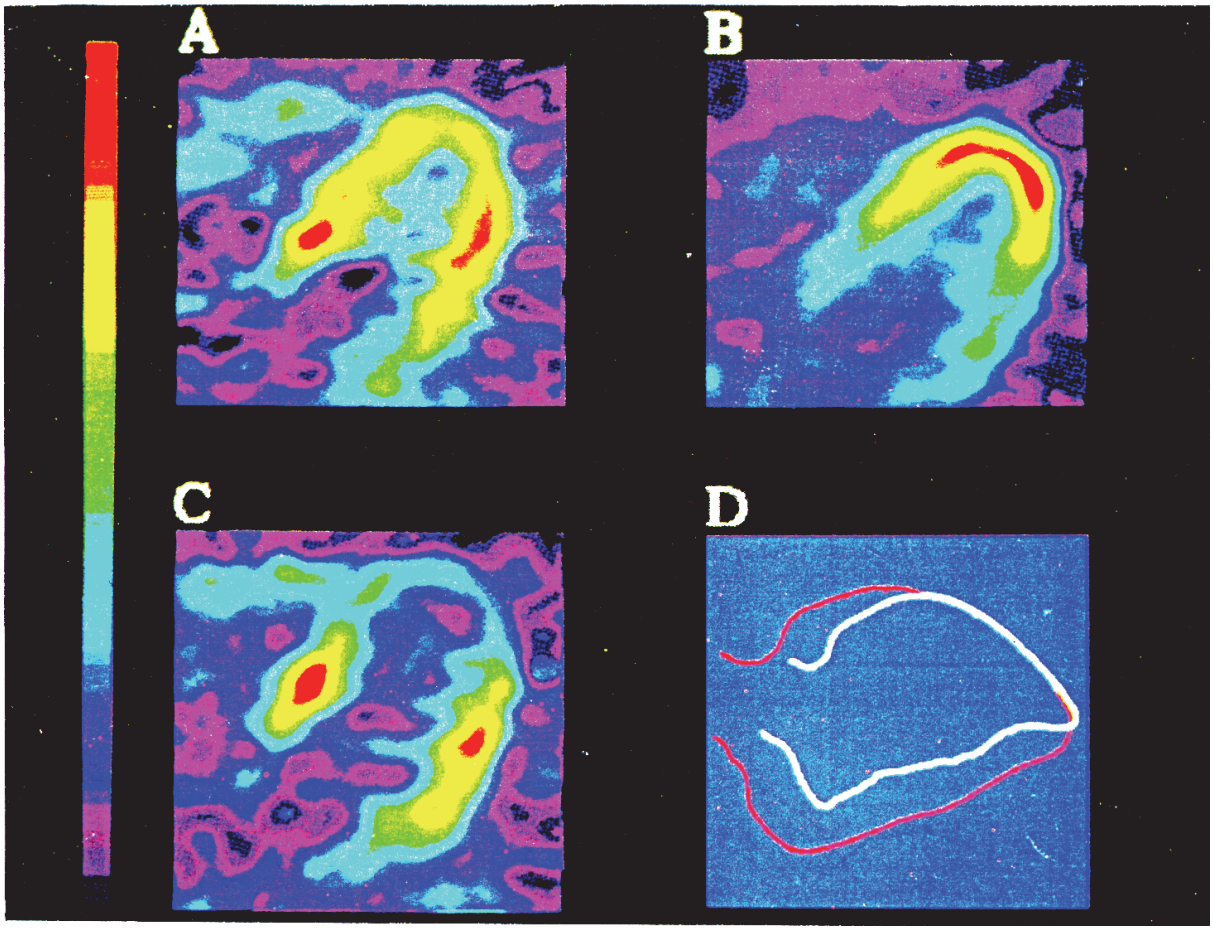

Plate 3-2 Representative cross-sectional tomographic images (linear scale, no background correction) are shown together with the end-diastolic and end-systolic contours from left ventriculography (D). *Panel A* shows the baseline flow image obtained with ^{13}N-ammonia. There is a 20 to 25% relative decrease in tracer uptake in the anterior wall (around 12 o'clock). Maximal uptake is observed in the basal septum and corresponds to an absolute flow value of 113 ml/min/100g, as opposed to an average value of 93 ml/min/100g in the anterior wall. *Panel B* shows the uptake of exogenous glucose, as measured with ^{18}F-FDG. The glucose utilization rate is highest (35 µmol/min/100g) in the area with the relative decrease in flow distribution (flow-metabolism "mismatch"). *Panel C* shows the flow images obtained during infusion of dipyridamole. There is a marked increase in the size of the anterior flow distribution defect. The absolute flow values were 223 ml/min/100g in the septum versus 64 ml/min/100g in the anterior wall.

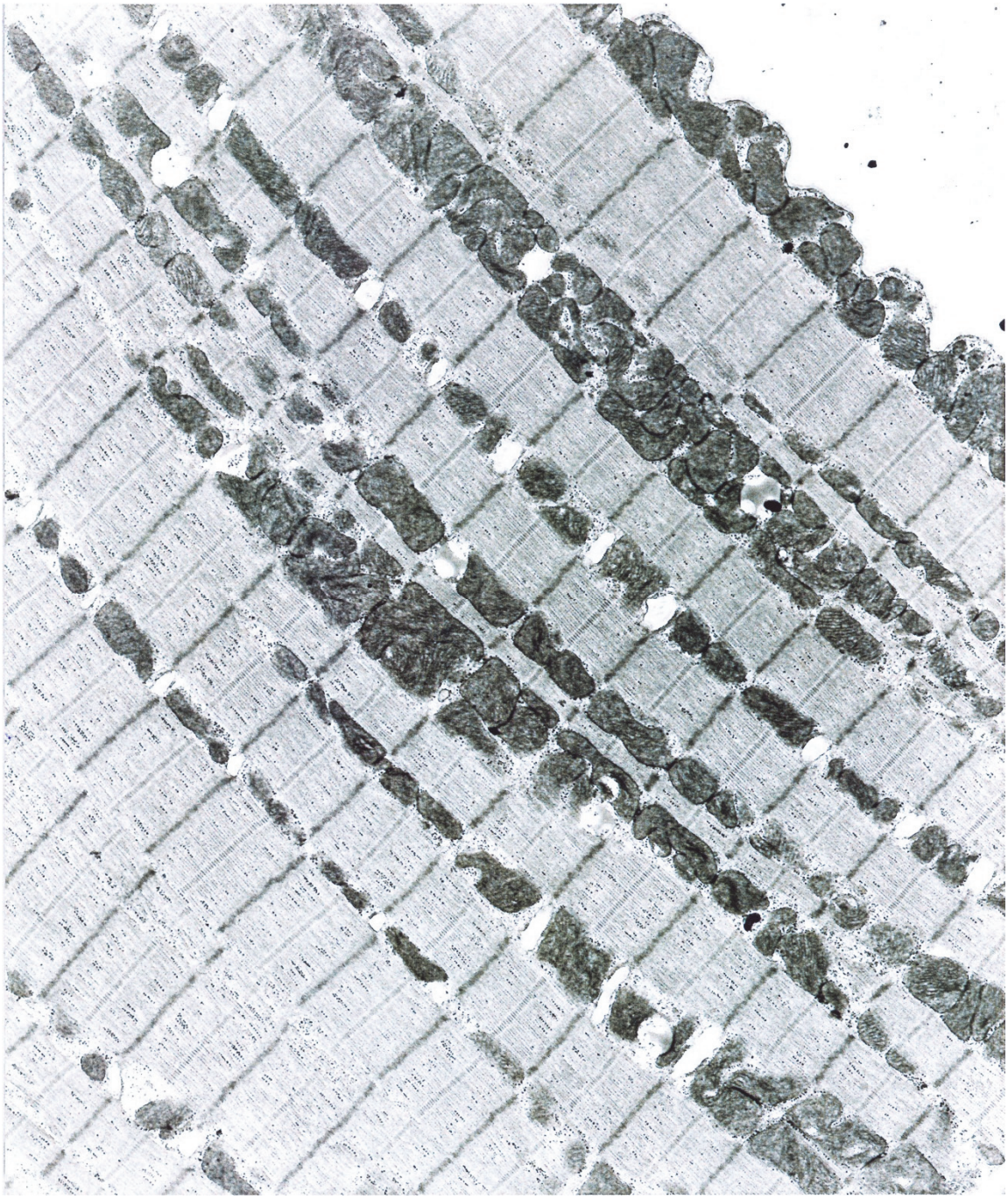

Plate 3-3 Transmission electron micrograph of a normal cardiomyocyte. Note the orderly arranged sarcomeres, interspersed with clusters of normal appearing mitochondria.

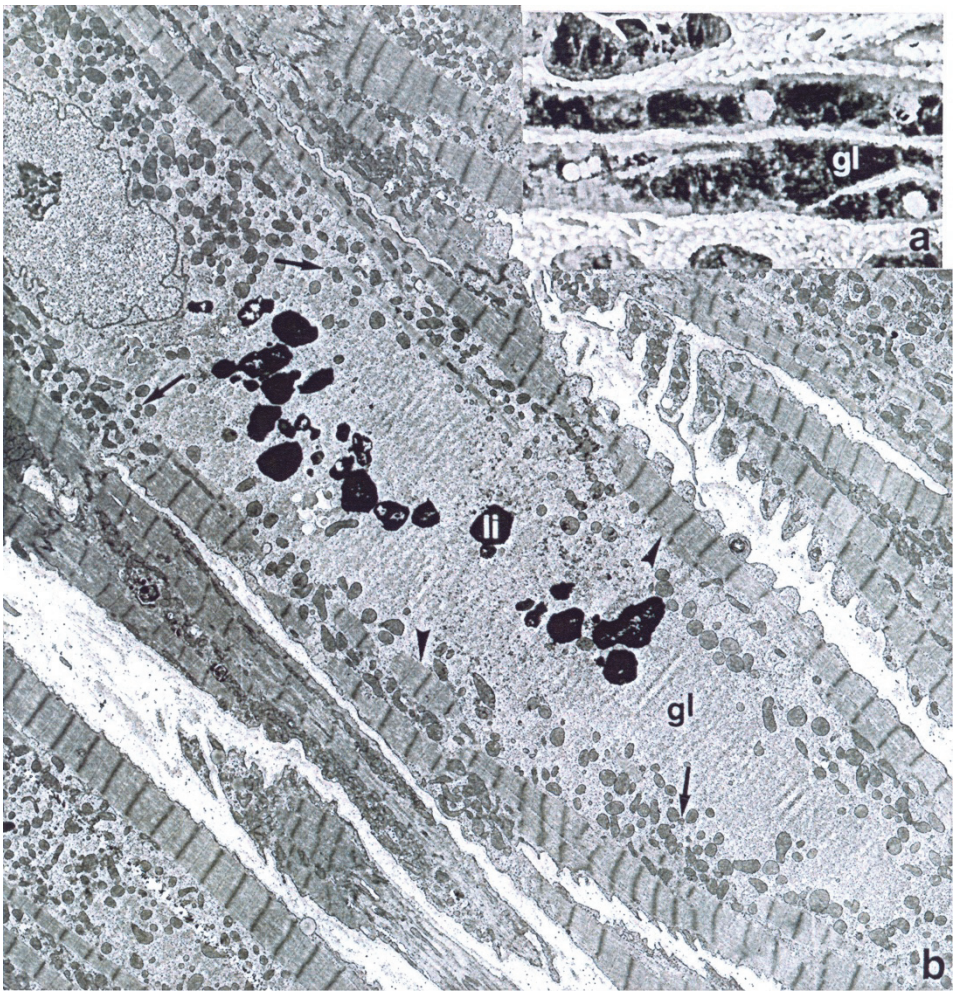

Plate 3-4 Electron and light (upper right) micrographs of myocardial samples derived from a cardiomyocyte affected by myolysis. The myolytic cytosol is filled with glycogen (gl) and small mitochondria (arrow). Sarcomeres (arrowheads) remain only at the cell periphery. Li: lipofuscin Magnification: x 3240.

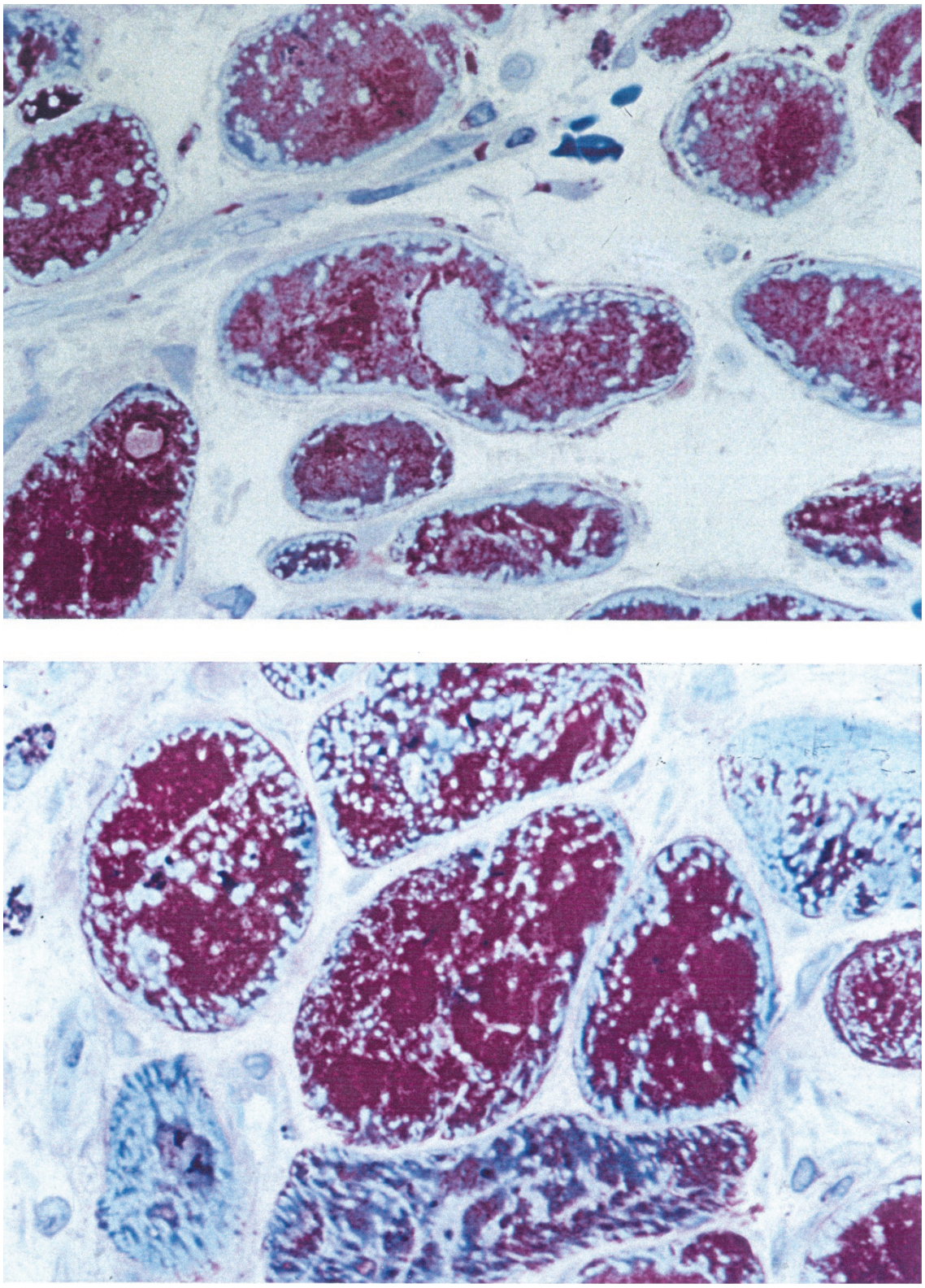

Plate 3-5 Light microscopy of semi-thick sections of dysfunctional myocardial segment stained with PAS and toluidine blue. The cytoplasm of the cells is devoid of sarcomeres and filled with abundant amount of glycogen (red stain). Note the increment of the extracellular space. Magnification is x 350.

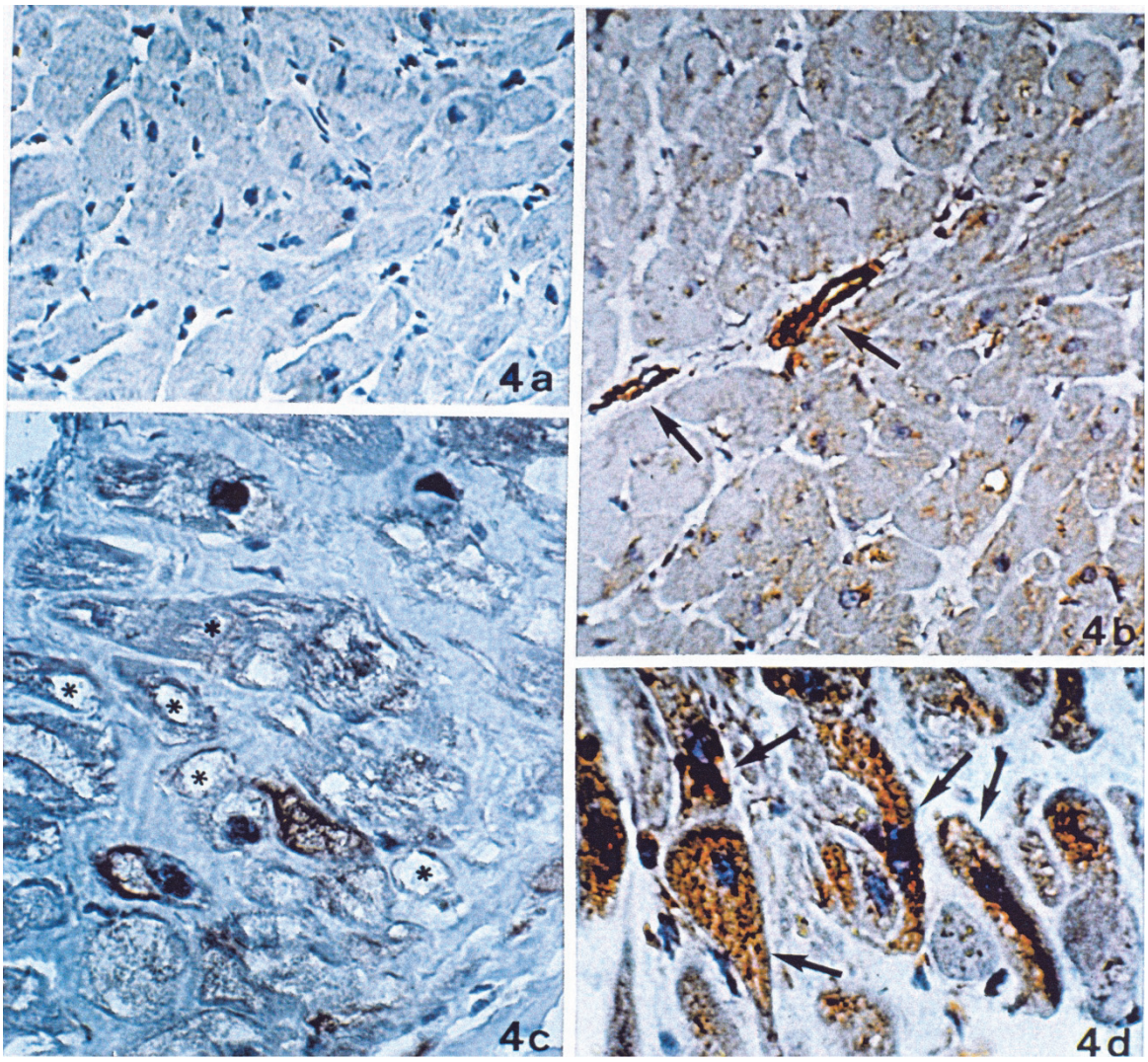

Plate 3-6 Immunoperoxidase labeling of α-smooth muscle actin. *Panel A.* α-smooth muscle actin in control myocardium: the normal adult myocardium is virtually devoid of any staining denoting the absence of α-smooth muscle actin expression in these cells. *Panel B.* α-smooth muscle actin is seen in moderate amounts in many cells of hibernating myocardium whereas it is strongly expressed in vascular smooth muscle cells (arrow). *Panels C* shows a segment in which some cardiomyocytes are strongly positive for α-smooth muscle actin, mainly at the cell periphery. Other cells with severe myolysis are negative for α-smooth muscle actin (asterisks). *Panel D* shows a segment of hibernating myocardium in which the majority of cardiomyocytes display high levels of α-smooth muscle actin (arrows). Magnification panels A and B: x 215; panels C and D: x 430.

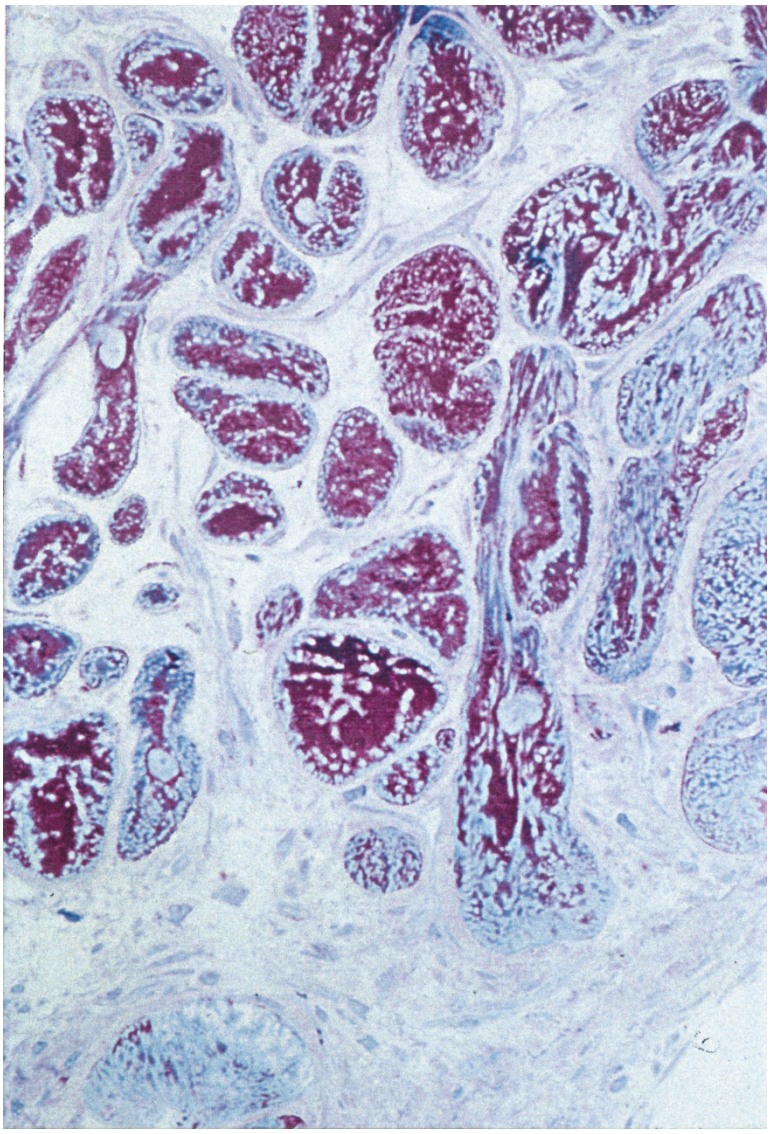

Plate 4-1 Light microscopy of a semi-thick section of dysfunctional myocardial segment stained with PAS and toluidine blue. The majority of cells is filled with abundant amount of glycogen (red stain). Note the increment of the extracellular space. Magnification is x 360.